Siste ...

LRTAP 9/75

LONG RANGE TRANSPORT OF AIR POLLUTANTS AS ESTIMATED BY A TRAJECTORY MODEL

BY

O. JENSEN, A. ELIASSEN, J. NORDØ AND J. SALTBONES

KJELLER, 25TH APRIL, 1975

NORWEGIAN INSTITUTE FOR AIR RESEARCH
P.O. BOX 115, N-2007 KJELLER
NORWAY

CONTENTS

CONTENTS (continuous)

LONG RANGE TRANSPORT OF AIR POLLUTANTS AS ESTIMATED BY A TRAJECTORY MODEL

ABSTRACT

Back trajectories are computed each 6 hours for a number of stations located within the boundaries of the participating OECD countries. As an air parcel moves along its trajectory sulphur dioxide is absorbed at a rate proportional to the strength of the underlying sources. Chemical transformation of SO_2 to SO_4, as well as deposition to the ground, are also simulated in a simple way.

The computed concentrations are compared with daily measurements in order to demonstrate the efficiency of the model, using various transport winds between the surface and the 850 mb. The transformation rates and the deposition rates are also varied in order to see the influence of these parameters on the model estimates.

INTRODUCTION

This preliminary report contains a great number of illustrations showing the results from pilot studies. It is hoped that some of the findings may become useful when deciding on the final computations for the LRTAP-project.

In order to study the possible effects of precipitation on the concentration of sulphur as an air parcel moves along its trajectory, the following relations are used:

$$\frac{\delta q}{\delta t} = \frac{Q}{H} - (k_0 + k_1 + \delta_N k_2 N)q \qquad (1)$$

$$\frac{\delta r}{\delta t} = 1.5 k_1 q - Kr \qquad (2)$$

q is the mixing ratio for SO_2 and r is the mixing ratio for SO_4 on filter. H is the height of the layer and is equal to 1 km in this preliminary study. Q is the emission of SO_2, k_0 the dry deposition rate, k_1 the chemical transformation rate of SO_2 to SO_4, N the precipitation intensity in mm/hour, $\delta_N = 1$ when N > 0.2 mm/hour and equal to zero for lower intensities and k_2 a factor between 0 and 8 x $10^{-5} s^{-1}$. K is the deposition rate of SO_4.
Zero concentrations are assumed at the starting point of each trajectory. Back trajectories are computed every 6 hours, and the mean of four consecutive concentrations form daily means. The precipitation amounts in each 12 hours interval are analysed and hourly amounts are derived by interpolation. A series of calculations are carried out for the period December 15th 1973 - March 31st 1974, varying the parameters of equations (1) and (2).

Back trajectories are computed from different wind fields. The winds at 850 mb and near surface form two of these fields. The remaining two are estimates of the winds in the friction layer and are described below.

The "Ekman" winds $\vec{v}_E$ are calculated from the 850 mb winds using expressions valid for a stationary, horizontally homogeneous and barotropic boundary layer with a constant eddy viscosity K (see Eliassen and Klein-Schmidt, Dynamic Meteorology, Handbuch der Physik sect. 16, pp 40-41). These expressions relate the geostrophic wind to the wind at a level sufficiently low so that the stress and the wind velocity have practically the same direction:

$$|\vec{v}_E| = (\cos\alpha - \sin\alpha)|\vec{v}|$$

$$\frac{\sin\alpha}{(\cos\alpha - \sin\alpha)^2} = \frac{C_D|\vec{v}|}{\sqrt{2fK}}$$

α is the angle between $\vec{v}$ and $\vec{v}_E$, (the cross-isobar angle), C_D is a drag coefficient, and f is the Coriolis parameter. In the calculations we have used the following values:

$$K = 5\ m^2 s^{-1}$$

$$C_D = \begin{array}{l} 0.0017 \text{ over sea.} \\ 0.0075 \text{ over land.} \end{array}$$

The value of C_D refers to a height of 50 m above ground level.

As an alternative to the "Ekman" winds, the "Clarke" low-level winds are calculated by a procedure described in detail in the report on the two-layer model. This wind field depends on the temperature stratification, but barotropic conditions are still assumed.

EFFECT OF VARIABLE k_2, FIGURES A1 - A2

In order to investigate the effects of a variable k_2, the following SO_2 estimates were computed for the 14 stations of Figure A0.

When $k_2 N \geq 0.6 s^{-1}$;

X1* with $k_0=0$, $k_1=2\ 10^{-6} s^{-1}$ $k_2=2\ 10^{-5} s^{-1}$,

X2* with $k_0=0$, $k_1=2\ 10^{-6} s^{-1}$, $k_2=4\ 10^{-5} s^{-1}$,

X3* with $k_0=0$, $k_1=2\ 10^{-2} s^{-1}$, $k_2=8\ 10^{-5} s^{-1}$

When $k_2 N < 0.6 s^{-1}$;

X1*=X2*=X3* with $k_0=0.6\ 10^{-5} s^{-1}$, $k_1=2\ 10^{-6} s^{-1}$, $k_2=0$

The hourly precipitation amounts in this sample is usually less than 0.2 mm/hour and the estimates $\overline{X1}$*, $\overline{X2}$* and $\overline{X3}$* are therefore almost equal. Figure A1 shows that the ratios between $\overline{X_i}$* and $\overline{SO_2}$ (observed) do not differ much from one for 9 of the 14 stations. The Danish stations measure relatively low concentrations while the "background" station SF 5 might have some local sources. The limited accuracy of the SO_2 observations may also lead to higher records at remote places. The SO_2 estimates are based on 850 mb trajectories, and the correlations are given as hundreds in Figure A2. The correlations are almost equal at a given station for the reasons mentioned above. Only modest correlations are derived for the OECD stations close to significant emission sources.

LIST OF SO_2 AND SO_4 ESTIMATES USED IN FIGURES A3 - A45

In the list below X2 is identical to the SO_2 estimate of X2*. X1, the other SO_2 estimate, is the "best" one derived for days with precipitation, see Jensen and Nordø (1975).

SO_2 estimates	$\delta_N=1$	$\delta_N=0$ or k_2 N < $0.6s^{-1}$
X1	$k_0+k_1=3\times10^{-5}$, $k_1=2\times10^{-6}$, $k_2=0$	$k_0+k_1=0.8\times10^{-5}$, $k_1=2\times10^{-6}$, $k_2=0$
X2	$k_0=0$, $k_1=2\times10^{-6}$, 4×10^{-5}	" , " , "

SO_4 on filter estimate		δ_N = 1. k_0+k_1	k_1	k_2	K	δ_N= 0 or k_2 N < $0.6s^{-1}$ k_0+k_1	k_1	K
(X1 as	X4	3×10^{-5}	2×10^{-6}	0	2×10^{-6}	0.8×10^{-5}	2×10^{-6}	2×10^{-6}
	X5	"	5×10^{-6}	0	"	"	"	"
	X6	"	10^{-5}	0	"	"	"	"
SO_2	X7	3×10^{-5}	2×10^{-6}	0	5×10^{-6}	"	"	"
	X8	"	5×10^{-6}	0	"	"	"	"
estimate)	X9	"	10^{-5}	0	"	"	"	"
	X10	3×10^{-5}	2×10^{-6}	0	10^{-5}	"	"	"
	X11	"	5×10^{-6}	0	"	"	"	"
	X12	"	10^{-5}	0	"	"	"	"
(X2 as	X13	2×10^{-6}	2×10^{-6}	4×10^{-5}	2×10^{-6}	0.8×10^{-5}	2×10^{-6}	2×10^{-6}
	X14	5×10^{-6}	5×10^{-6}	"	"	"	"	"
	X15	10^{-5}	10^{-5}	"	"	"	"	"
SO_2	X16	2×10^{-6}	2×10^{-6}	4×10^{-5}	5×10^{-6}	"	"	"
	X17	5×10^{-6}	5×10^{-6}	"	"	"	"	"
estimate)	X18	10^{-5}	10^{-5}	"	"	"	"	"
	X19	2×10^{-6}	2×10^{-6}	4×10^{-5}	10^{-5}	"	"	"
	X20	5×10^{-6}	5×10^{-6}	"	"	"	"	"
	X21	10^{-5}	10^{-5}	"	"	"	"	"

Table A1: SO_2 and SO_4 on filter estimates referred to in the following figures. k_0, k_1 and K have dimention s^{-1}.

If the precipitation is light or absent, the decay of SO_2 is $0.8 \times 10^{-5}s^{-1}$. This value may be representative for western Europe and the North Sea even in winter. But over snowcovered land the decay is likely to become much slower, see Whelpdale and Shaw (1974). Consequently there is some possibility of underestimating the SO_2 concentrations over cold land in the winter season.

The SO_4 (on filter) estimates are computed from the two SO_2 estimates X1 and X2, with some variants of the transformation rate k_1 when precipitation occurs. The deposition rate of SO_4, K, is also varied when the air parcel is exposed to precipitation. Table A1 shows that both k_1 and K may vary between $2 \times 10^{-6}s^{-1}$ and $10^{-5}s^{-1}$.

COMPARISON OF SO_2 ESTIMATES USING WINDS AT DIFFERENT LEVELS, FIGURES A3 - A8

Figure A3 shows the ratios between the estimated means and the observed ones, when using the SO_2 estimate of X2. Concerning the upper ratio, the 850 mb estimate, it is close to unity for 9 stations. The high ratios for the Danish stations and the station S 4 are noticeable. The "background" stations SF5 has on the other hand a rather low ratio, and some possible explanations are already indicated above. The ratios for the remaining trajectory estimates are more variable and may not be used without regional corrections.

Figure A4 gives the corresponding correlations. The correlations for SO_2 estimates according to 850 mb trajectories, show poor correlations near the main emission centres. But there significant correlations are found when low level winds are used. Most remarkable is the rise at the station D 2. This result was expected as the air pollutants are emitted at low levels and only gradually spread upwards.

Figure A5 gives the ratios for the four trajectory estimates when the SO_2 estimates of X1 is used. The mean amplitudes are less than those of X2 as X1 has a much stronger decay when light precipitation occurs. The ratios are less dependent on the wind estimate used in the trajectory calculations. Besides the Danish stations, the ratios are close to one for most of the selected stations. The ratios are rather low for the Finnish stations and the station S 5 in Northern Sweden. This decrease might have been reduced if a slower decay had been used over snowcovered land.

Figure A6 shows the correlations for X1, and they are similar to those found for X2.

Figures A5 and A6 indicate that one should perhaps construct trajectories at two levels using 850 mb (or possibly "Clarke") wind trajectories for transport of tall stack emissions and surface wind trajectories for low emissions.

At the 1973 meeting at Gausdal some correlations were presented between the observed SO_2 value and the total emission of SO_2 along the trajectory. Figure A7 gives the ratio between the averages of observed and computed SO_2 concentrations. The ratios at SF3 and SF5 may indicate some local emission sources.

Figure A8 shows that the correlations are sometimes better than those of X1 for some stations at a great distance from large emission sources. But the correlations of A 8 are remarkably low for the stations D 2 and NL1.

FIGURES A9 AND A10, A COMPARISON OF TOTAL EMISSION ALONG A TRAJECTORY AND THE OBSERVED SO_4 ON FILTER

Figure A9 shows the ratios between the mean values. F 1 and SF5 have the highest values. - Figure A10 gives the correlations which in general are best for the 850 mb wind estimates. The correlations are mostly low for estimates based on surface winds, the exceptions being UK1 and F 1.

DEPENDENCE ON DECAY RATE OF SO_4 WHEN X2 IS THE SO_2 ESTIMATE, FIGURES A11 - A16

The SO_4 estimates of X13, X16 and X19 have decay rates (K values) of $2 \times 10^{-6}s^{-1}$, $5 \times 10^{-6}s^{-1}$ and $10^{-5}s^{-1}$ respectively (if precipitation occurs). Figure A11 shows that the SO_4 concentrations are underestimated at all stations but D 2. F 1 has high values compared to the computed ones. The variations of the ratios are small elsewhere.

The computations based on "Clarke" winds are more variable when the ratios are concerned, see Figure A12. The same applies to the ratios for the surface wind computations given in Figure A13.

Figure A14 shows the correlations when 850 mb winds are used. A comparison with Figure A10 shows almost identical results. The result of raising K is therefore mainly a reduction of the amplitude of the SO_4 estimates.

Figure A15 gives on the other hand a modest rise of the correlations for "Clarke" wind estimates compared to those of Figure A10.

Figure A16 shows a higher rise for the SO_4 estimates based on surface winds, and the stations D 2 and NL1 have now reasonably good correlations.

DEPENDENCE ON DECAY RATE OF SO_4- WHEN X1 IS THE SO_2 ESTIMATE, FIGURES A17 - A22

If X1 is used as SO_2 estimate, the SO_4 estimates of X4, X7 and X10 have exactly the same decay rates as the variables X13, X16 and X19 above.

Figure A17 gives slightly lower mean SO_4 concentrations than those of Figure A11. The same applied for the average SO_2 concentrations. - The ratios based on "Clarke" wind estimates are somewhat more variable, see Figure A18. This result was also derived above (Figure A12). But it may be noticed that the SO_4 estimate of X10 has an amplitude near unity, the main exceptions being D 1 and F 1. - Figure A19 shows finally the ratios for the surface wind estimates. They seem to vary somewhat more than the "Clarke" wind estimates.

The correlations for the 850 mb estimates are given in Figure A20. The values are similar to those derived when X2 was used. The same comments apply to Figures A21 and A22, showing correlations for SO_4 estimates based on "Clarke" and surface wind trajectories.

EFFECT OF RISING THE PRODUCTION RATE OF SO_4, FIGURES A23 - A28

When humidity comes near saturation the transformation rate k_1 may increase. The SO_4 estimates of X4, X5 and X6 have values of k_1 equal to $2 \times 10^{-6}s^{-1}$, $5 \times 10^{-6}s^{-1}$ and $10^{-5}s^{-1}$, respectively. When 850 mb winds are used, the ratios of the estimated means to the mean of observed SO_4 on filter are given in Figure A23. For the fixed mixing height of 1000 m the X6 estimate seems to have the best ratio. Exceptions are D 2 and F 1, as above. - The correlations are plotted in Figures A24 and are quite similar at a given station.

Only the X4 estimate seems to give a reasonable amplitude when "Clarke" winds are used, see Figure A25. X4 is also better correlated to the observed SO_4 on filter according to Figure A26. - Similar results are found when surface winds are used (Figures A27 - A28).

EFFECTS OF INCREASED PRODUCTION AND DECAY OF SO_4 WHEN PRECIPITATION OCCURS, FIGURES A29 - A34

During precipitation one may simulate a rise in k_1 as well as K. For the SO_4 estimate of

X4 $k_1 = K = 2\times10^{-6}s^{-1}$,

X8 $k_1 = K = 5\times10^{-6}s^{-1}$,

X12 $k_1 = K = 10^{-5}s^{-1}$

These three estimates are compared to observed values on the following figures.

Figure A29 shows the ratios between the mean estimates and the observed mean. The mean of X12 seems to be closest to unity when 850 mb winds are used (Figure A29). The correlations in Figure A30 show, however, no special preference.

When "Clarke" winds are used, Figures A31 and A32, the ratios seem to vary more. The estimates at the surface look somewhat better with regard to the amplitudes, see Figures A33 and A34.

FIGURES A35 - A37, COMPARISONS BETWEEN OBSERVED SO_4 ON FILTER CONCENTRATIONS AND TRAJECTORY ESTIMATES OF SO_2

Figure A35 shows the correlations between observed SO_4 on filter and the SO_2 estimates of X1 and X2 when 850 mb winds are used. The X2 correlations are somewhat better. - When "Clarke" winds are used, Figure A36, there is a slight preference of X1, but X2 is still best near the large emission sources. The latter result is also derived for the estimates based on surface wind trajectories, see Figure A37.

FIGURES A38 - A41, CORRELATIONS OF TOTAL EMISSION OF SO_2 ALONG TRAJECTORY TO OBSERVATIONS AND SO_2 ESTIMATES

It may be interesting to see a comparison of these four correlations over western Europe and the Nordic countries. Figures A38 shows the correlations when 850 mb winds are used. The correlations between X2 and the total emission are very high all over the map. The same result is derived for most of the SO_4 estimates and explains why the correlations vary so little from one estimate to another. The main effect of the k_1 and K variations is amplitude modifications, as demonstrated by some of the figures above. But an amplitude estimate near the observed one is of course desired when budget calculations are going to be carried out. - The estimate X1 shows also too high correlations to the total emission along the trajectory. The correlations between total emission and observed SO_2 and SO_4 have been discussed above.

Figure A39 gives the same four correlations when "Clarke" winds are used. The drops for D 2, NL1 and F 1 are noticeable.

Figure A40 shows a similar drop for D 1 and NL1 when "Ekman" winds are used. The correlations at F 1 are high again. - Figure A41 presents finally the correlations when surface winds are used. Low correlations of X1 and X2 are also found for the two Danish stations.

BACK TRAJECTORY ESTIMATES FOR THE EPISODE ON MARCH 27, 1974

This episode has been discussed in a report by Nordø (1974). During the end of March 1974 easterly winds prevailed between Scandinavia and the continent (see also Figures A46 - A47 below). On March 27 the NILU aircraft sampled the air between southern Norway and the Channel. The SO_2 concentrations rose from a few microgrammes to 135 microgrammes west of the Netherlands (500 m above ground). Figure A42 gives the observed SO_2 concentrations as well as the estimated ones, when 850 mb trajectories are used. The estimates corresponds reasonably well with the aircraft values, but the stations in the Netherlands report rather low values. UK1 does the same, but another station nearby report high concentrations. The computations gave high estimates at D 2 and low estimates at F 1, quite opposite of the observations.

Figures A43 and A44 show the same correlations for the "Clarke" and "Ekman" trajectory estimates. The computed concentrations are somewhat lower at NL2 and D 2, and they are slightly higher at F 1.

The surface trajectory estimates are reproduced in Figure A45. The correspondence is now rather good at F 1 and D 2, showing once again that low level winds are preferable near the sources. But the station NL1 has still high estimates which agree well with the concentrations aloft. This result demonstrates that sharp vertical gradients may last for days in stable stratifications.

Figures A46 and A47 show the back trajectories every six hours for 850 mb and surface. At the station F 1 the 850 mb transport is from the east from regions with relatively weak emission sources. Near the surface transport is from the north and northeast resulting in signifiant pollution from nearby and remote sources. - At the station D2 850 mb transport is from southeast, across some large emission sources. But the low level transport is due east and the result is a moderate pollution level.

COMPARISON OF OBSERVED HIGH SO_2 CONCENTRATIONS WITH TRAJECTORY ESTIMATES

At the end it might be of interest to see how well "extreme" SO_2 concentrations are estimated by the trajectory approach above. Somewhat arbitrarily only days with SO_2 concentrations higher than 100 micorgrammes per m^3 are listed in Table A2.

STATION	DATE D M Y	OBSERVED AT SURFACE	COMPUTED VALUES OF X1 AND X2 USING			
			850 MB	"CLARKE"	"EKMAN"	SURFACE
D2	03 01 74	169	44-49	66-94	68-98	113-229
-	05 - -	153	23-26	68-74	56-59	128-133
-	06 - -	130	44-51	70-84	106-116	144-166
-	16 02 -	119	29-34	89-94	87-93	123-168
-	12 03 -	114	74-75	122-125	207-208	160-162
NLI	20 12 73	128	22-23	56-57	61-61	76-77
-	02 01 74	108	53-67	84-109	90-110	85-119
-	28 02 -	103	66-67	130-130	134-134	100-101
-	11 03 -	111	31-47	61-104	51-96	92-137
FI	27 03 74	127	30-32	36-52	42-52	75-110
-	28 - -	121	29-40	33-42	36-42	52-76

Table A2: December 73 - March 74.
Trajectory computations for days when observed SO_2 concentrations were more than 100 microgrammes per m^3. Left estimate is X1, right estimate is X2.

Table A2 shows that high values are only found for stations not far from large emission sources. The surface trajectory estimates are best, the 850 mb ones worst. The "Ekman" and "Clarke" wind estimates are in between.

As for March 27, 1974 surface and 850 mb trajectories will be presented for a few more days with high concentrations. Figure A48 shows the trajectories for January 3, 1974. The direction of the 850 mb transport is more southerly and much stronger than the surface transport. The weak southeasterly surface winds are crossing high emission sources (according to our present emission estimates) and must give high SO_2 estimates in accordance with observations.

During the days of January 5 - 6, 1974 the 850 mb transport is southwesterly, confer Figure A49. The 850 mb estimates of SO_2 are therefore of moderate size at D 2. Near the surface, however, the winds are southeasterly and weak. The upwind emission sources are strong. The SO_2 estimates become high and agree well with observations.

CONCLUSIONS

This preliminary investigation indicate that low level winds give the best SO_2 estimates at a distance less than about 500 km from large emission sources. At greater distances the 850 mb winds seem to give the best concentrations.

The correlation analysis cannot discriminate too well among the various SO_4 (on filter) estimates as most of these are highly intercorrelated. But the mean amplitudes may vary much from one estimate to another. The computations show that some of the SO_4 on filter estimates have means close to the observed ones. The same is partly true for the SO_2 estimate of X1. It should therefore be possible to carry out budget studies for SO_2 and SO_4 on filter using surface winds for low level emissions and 850 mb winds for high stack emissions.

The wet deposition of SO_4 may have a higher score, as already indicated by an investigation by Jensen and Nordø (1975).

REFERENCES

D.M. Whelpdale and R.W. Shaw — Sulphur dioxide removal by turbulent transfer over grass, snow and water surface. TELLUS, Volume 26, No. 1-2, 1974.

O. Jensen and J. Nordø — A summer episode, decay of SO_2 on days with precipitation and preliminary budget studies. LRTAP report 1975.

J. Nordø — Sulphur pollution arising from distant emission sources. ELMIA conference, Jönköping, Sweden, 1974.

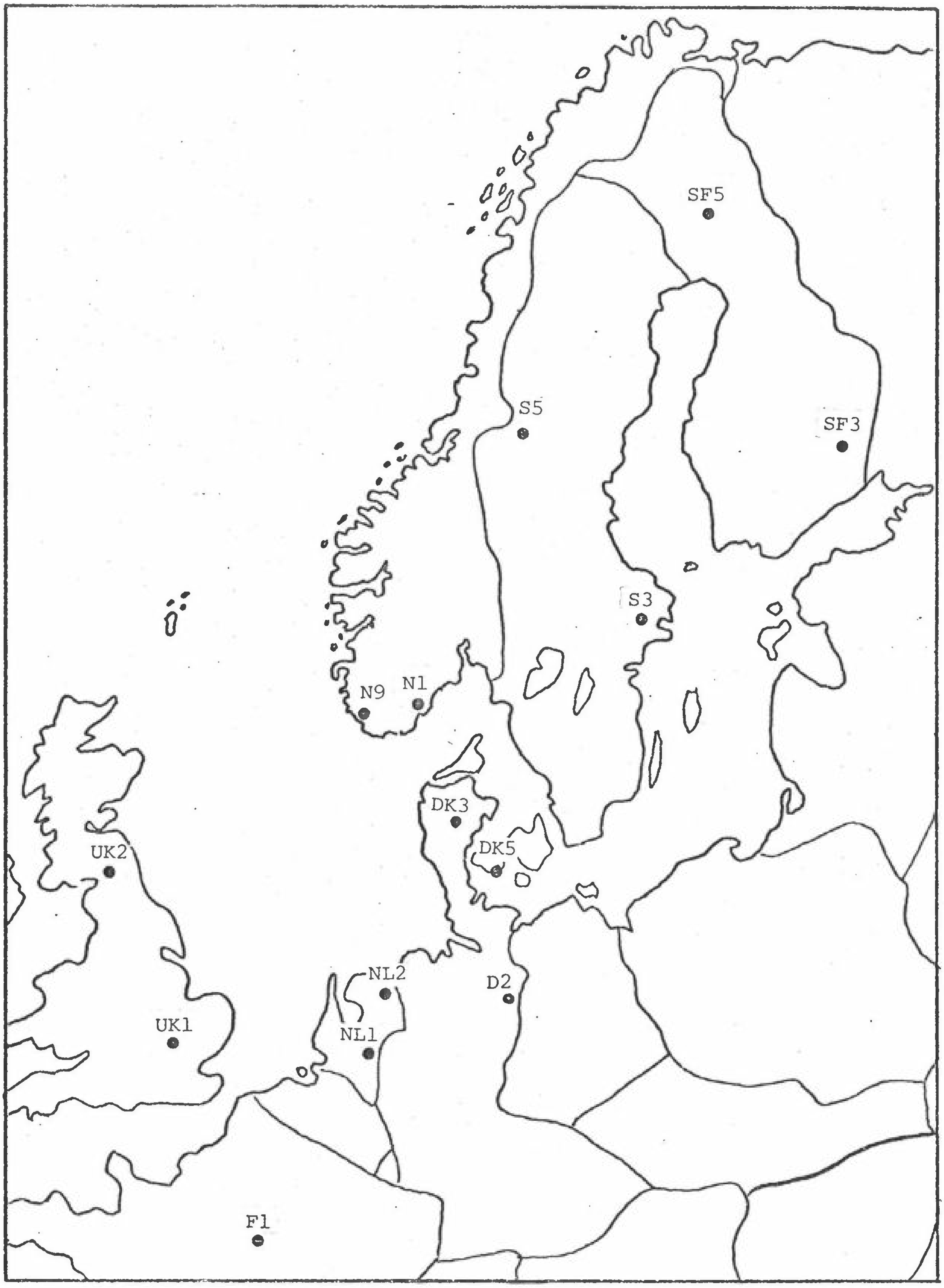

FIG. A0 DEC 73 - MARCH 74
STATIONS USED IN
FIGS. A1 - A 50

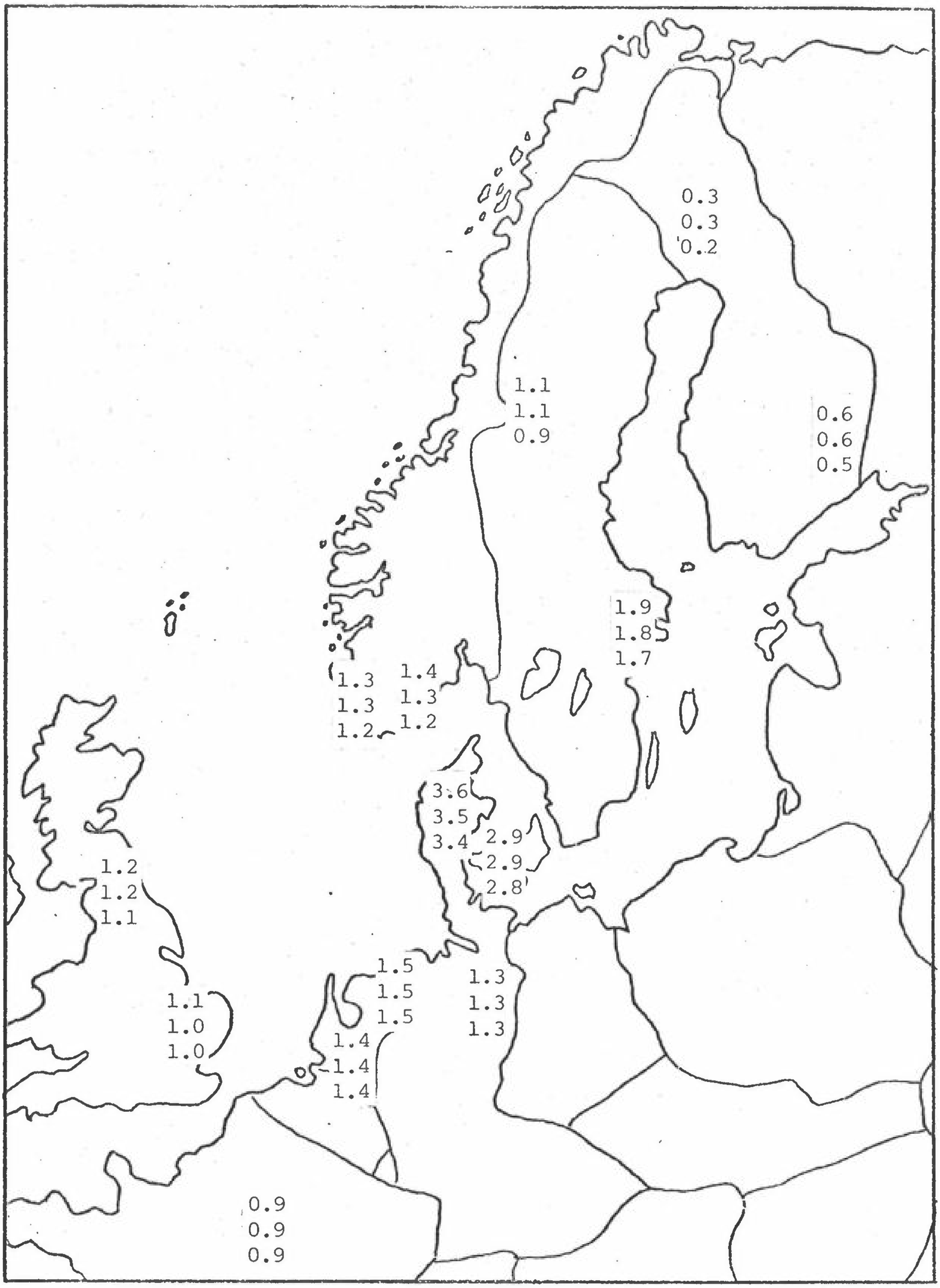

FIG. A1 DEC 73 - MARCH 74
48 HOURS BACK TRAJECTORIES
AT 850 MB

RATIOS $\overline{X1}^{*}, \overline{X2}^{*}, \overline{X3}^{*} / \overline{SO_2}$ (OBS.)

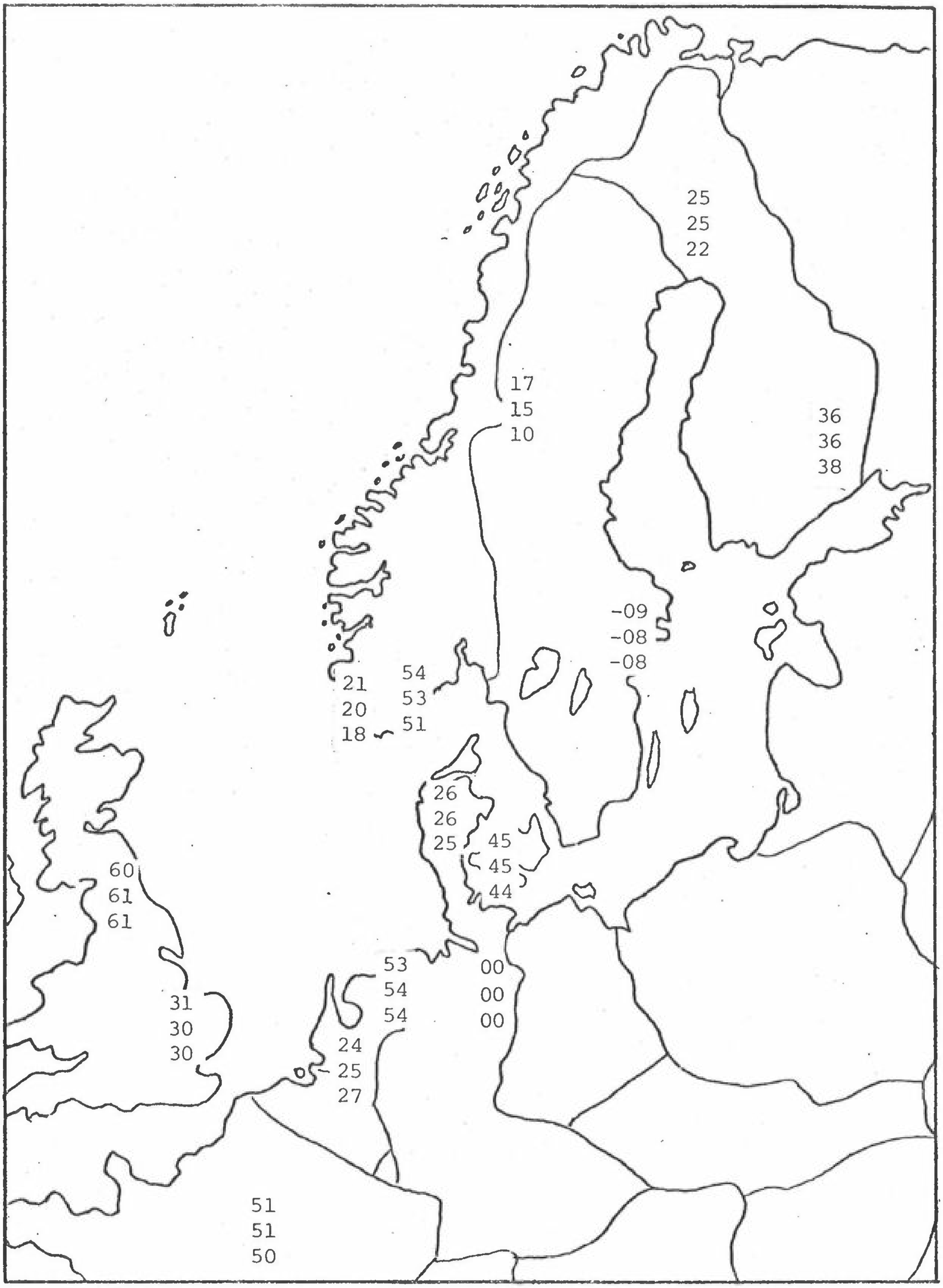

FIG. A2 DEC 73 - MARCH 74

48 HOURS BACK TRAJECTORIES AT 850 MB

CORRELATIONS BETWEEN OBSERVED SO_2 AND X^*_1, X^*_2 AND X^*_3.

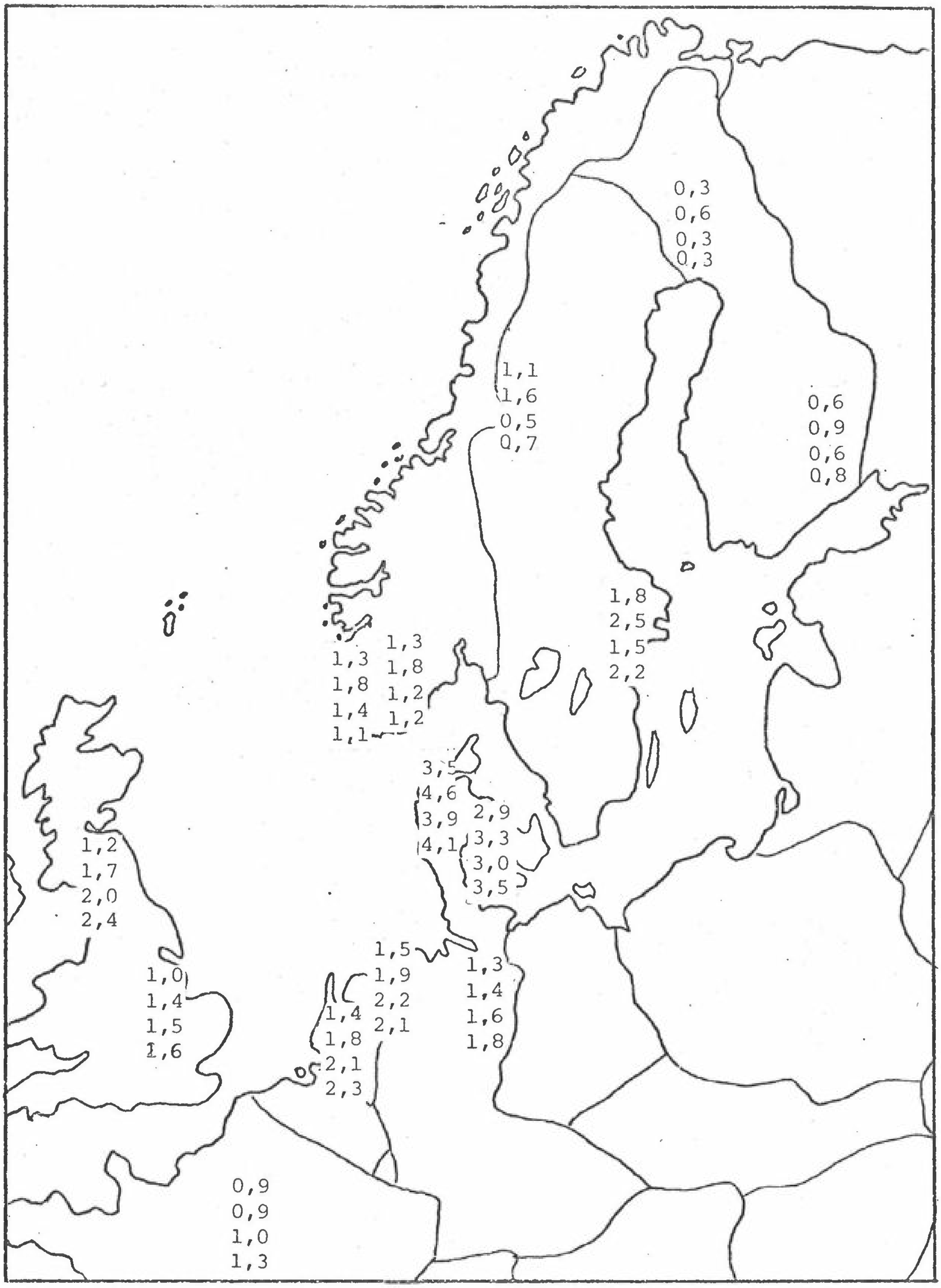

FIG. A3 BACK TRAJECTORY ESTIMATES
FOR DEC 73 - MARCH 74

RATIOS BETWEEN 4 ESTIMATED X_2
MEANS AND OBSERVED SO_2 MEAN
UPPER VALUE REFERS TO 850 MB WIND (48H)
NEXT " " " "CLARKE" " (96H)
THIRD " " " "EKMAN" " (48H) AND
LOWER " " " SURFACE " (96H)

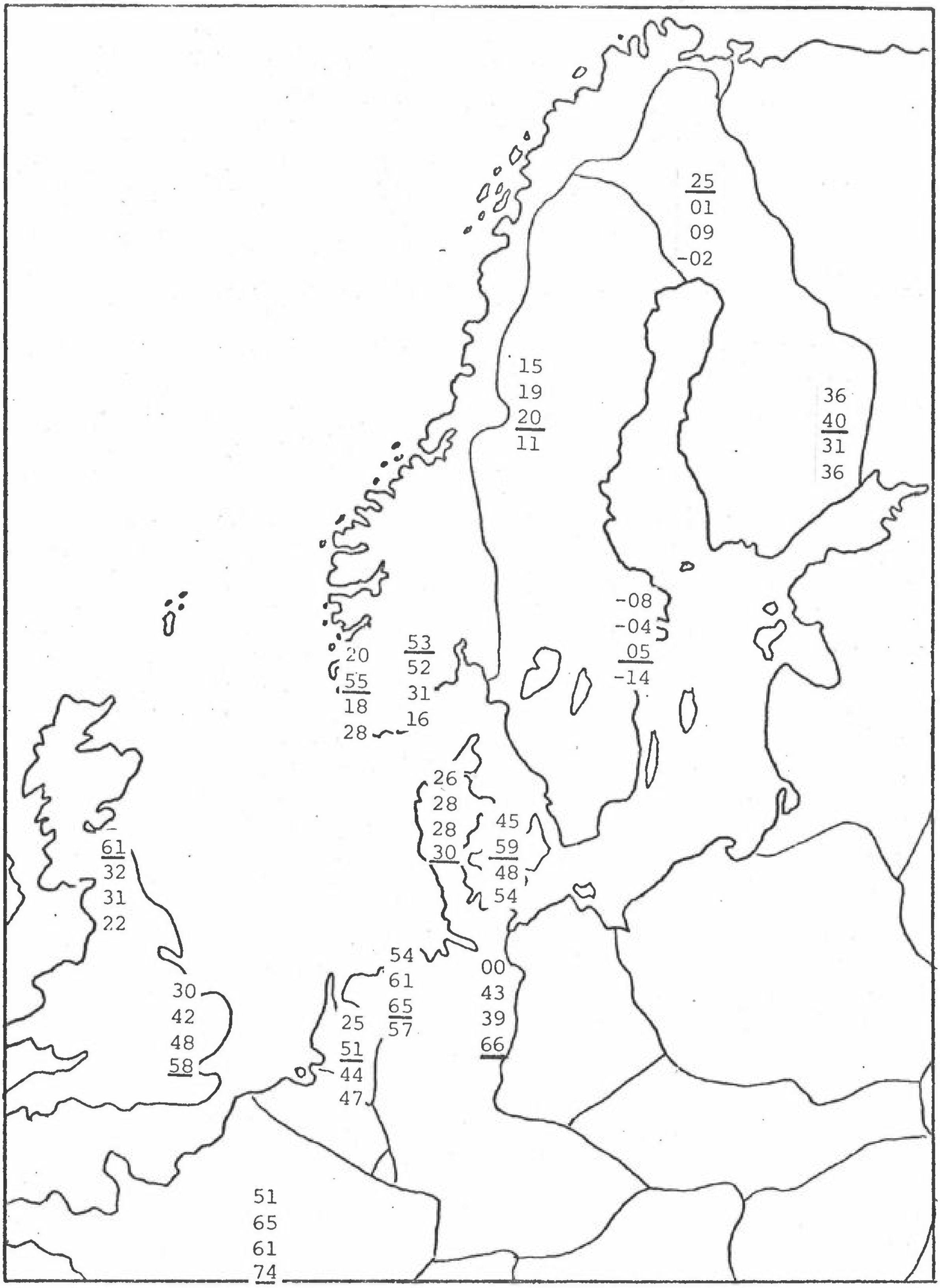

FIG. A4 BACK TRAJECTORY ESTIMATES
FOR DEC 73 - MARCH 74

CORRELATIONS BETWEEN 4 X_2
ESTIMATES AND OBSERVED SO_2

UPPER VALUE REFERS TO 850 MB WIND (48H)
SECOND " " " "CLARKE" " (96H)
THIRD " " " "EKMAN" " (48H)
FOURTH " " " SURFACE " (96H)

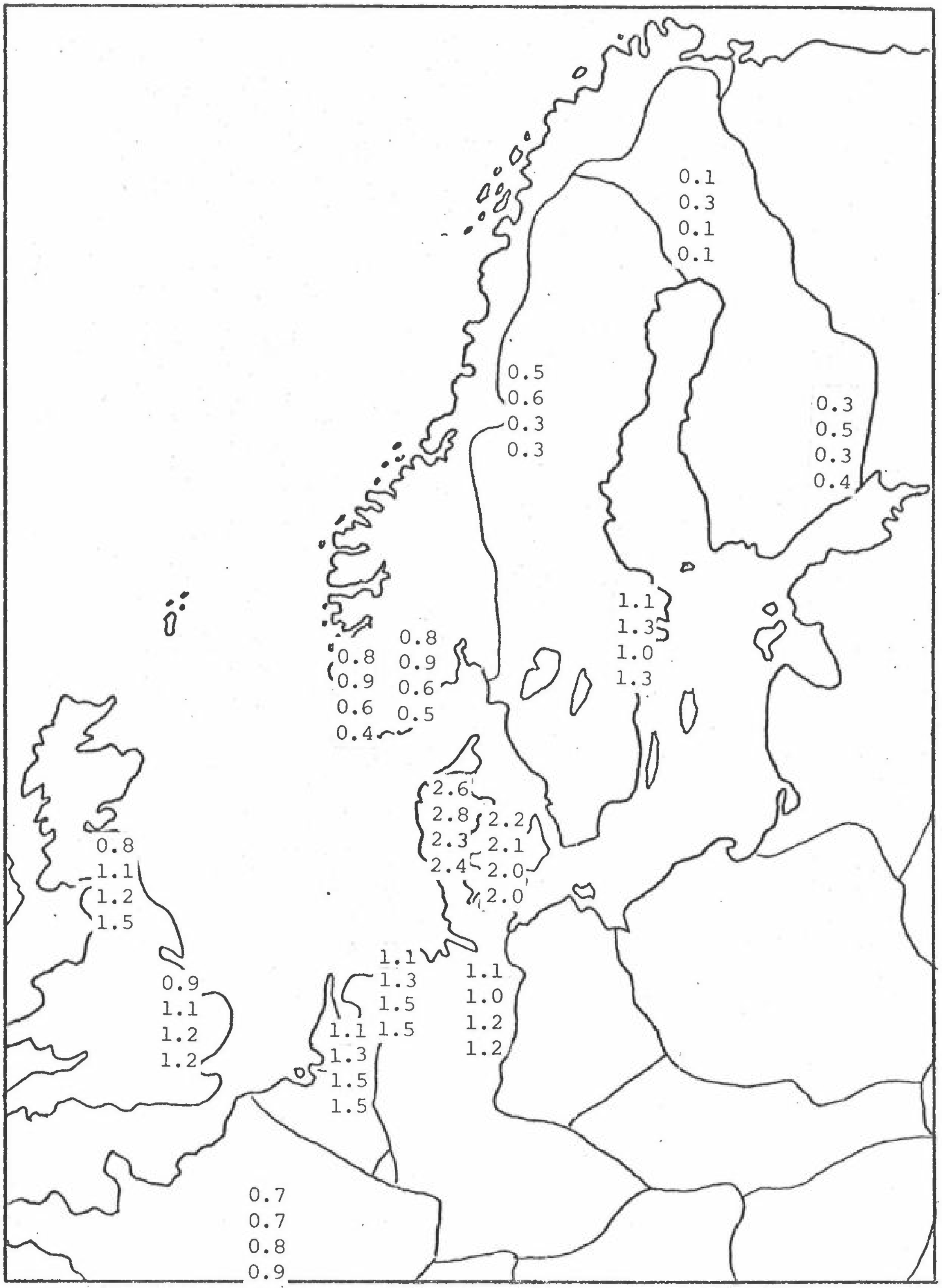

FIG. A5 BACK TRAJECTORY ESTIMATES
FOR DEC 73 - MARCH 74

RATIOS BETWEEN 4 X1 MEANS AND THE
OBSERVED SO_2 MEAN
UPPER VALUE REFERS TO 850 MB WIND (48H)
SECOND " " " "CLARKE" " (96H)
THIRD " " " "EKMAN" " (48H)
FOURTH " " " SURFACE " (96H)

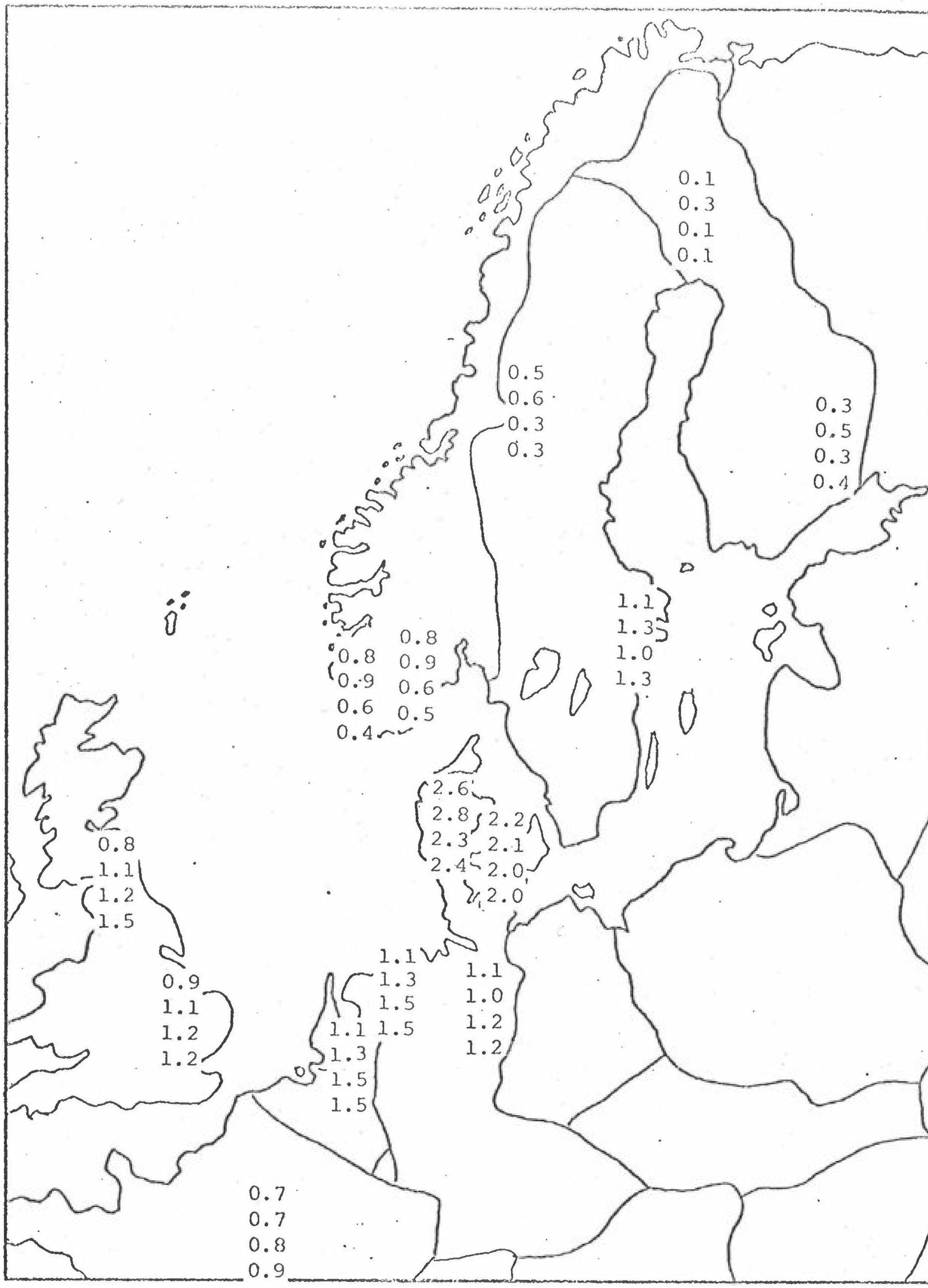

FIG. A5 BACK TRAJECTORY ESTIMATES FOR DEC 73 - MARCH 74

RATIOS BETWEEN 4 X1 MEANS AND THE OBSERVED SO_2 MEAN

UPPER VALUE REFERS TO 850 MB WIND (48H)
SECOND " " " "CLARKE" " (96H)
THIRD " " " "EKMAN" " (48H)
FOURTH " " " SURFACE " (96H)

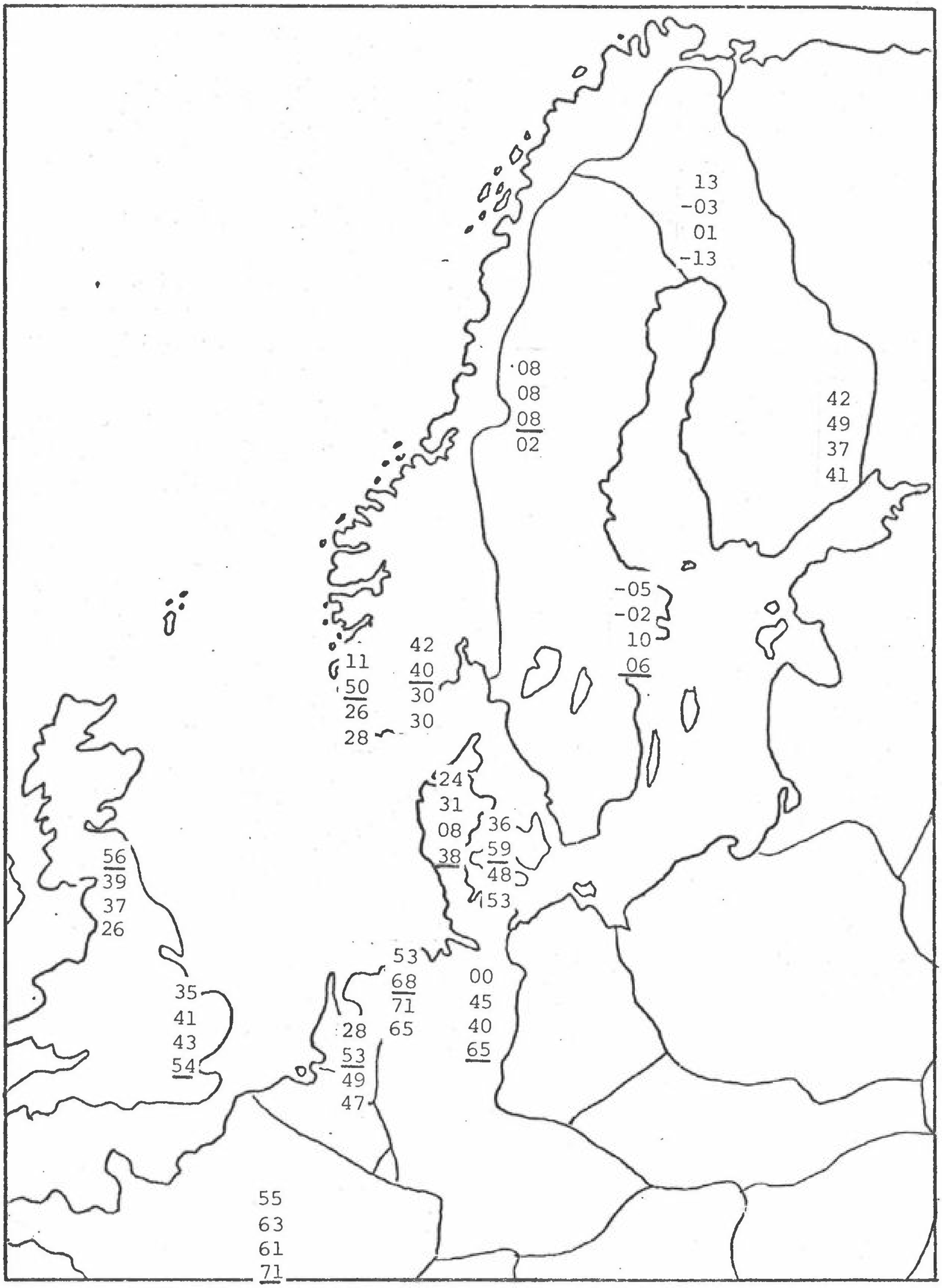

FIG. A6 BACK TRAJECTORI ESTIMATES
FOR DEC 73 - MARCH 74

CORRELATIONS BETWEEN 4 X1
ESTIMATES AND OBSERVED SO_2
UPPER VALUE REFERS TO 850 MB WIND (48H)
SECOND " " " "CLARKE" " (96H)
THIRD " " " "EKMAN" " (48H)
FOURTH " " " SURFACE " (96H)

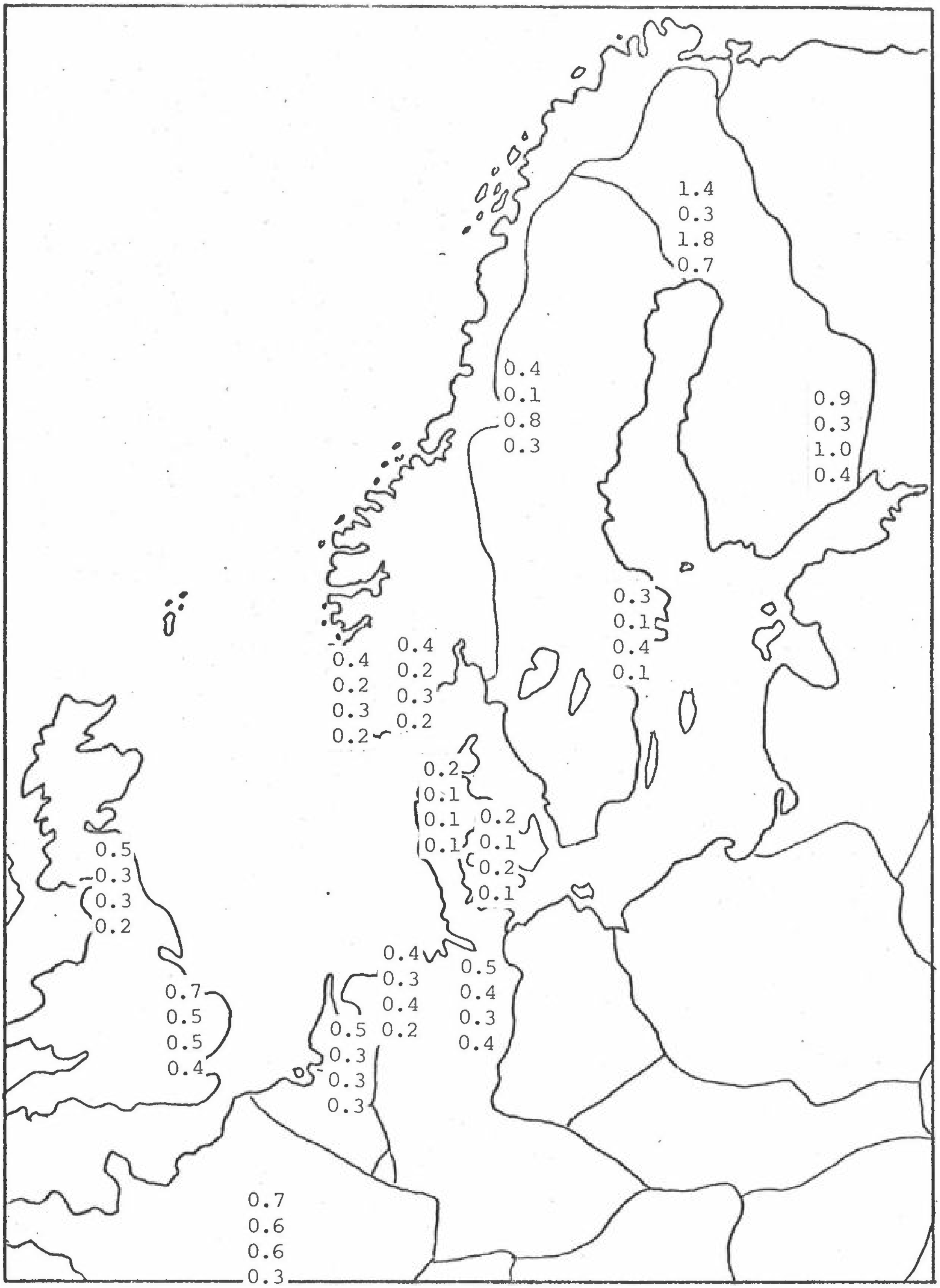

FIG. A7 BACK TRAJECTORY ESTIMATES FOR DEC 73 - MARCH 74

RATIOS BETWEEN MEANS OF OBSERVED SO_2 AND TOTAL EMISSION ALONG TRAJECTORY FOR

850 MB WIND (TOP VALUE), "CLARKE" WIND, "EKMAN" WIND AND SURFACE WIND.

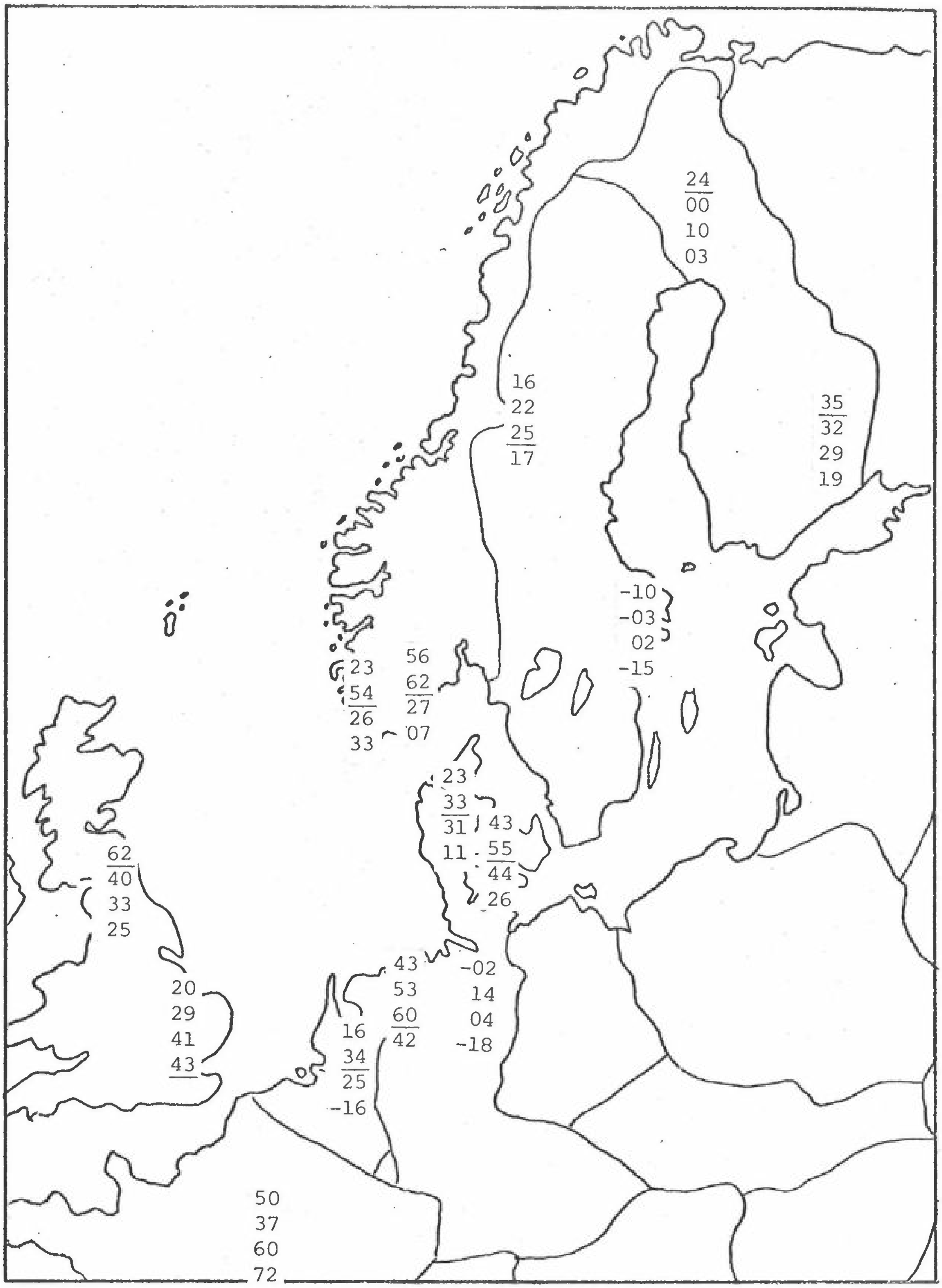

FIG. A8 BACK TRAJECTORY ESTIMATES FOR DEC 73 - MARCH 74

CORRELATION BETWEEN SO_2 AND EMISSION ALONG TRAJECTORY FOR 850 MB WIND (TOP VALUE), "CLARKE" WIND, "EKMAN" WIND AND SURFACE WIND

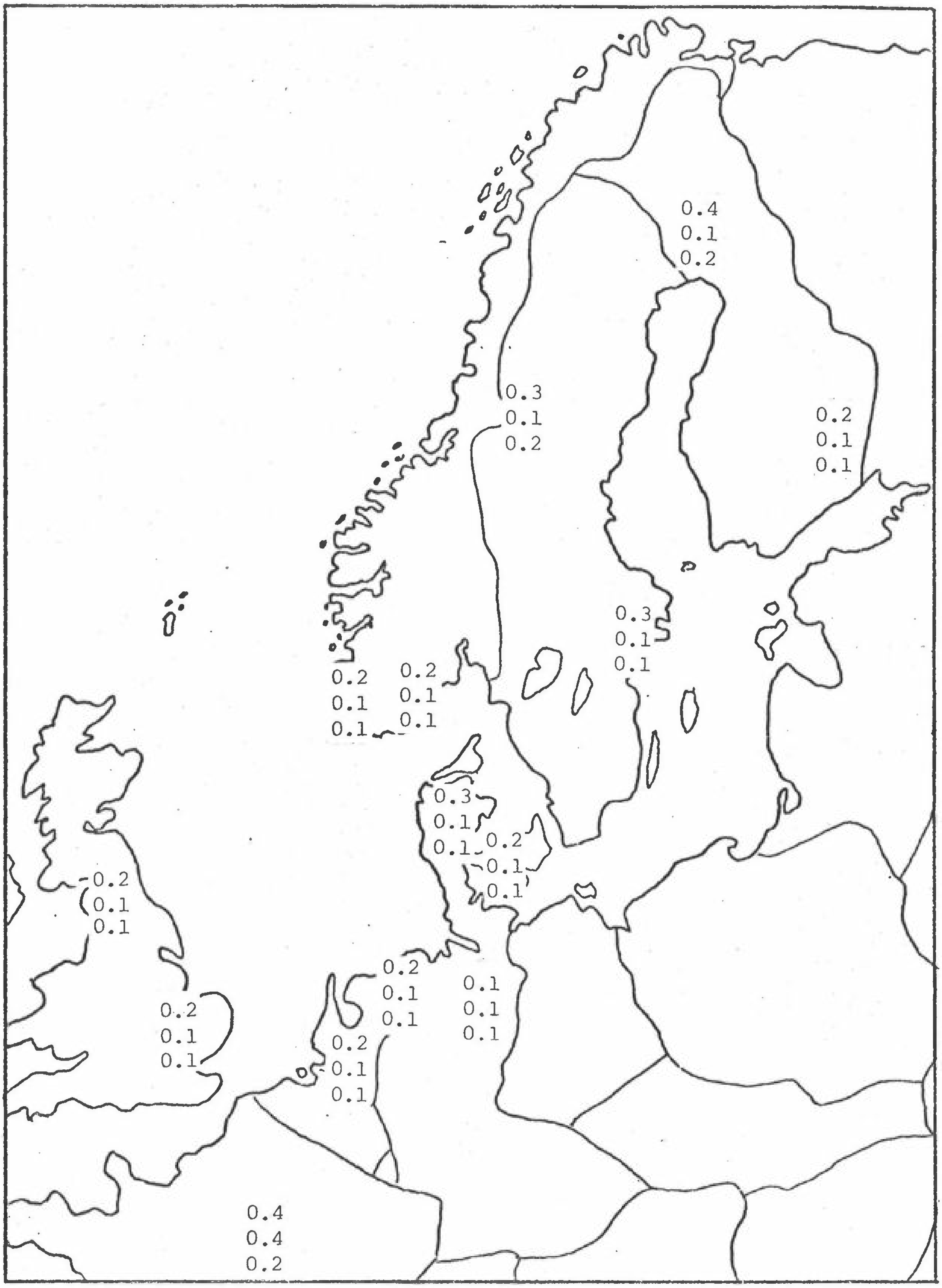

FIG. A9 BACK TRAJECTORY ESTIMATES FOR DEC 73 - MARCH 74

RATIONS BETWEEN MEANS OF OBSERVED SO_4 ON FILTER AND TOTAL EMISSON ALONG TRAJECTORY FOR 850 MB WIND (TOP VALUE), "CLARKE" WIND AND SURFACE WIND

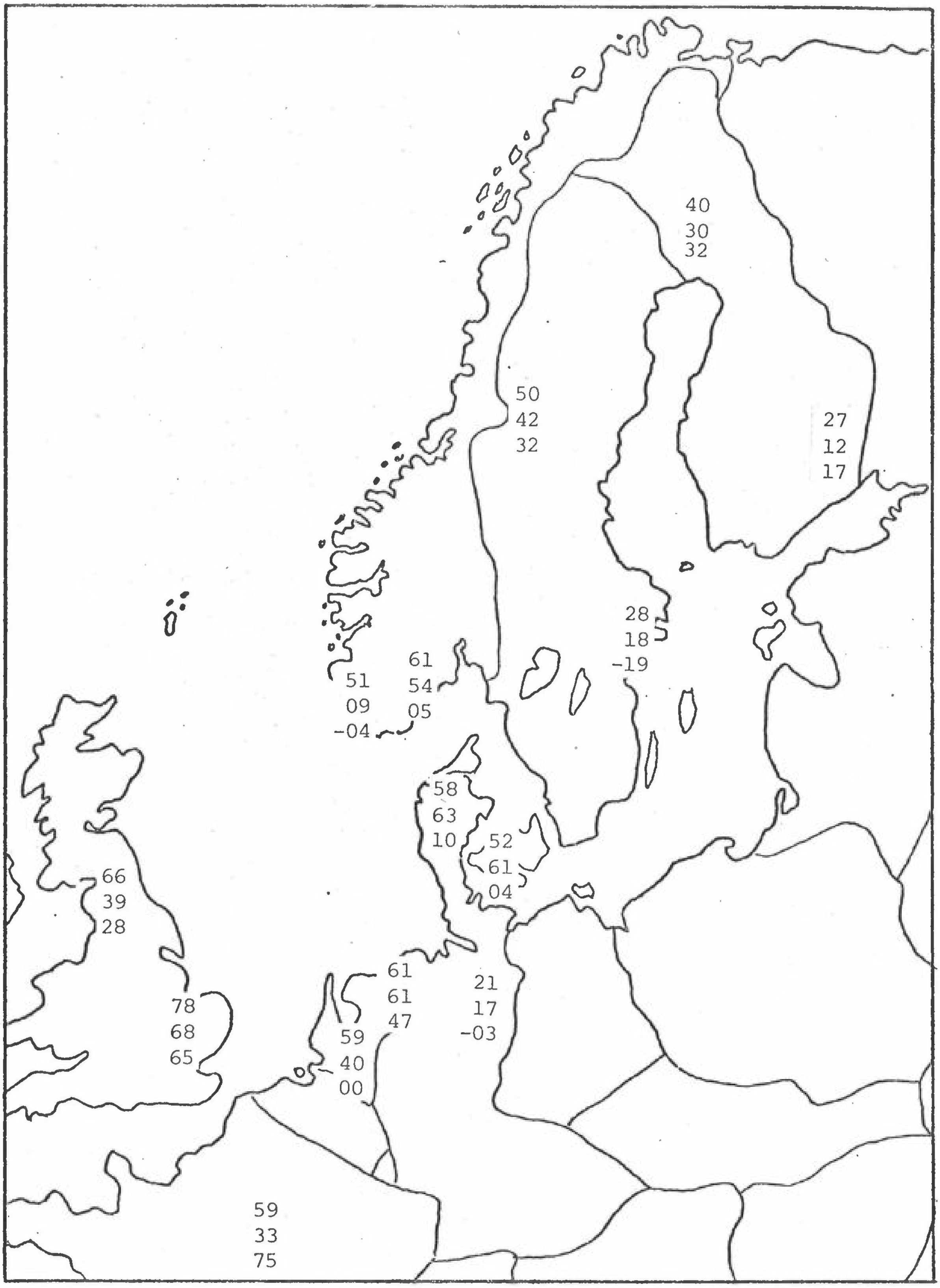

FIG. A10 BACK TRAJECTORY ESTIMATES FOR DEC 73 - MARCH 74

CORRELATIONS BETWEEN SO_4 ON FILTER AND TOTAL EMISSION ALONG TRAJECTORY FOR 850 MB WIND (TOP VALUE), "CLARKE" WIND AND SURFACE WIND.

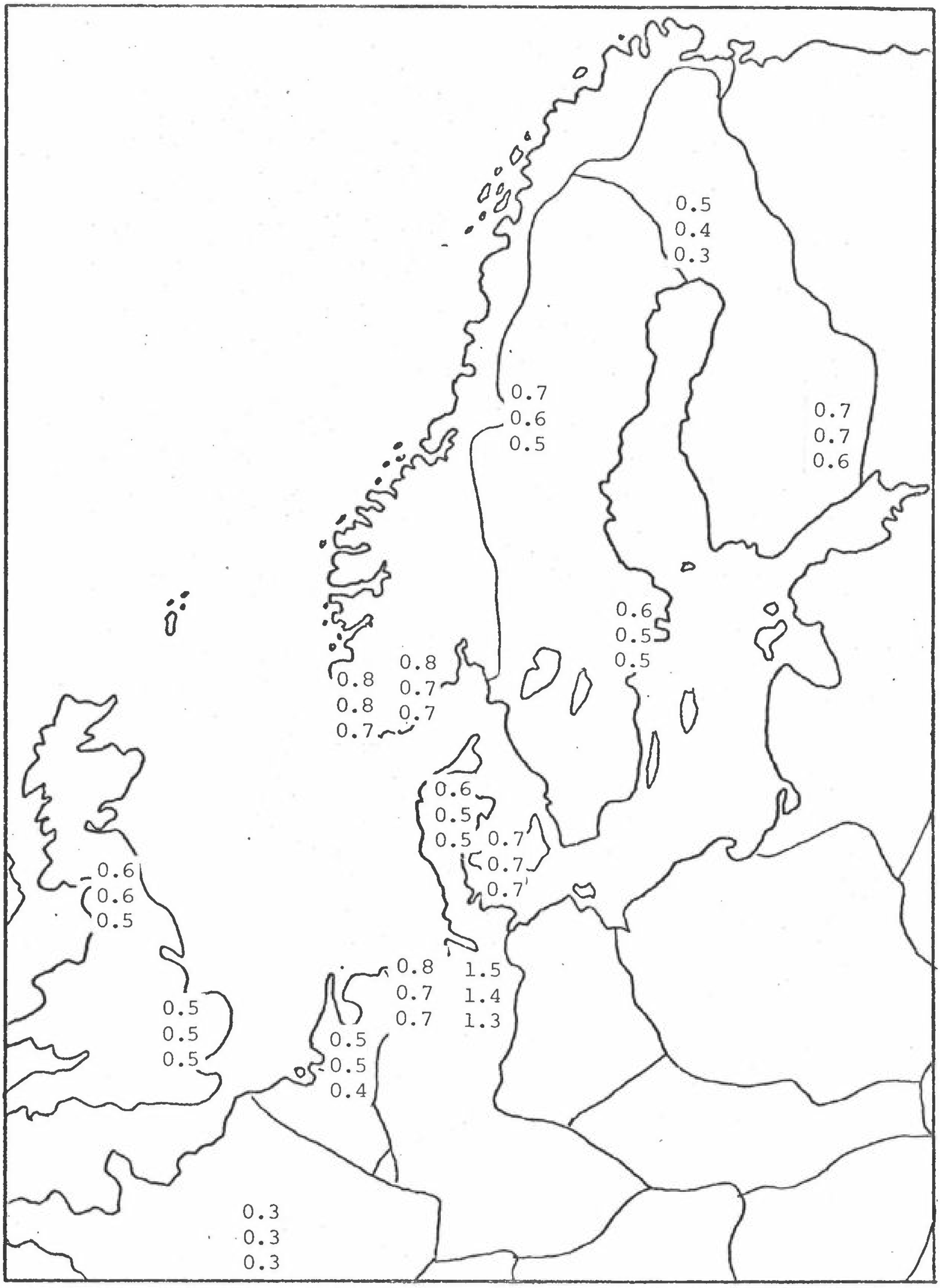

FIG. A11 DEC 73 - MARCH 74

48 HOURS 850 MB BACK TRAJECTORIES

RATIO $\overline{X13}$ / $\overline{X16}$ / $\overline{X19}$ TO $\overline{SO_4}$ ON FILTER

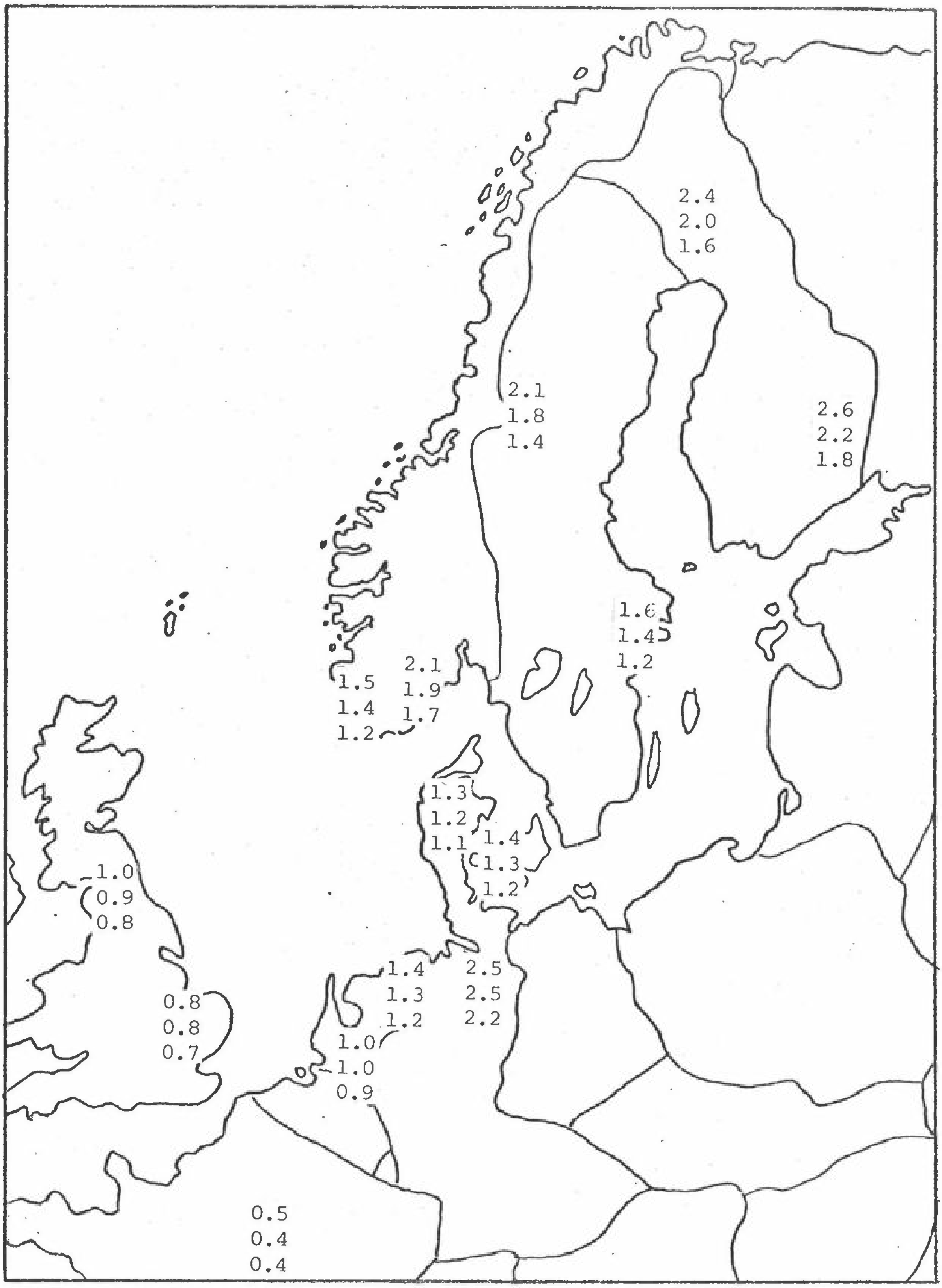

FIG. A12 DEC 73 - MARCH 74

96 HOURS "CLARKE" BACK TRAJECTORIES

RATIO $\overline{X13}$ / $\overline{X16}$ / $\overline{X19}$ TO $\overline{SO_4}$ ON FILTER

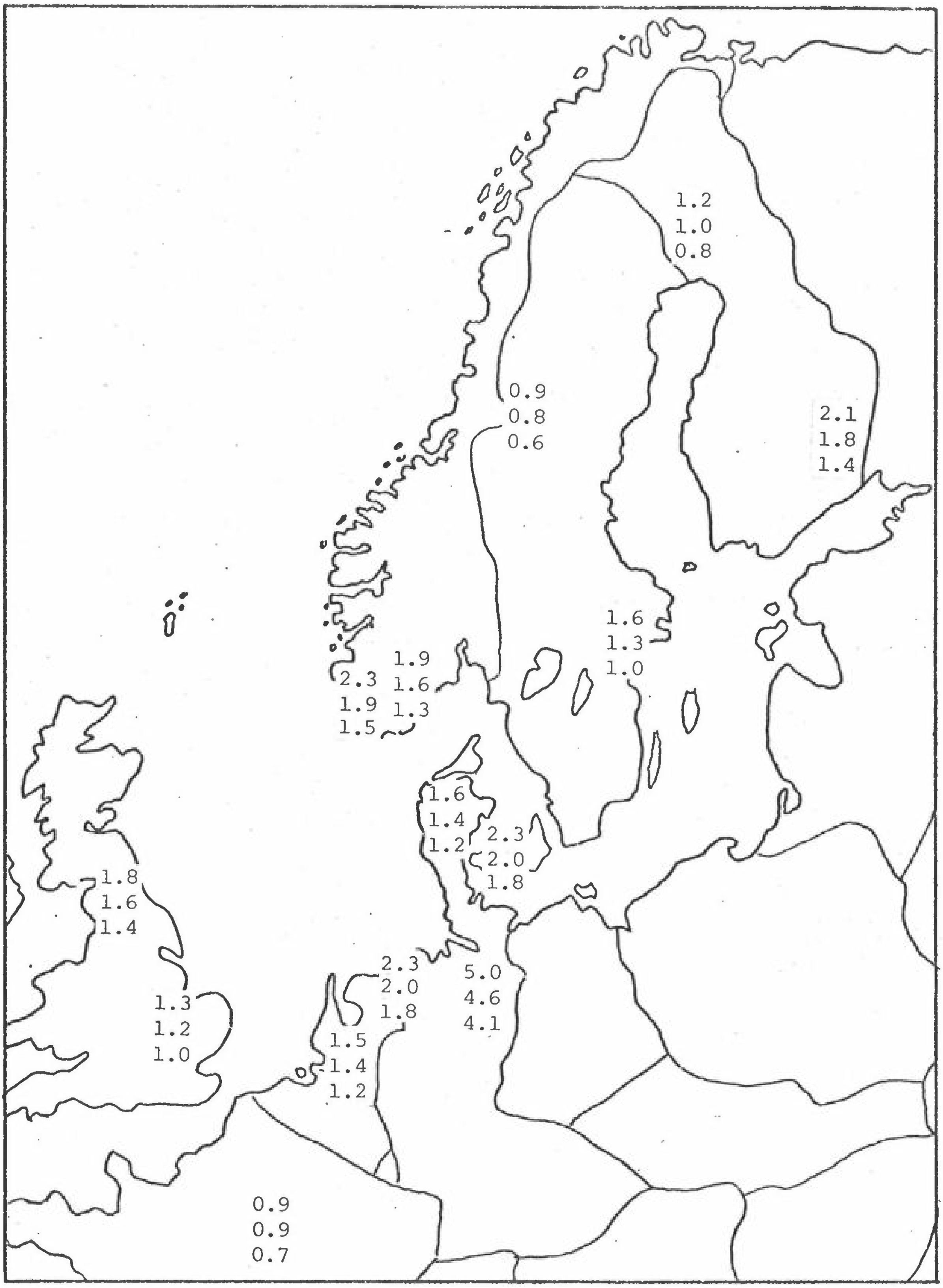

FIG. A13 DEC 73 - MARCH 74

96 HOURS SURFACE BACK TRAJECTORIES

RATIO $\overline{X13}$ / $\overline{X16}$ / $\overline{X19}$ TO $\overline{SO_4}$ ON FILTER

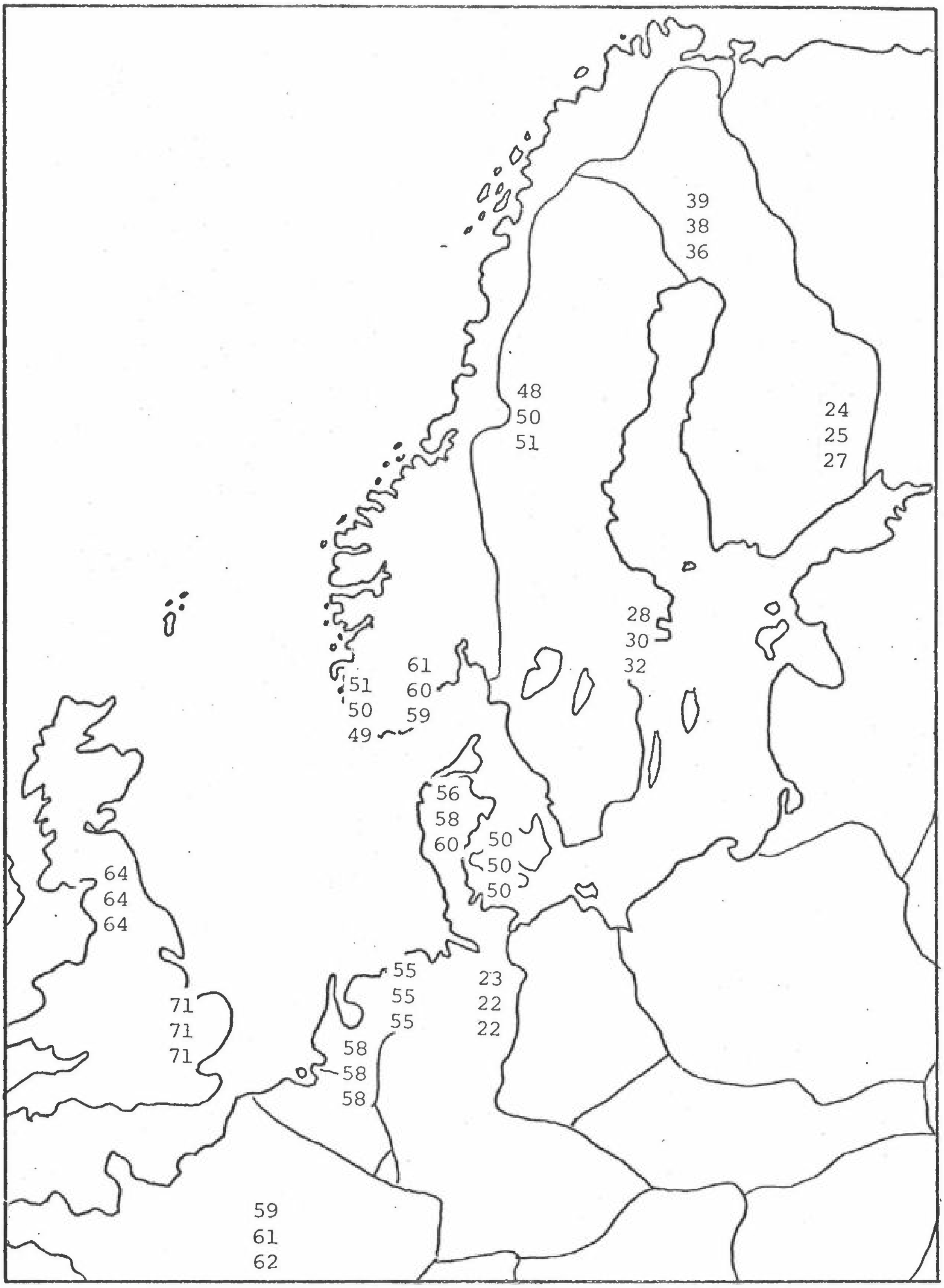

FIG. A14 DEC 73 - MARCH 74

48 HOURS 850 MB BACK TRAJECTORIES

X13

CORRELATIONS OF X16 TO SO_4 ON FILTER

X19

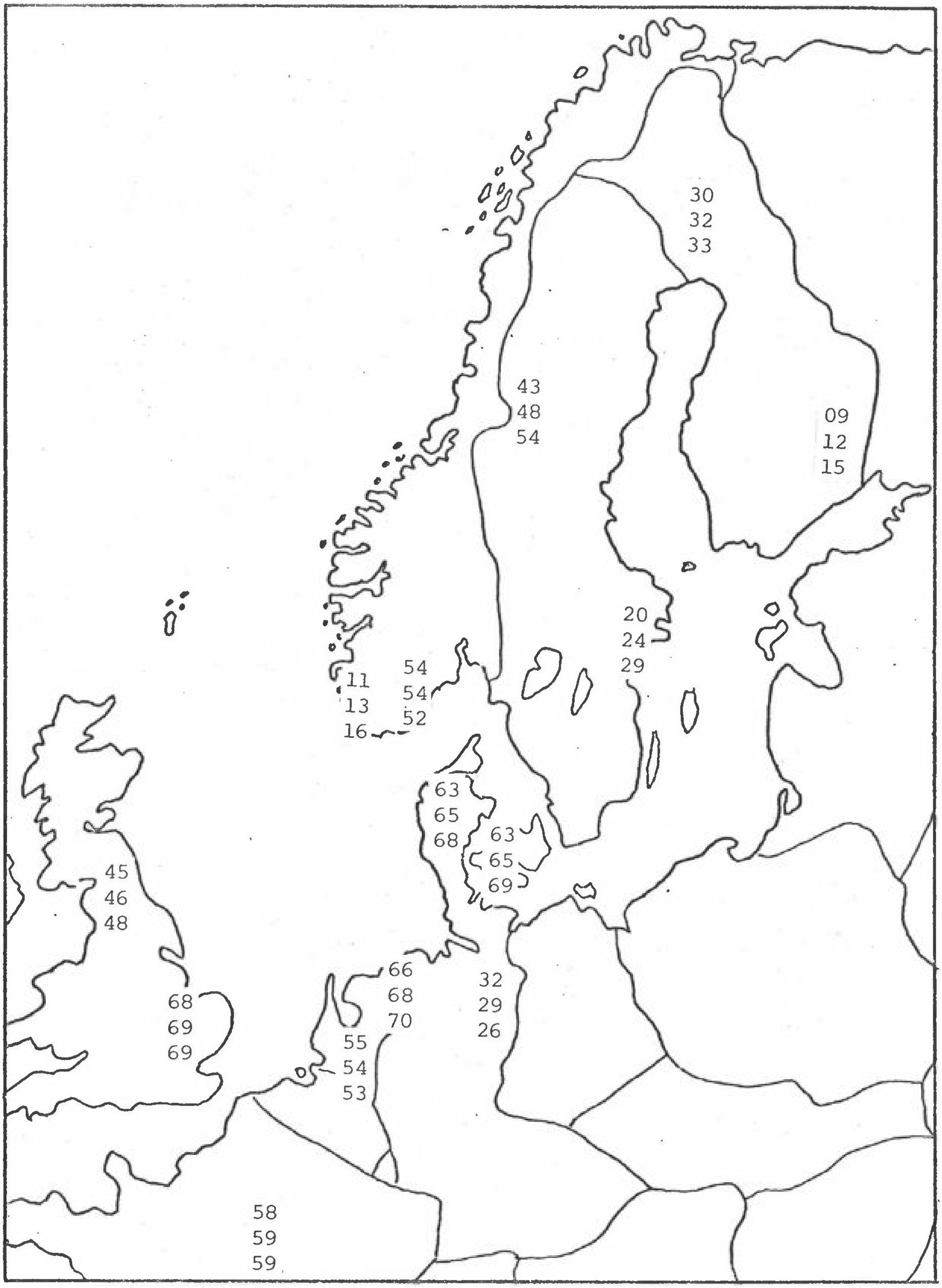

FIG. A15 DEC 73 - MARCH 74

96 HOURS "CLARKE" BACK TRAJECTORIES

X13

CORRELATIONS OF X16 TO SO_4 ON FILTER

X19

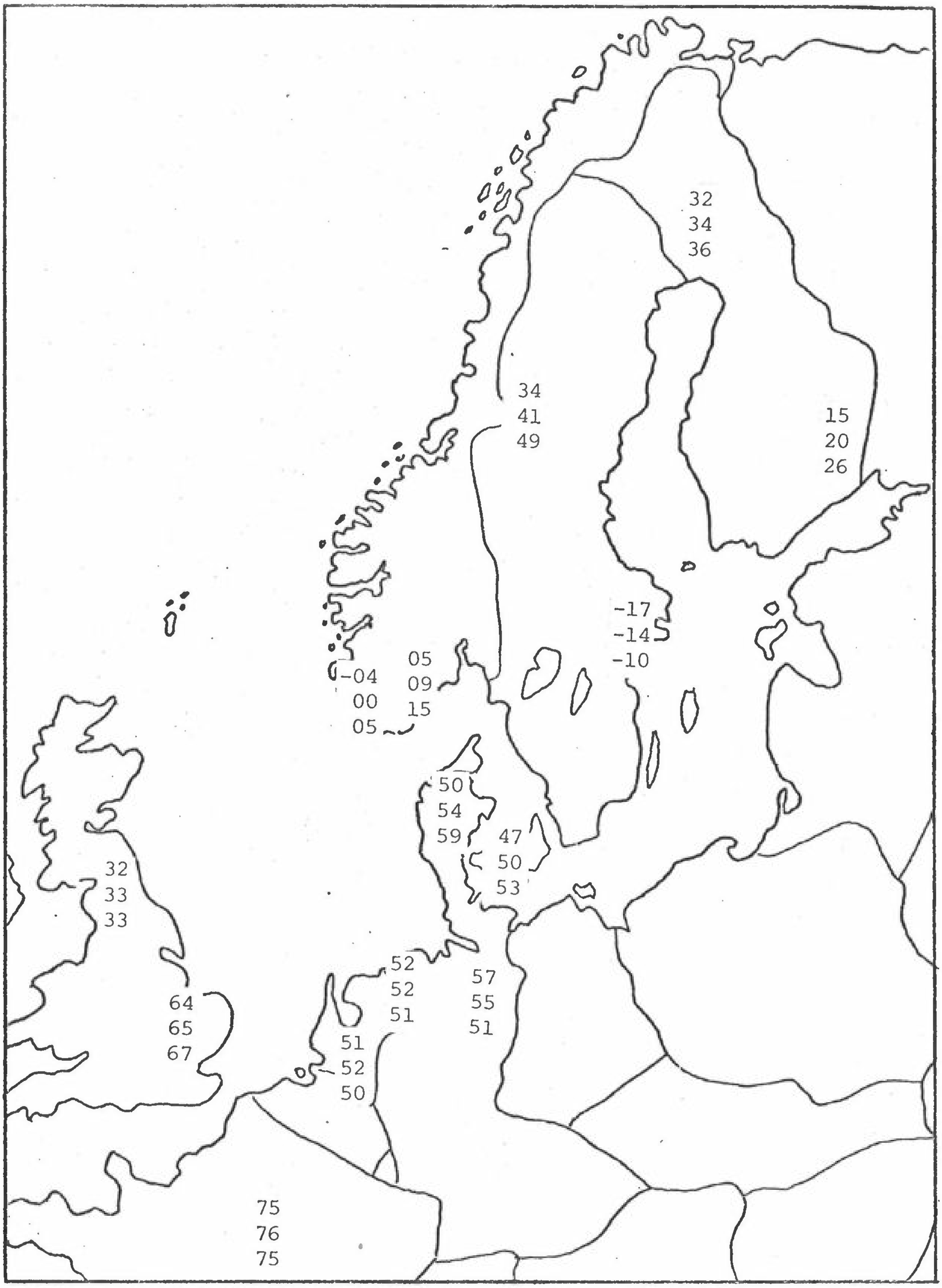

FIG. A16 DEC 73 - MARCH 74

96 HOURS SURFACE BACK TRAJECTORIES

X13

CORRELATION OF X16 TO SO_4 ON FILTER

X19

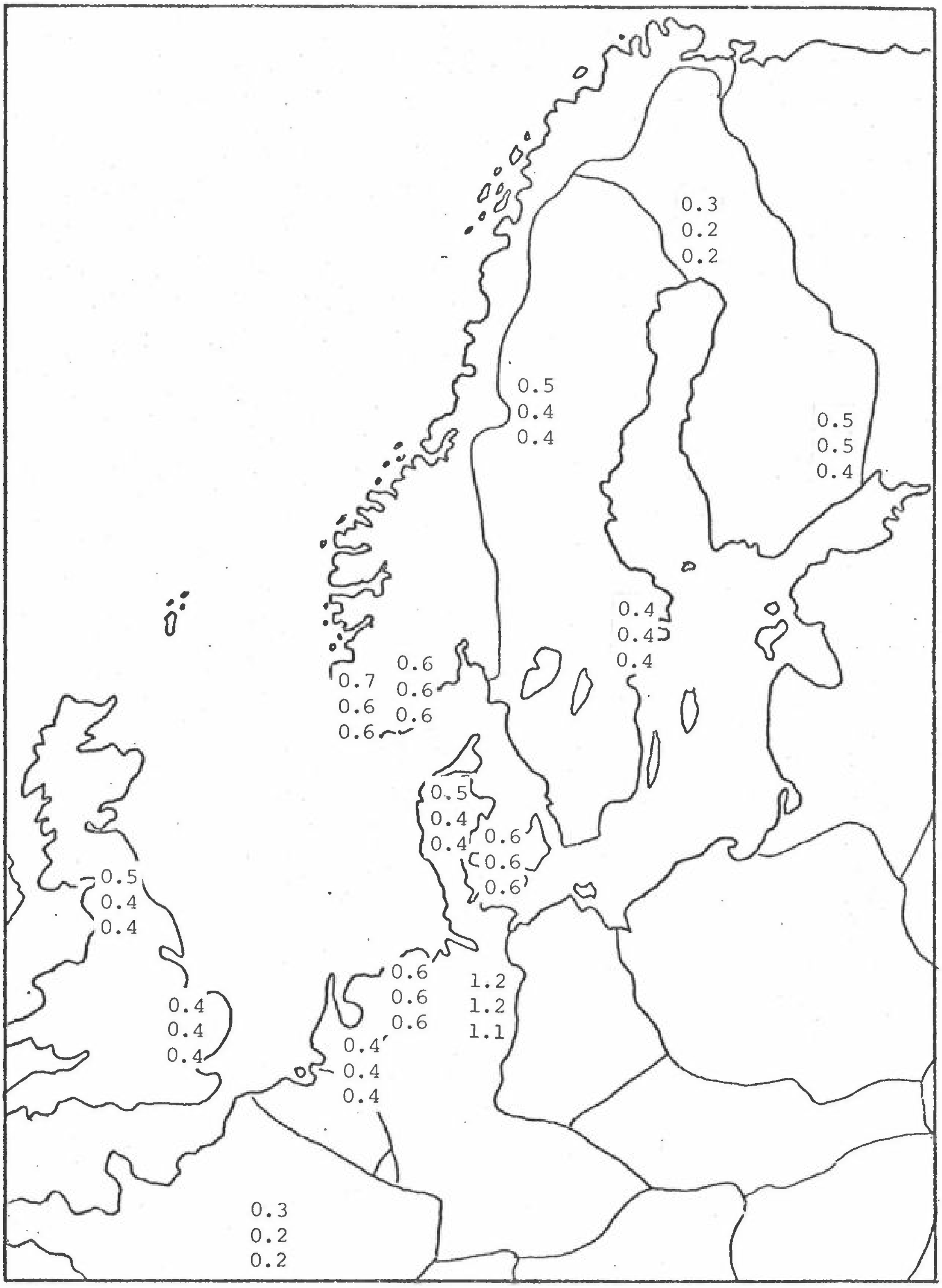

FIG. A17 DEC 73 - MARCH 74

48 HOURS 850 MB BACK TRAJECTORIES

RATIO OF $\overline{X4}$ / $\overline{X7}$ / $\overline{X10}$ TO $\overline{SO_4}$ ON FILTER

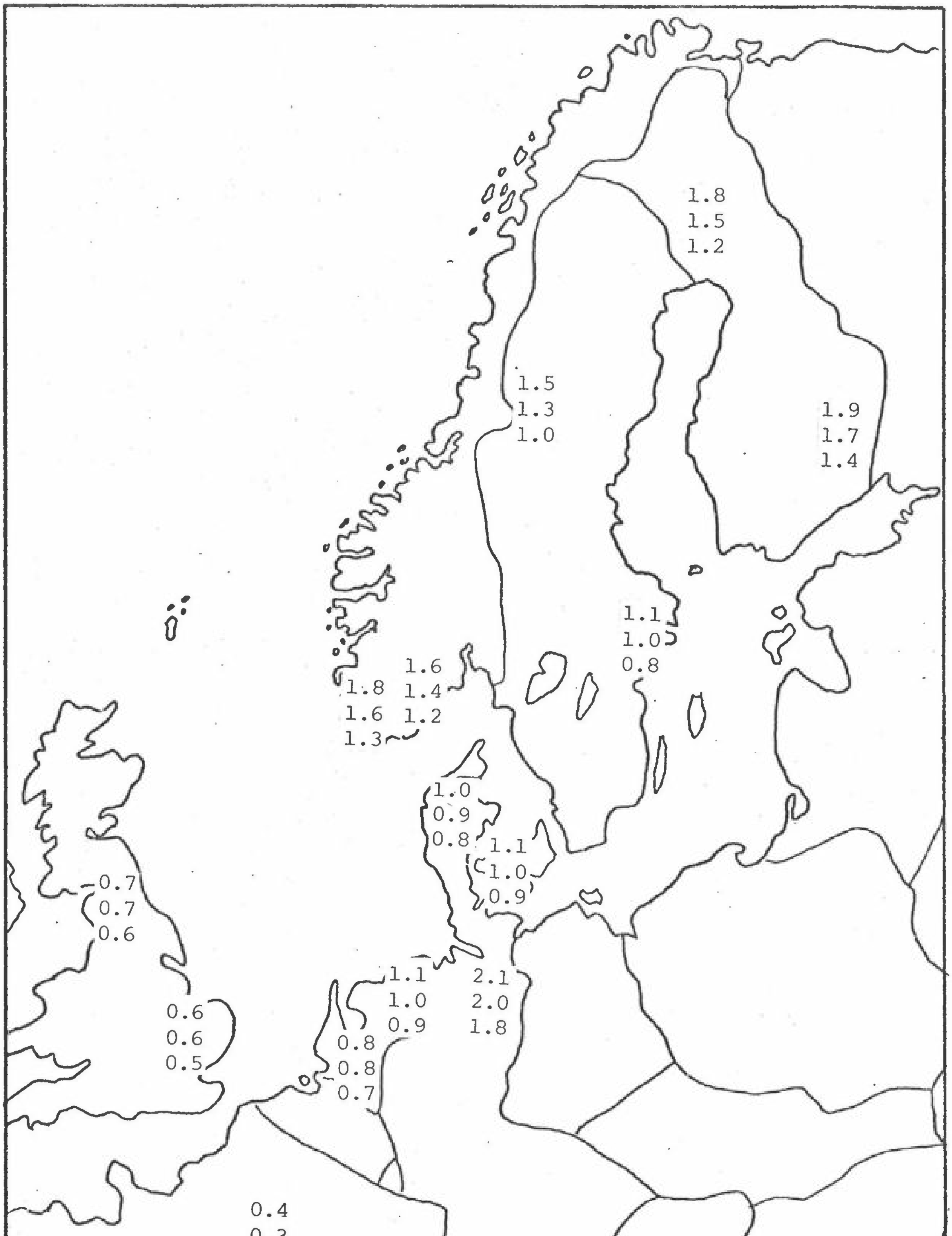

FIG. A18 DEC 73 - MARCH 74

96 HOURS "CLARKE" BACK TRAJECTORIES

RATIO OF $\overline{X4}$ / $\overline{X7}$ / $\overline{X10}$ TO $\overline{SO_4}$ ON FILTER

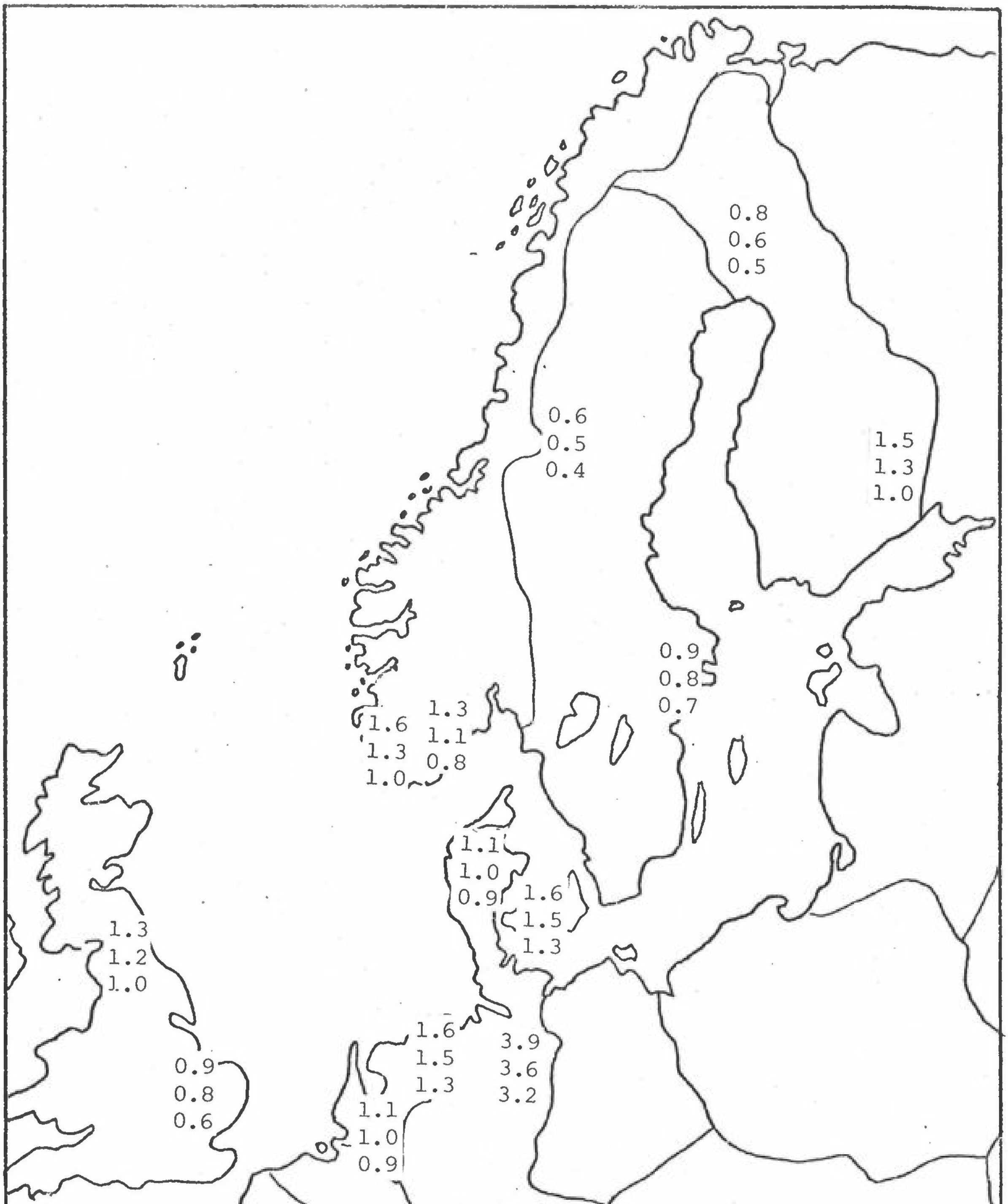

FIG. A19 DEC 73 - MARCH 74

96 HOURS SURFACE BACK TRAJECTORIES

RATIO OF $\overline{X4}$, $\overline{X7}$, $\overline{X10}$ TO $\overline{SO_4}$ ON FILTER

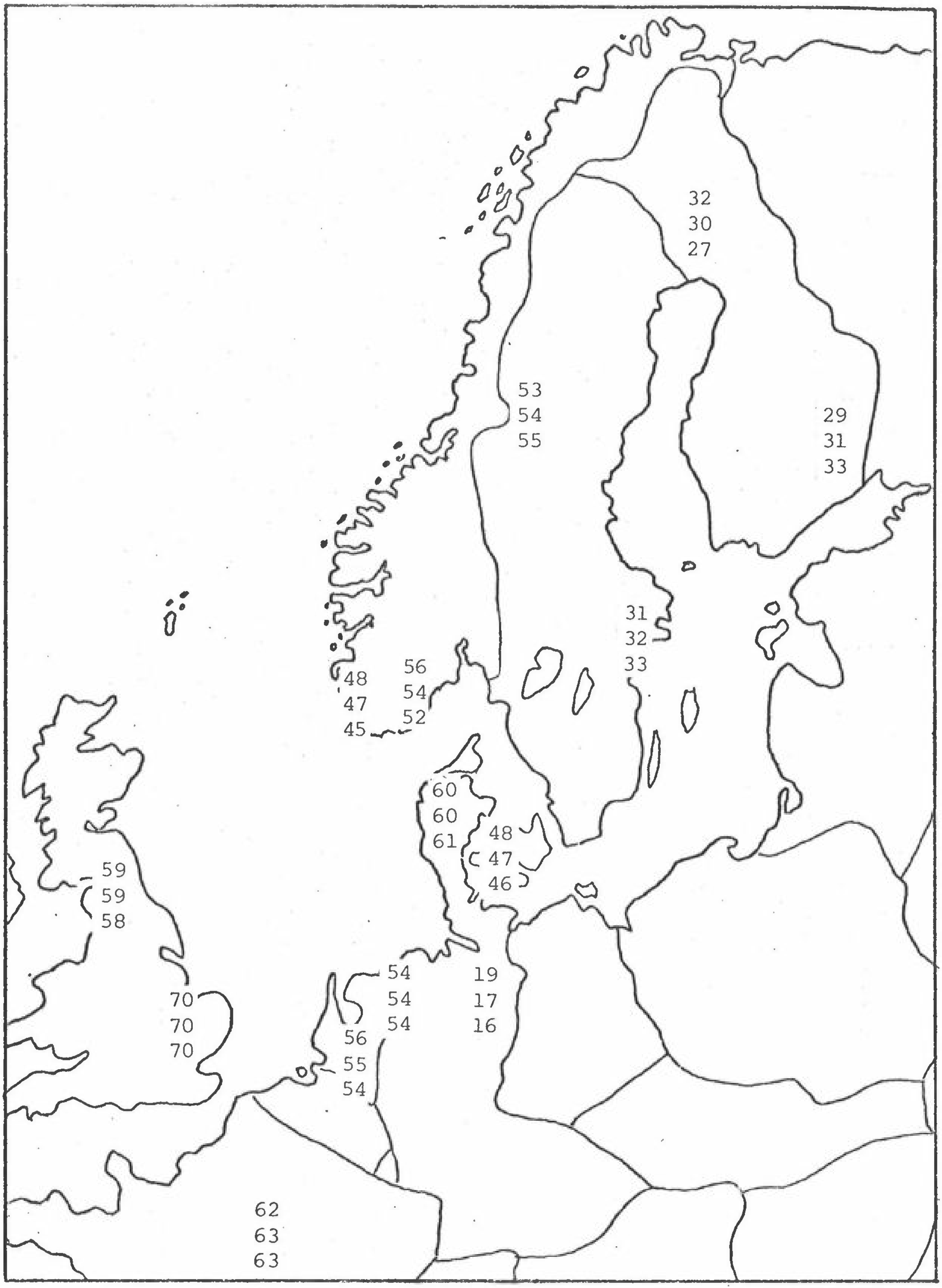

FIG. A20 DEC 73 - MARCH 74

48 HOURS 850 MB BACK TRAJECTORIES

X4

CORRELATION OF X7 TO SO_4 ON FILTER

X10

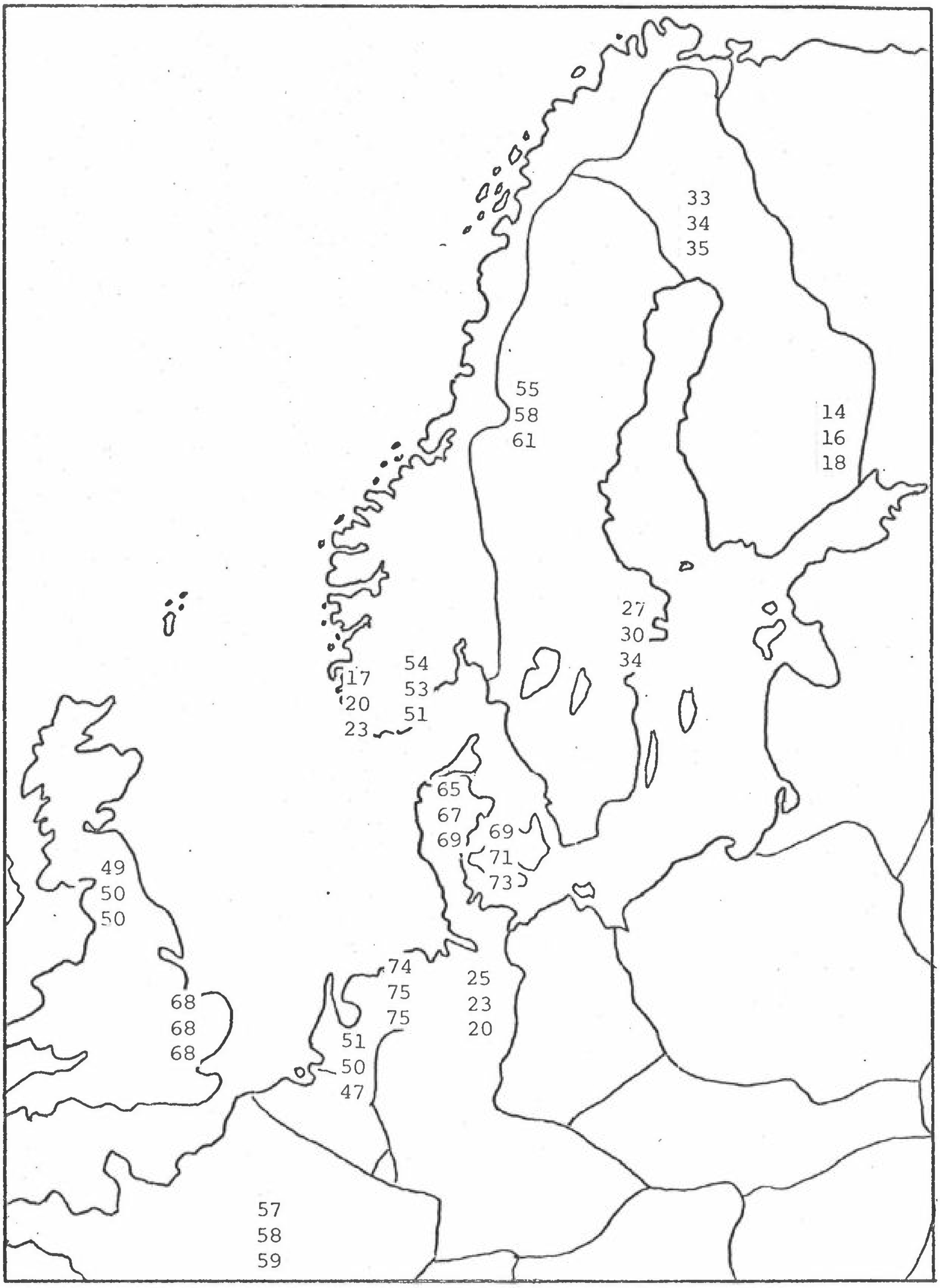

FIG. A21 DEC 73 - MARCH 74

96 HOURS "CLARKE" BACK TRAJECTORIES

X4

CORRELATION OF X7 TO SO_4 ON FILTER

X10

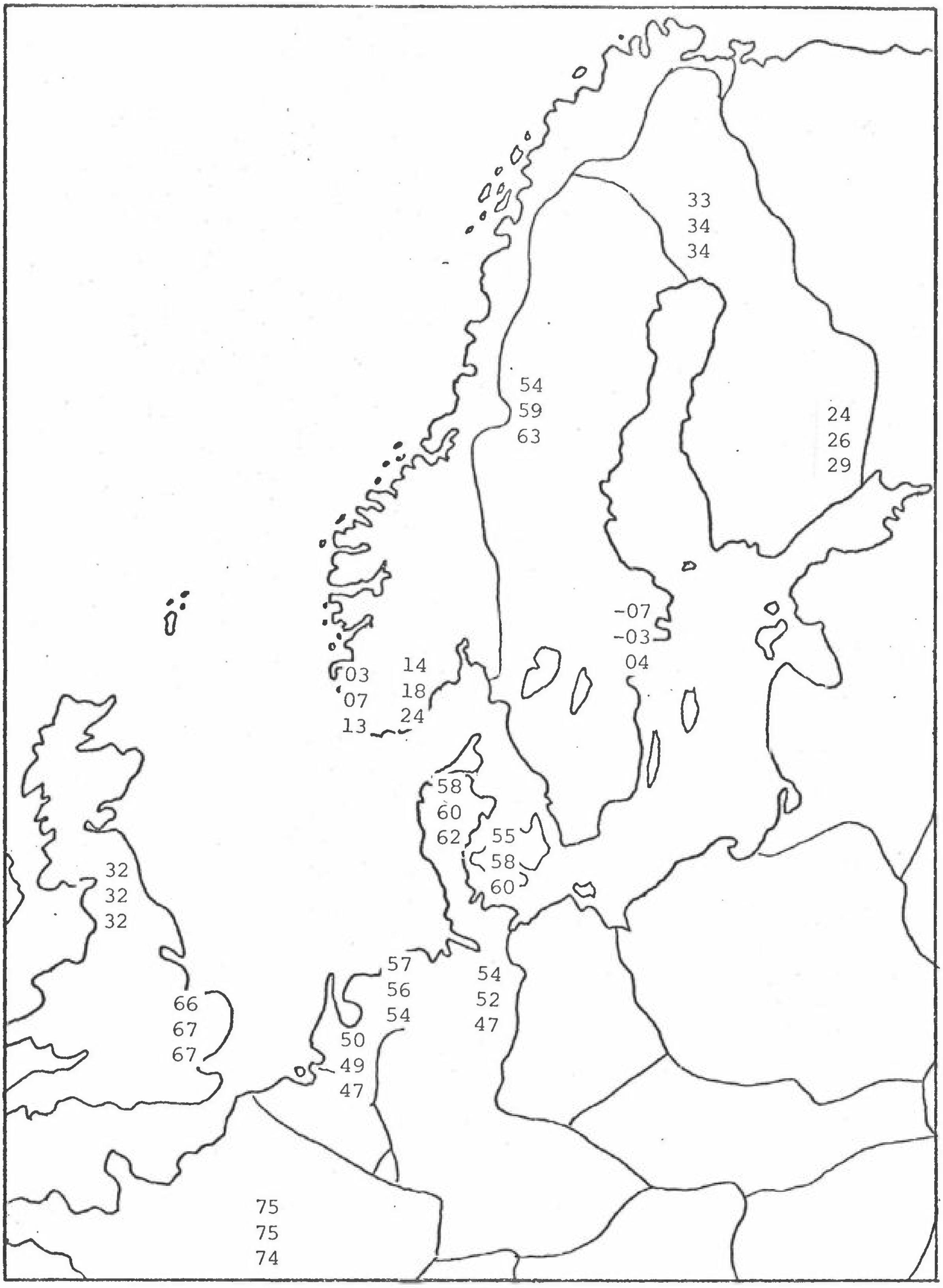

FIG. A22 DEC 73 - MARCH 74

96 HOURS SURFACE BACK TRAJECTORIES

X4
CORRELATION OF X7 TO SO_4 ON FILTER
X10

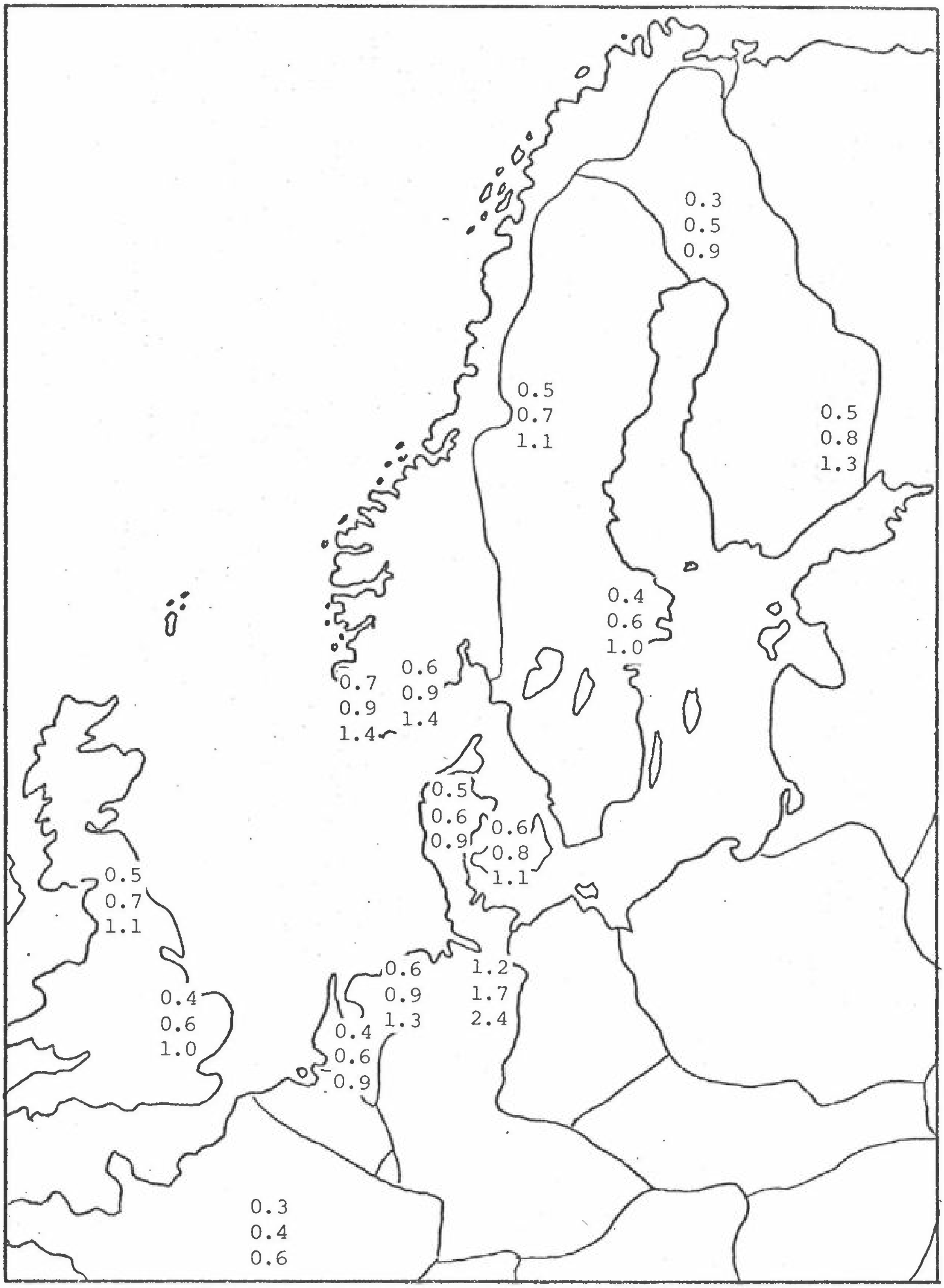

FIG. A23 DEC 73 - MARCH 74

48 HOURS 850 MB BACK TRAJECTORIES

RATIO OF $\overline{X4}$ / $\overline{X5}$ / $\overline{X6}$ TO $\overline{SO}_4$ ON FILTER

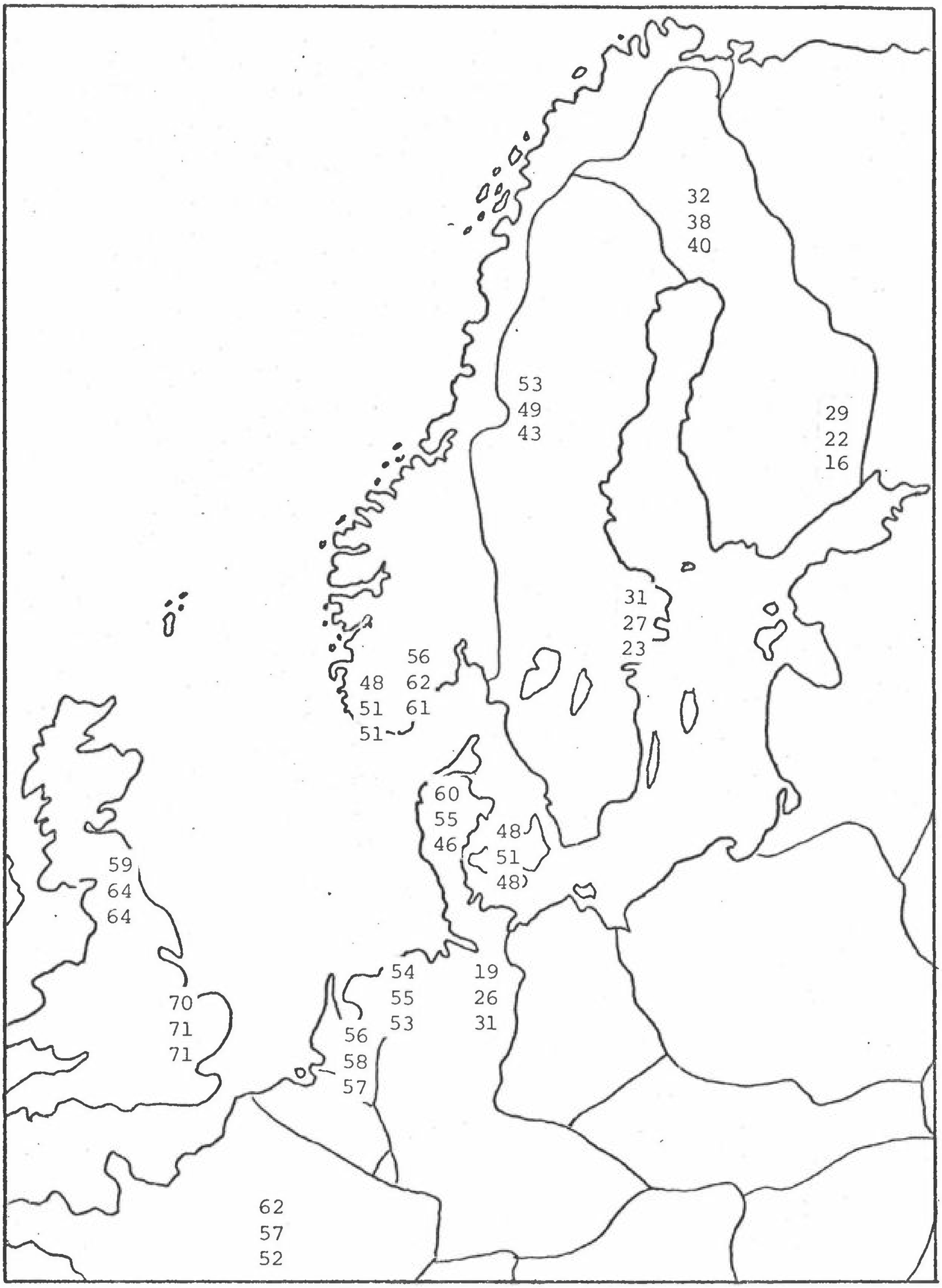

FIG. A24 DEC 73 - MARCH 74

48 HOURS 850 MB BACK TRAJECTORIES

X4

CORRELATION OF X5 TO SO_4 ON FILTER

X6

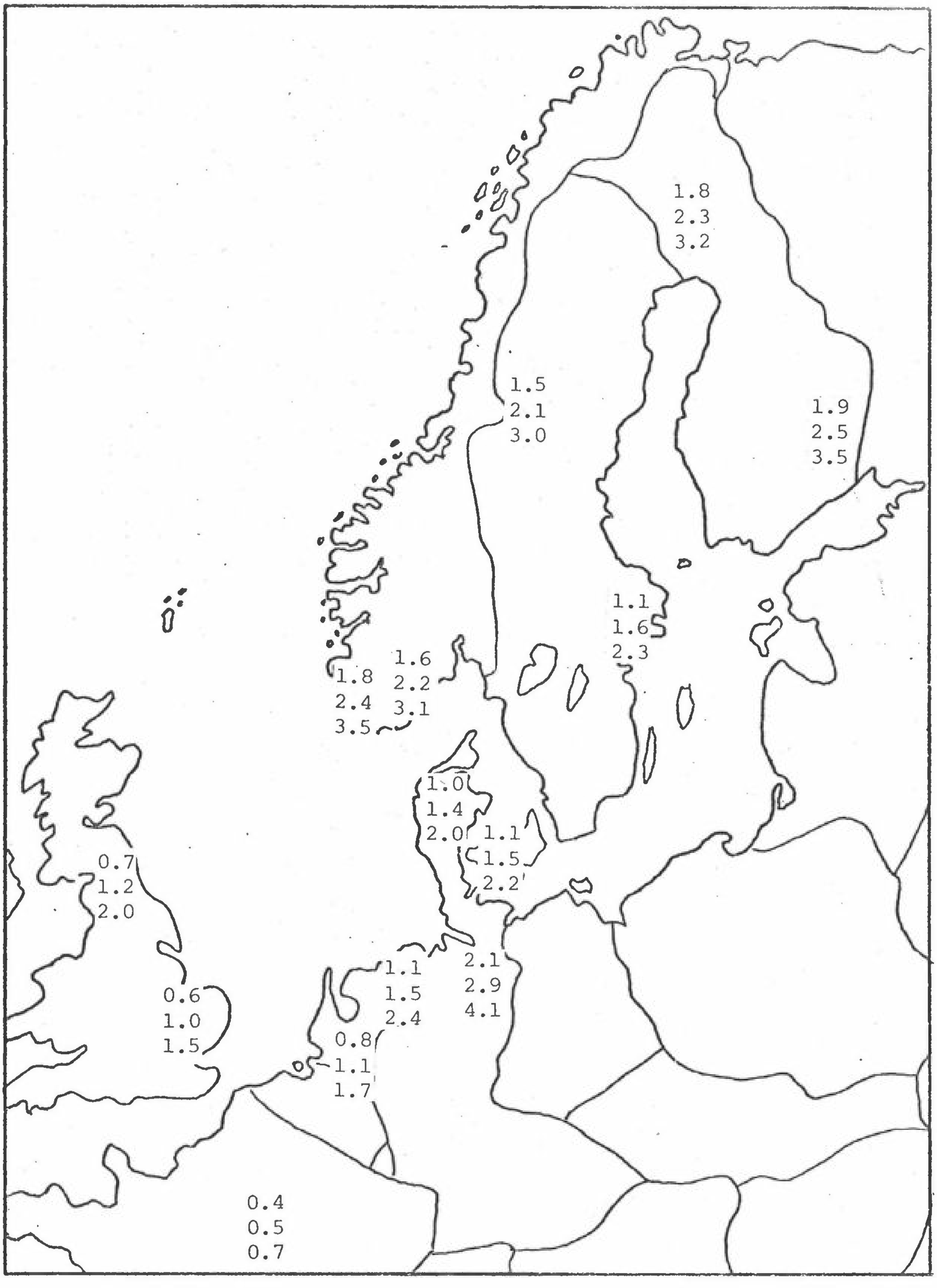

FIG. A25 DEC 73 - MARCH 74

96 HOURS "CLARKE" BACK TRAJECTORIES

RATIO OF $\overline{X4}$ / $\overline{X5}$ / $\overline{X6}$ TO $\overline{SO_4}$ ON FILTER

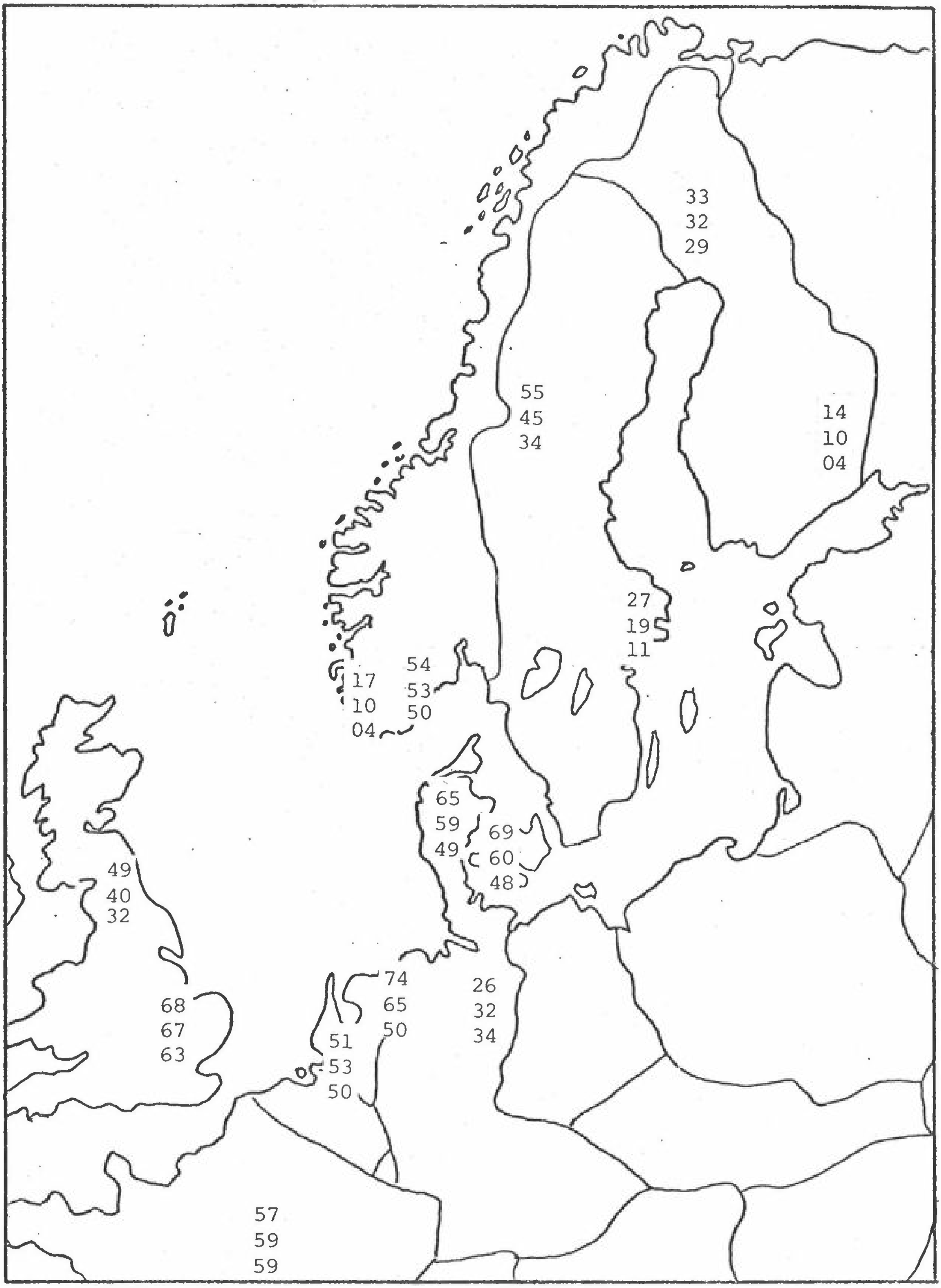

FIG. A26 DEC 73 - MARCH 74

96 HOURS "CLARKE" BACK TRAJECTORIES

X4

CORRELATION OF X5 TO SO_4 ON FILTER

X6

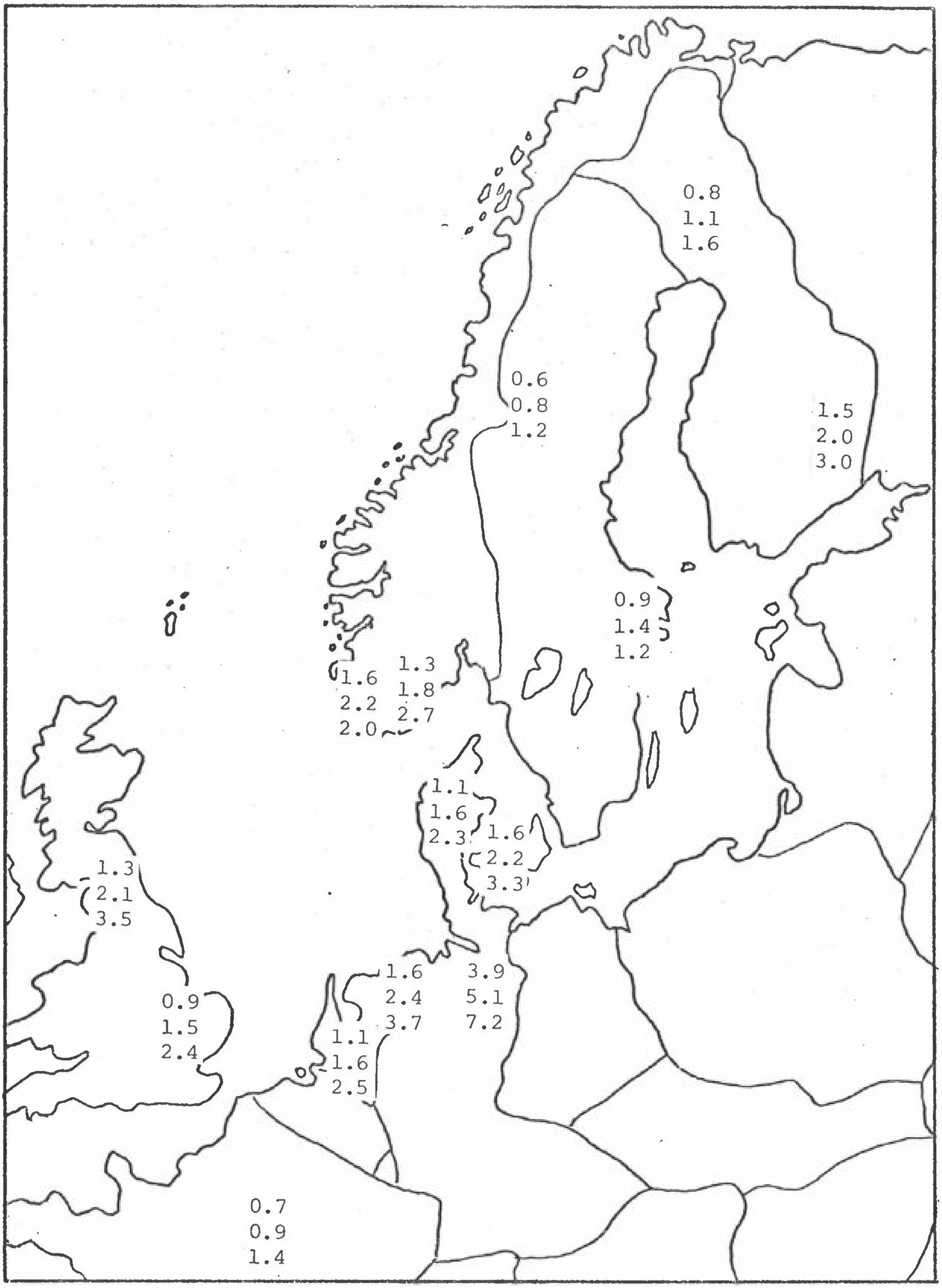

FIG. A27 DEC 73 - MARCH 74

96 HOURS SURFACE BACK TRAJECTORIES

RATIO OF $\overline{X4}$, $\overline{X5}$, $\overline{X6}$ TO $\overline{SO_4}$ ON FILTER

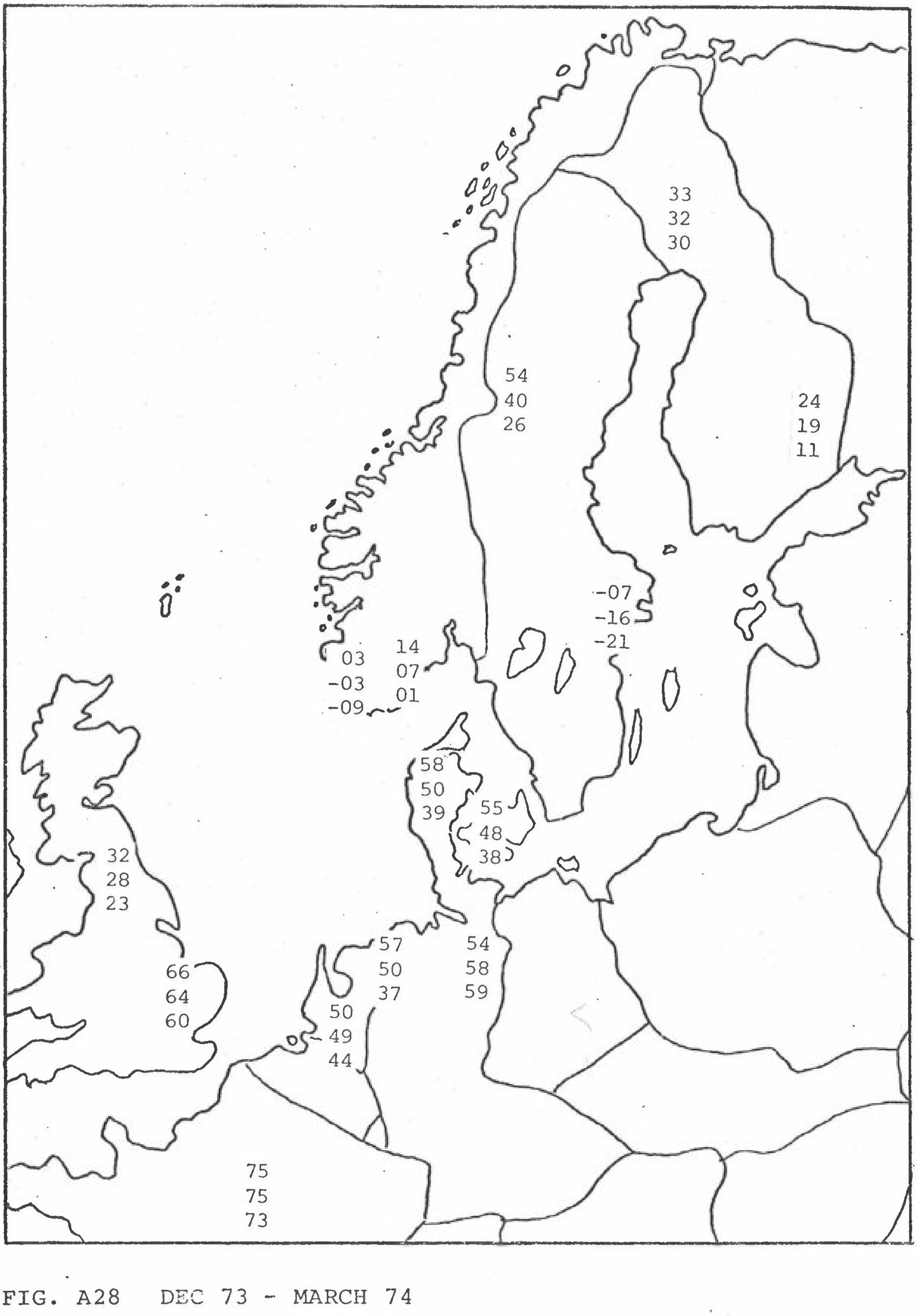

FIG. A28 DEC 73 - MARCH 74

96 HOURS SURFACE BACK TRAJECTORIES

X4

CORRELATION OF X5 TO SO_4 ON FILTER

X6

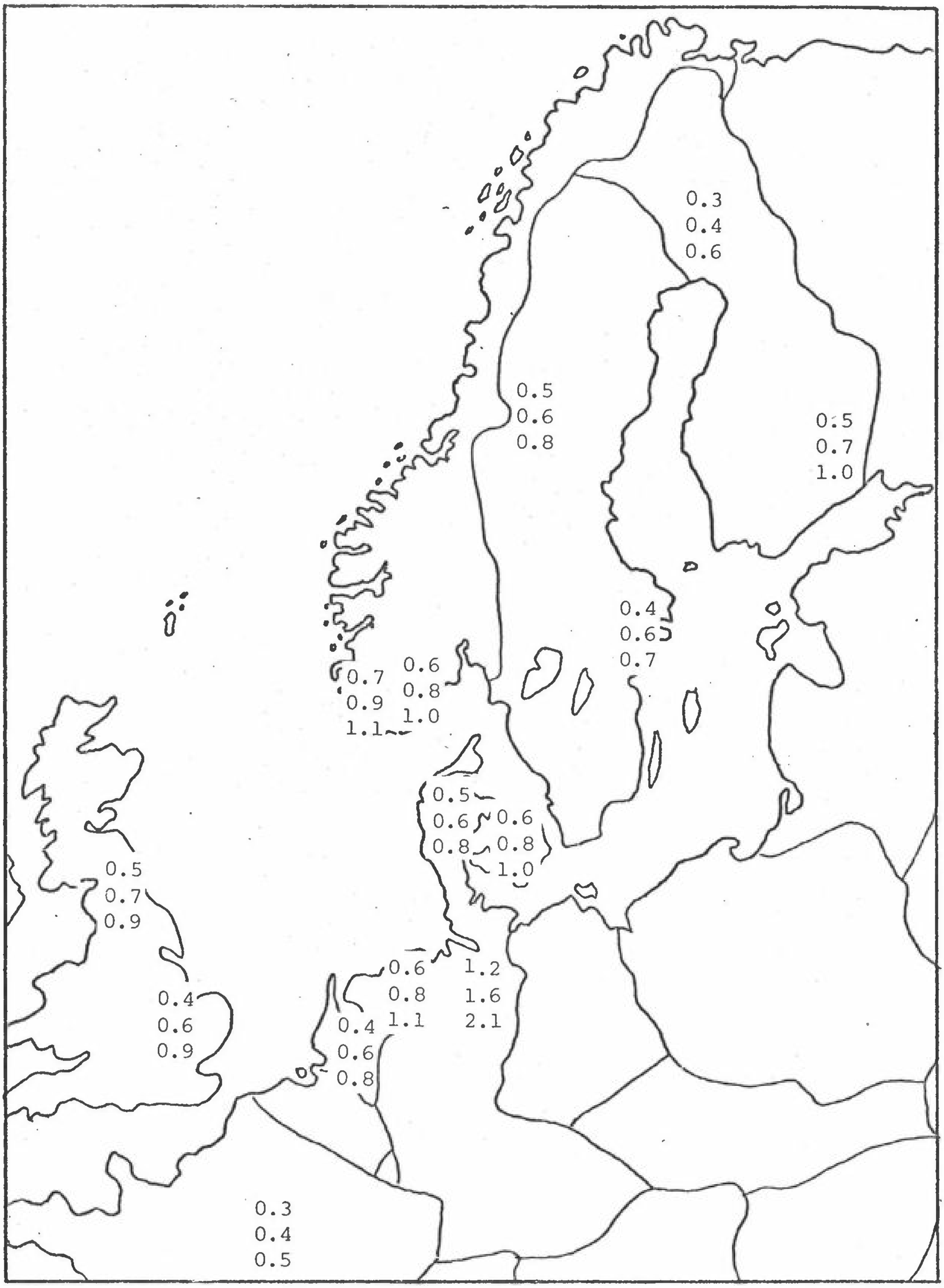

Fig. A29 DEC 73 - MARCH 74

48 HOURS 850 MB BACK TRAJECTORIES

RATIO OF $\overline{X4}$ / $\overline{X8}$ / $\overline{X12}$ TO $\overline{SO}_4$ ON FILTER

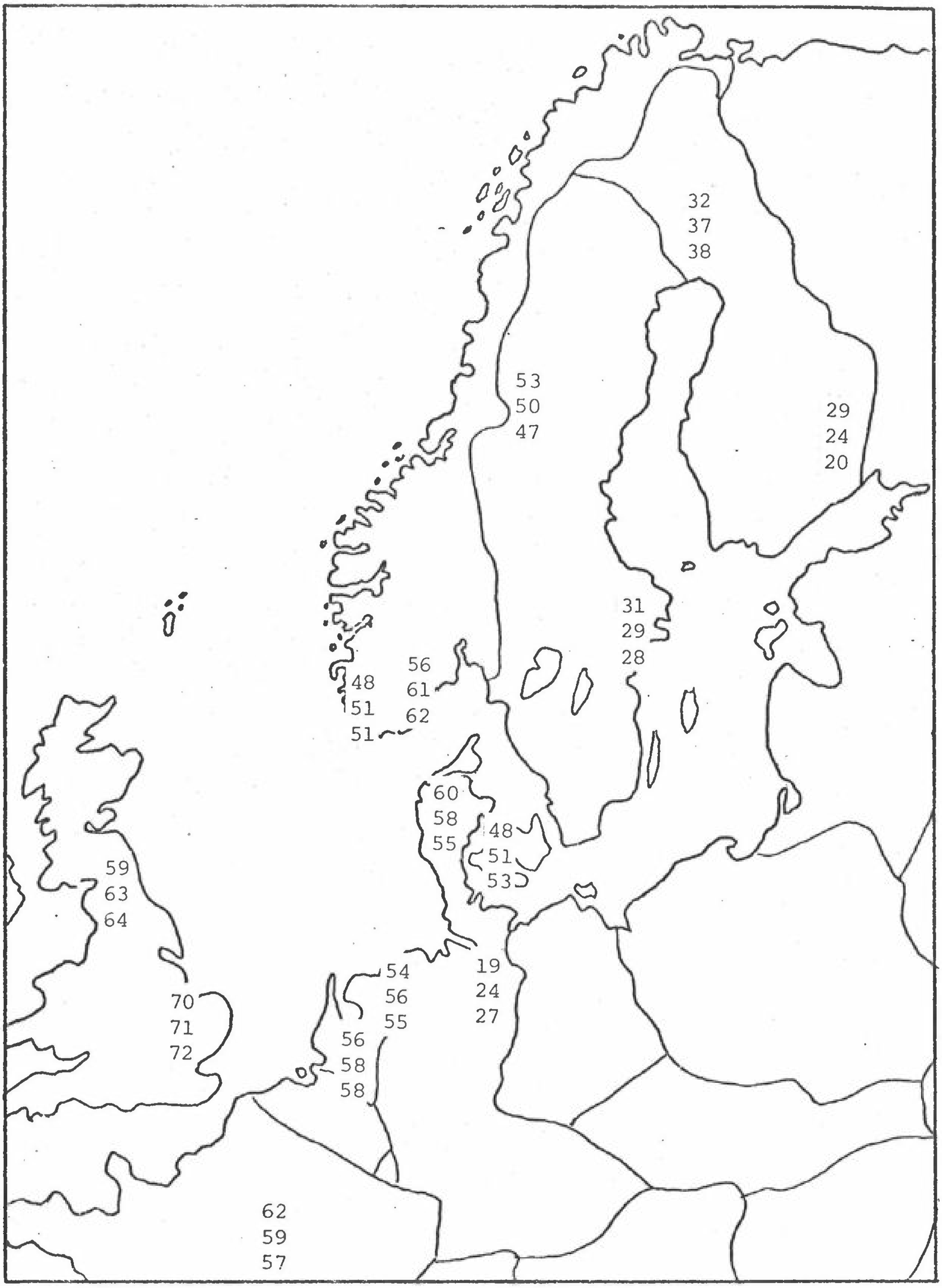

FIG. A30 DEC 73 - MARCH 74
48 HOURS 850 MB BACK TRAJECTORIES
X4
CORRELATION OF X8 TO SO_4 ON FILTER
X12

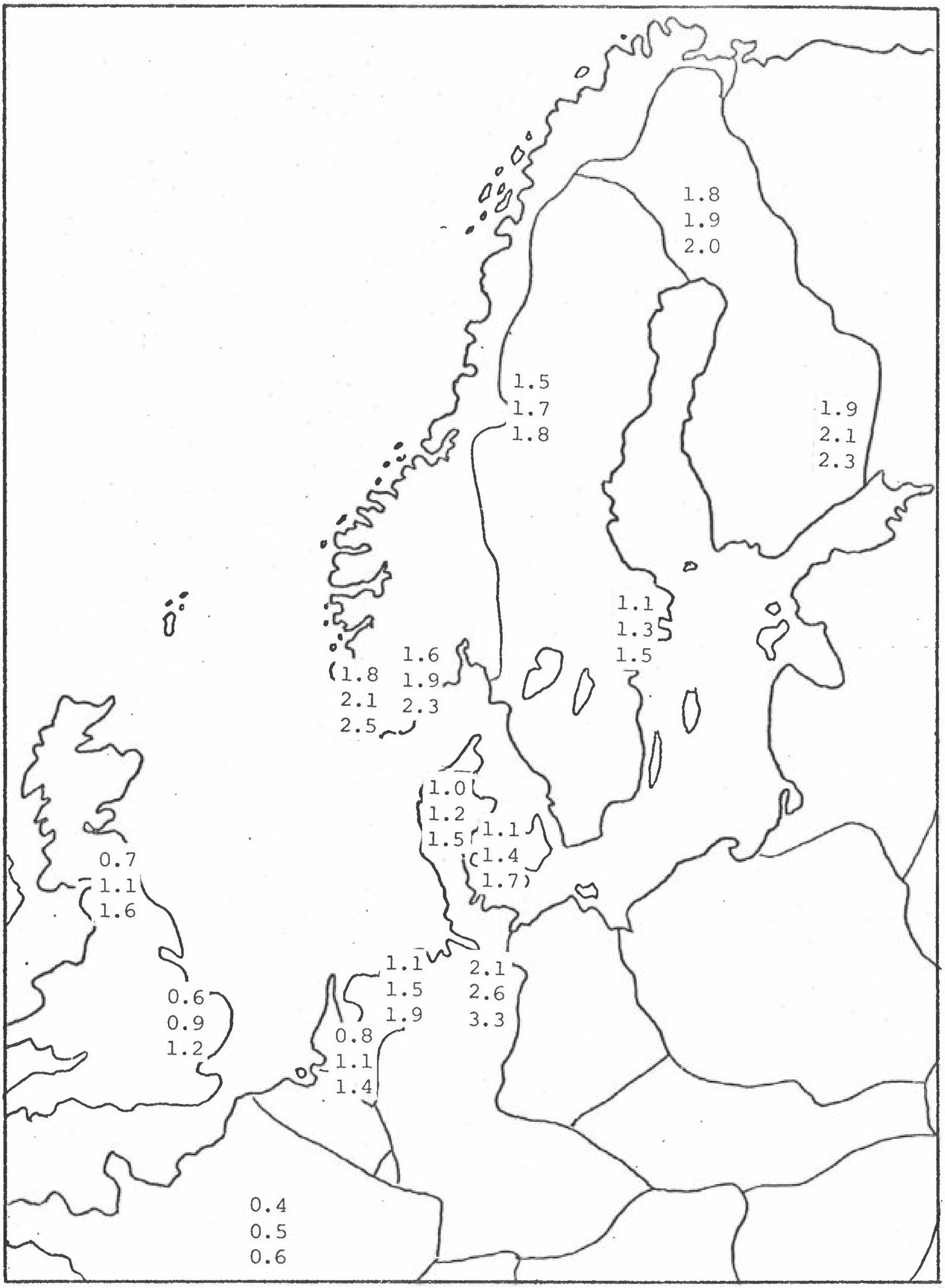

FIG. A31 DEC 73 - March 74

96 HOURS "CLARKE" BACK TRAJECTORIES

RATIO OF $\overline{X4}$, $\overline{X8}$, $\overline{X12}$ TO $\overline{SO_4}$ ON FILTER

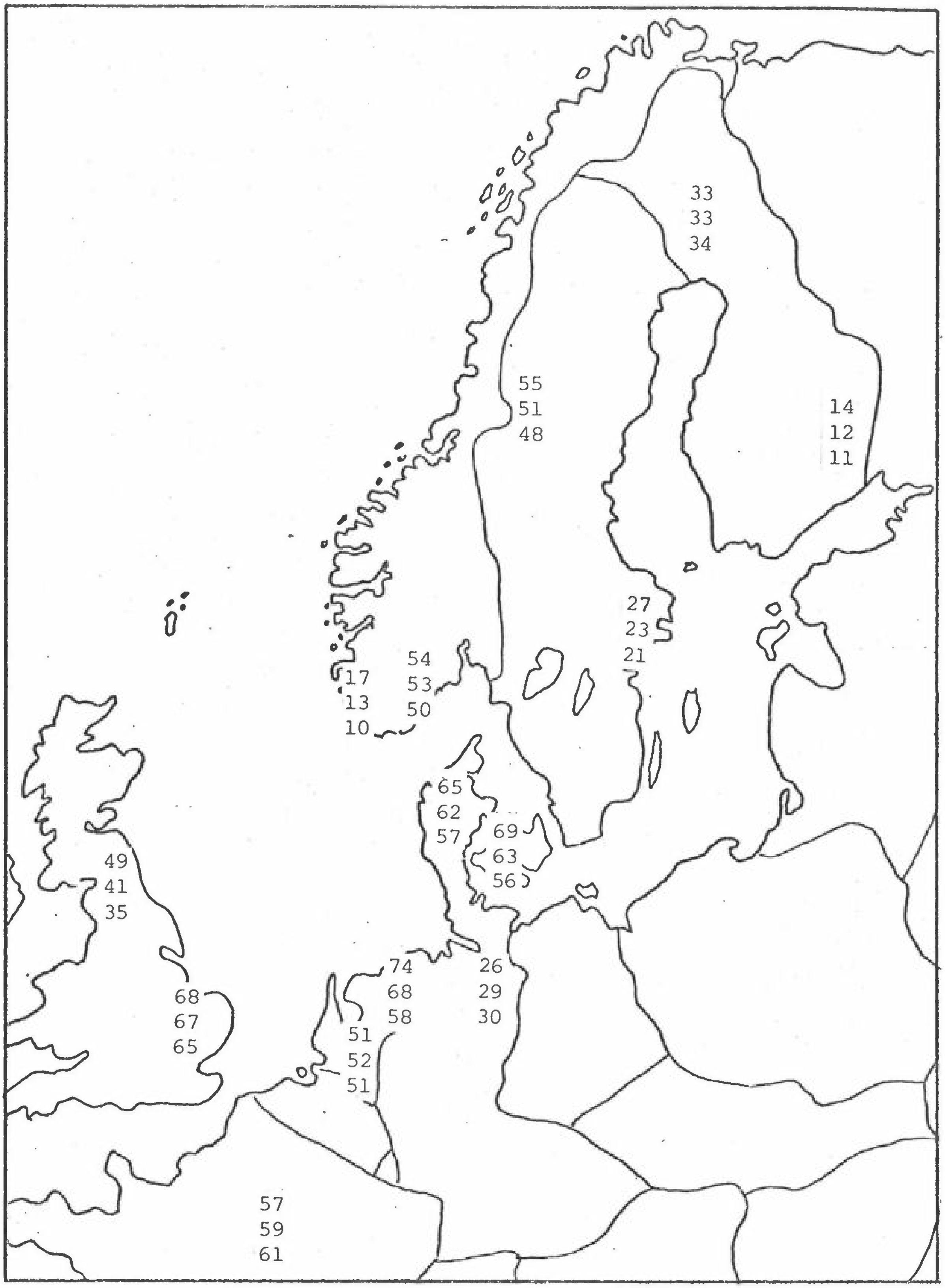

FIG. A32 DEC 73 - MARCH 74
96 HOURS "CLARKE" BACK TRAJECTORIES
X4
CORRELATION OF X8 TO SO_4 ON FILTER
X12

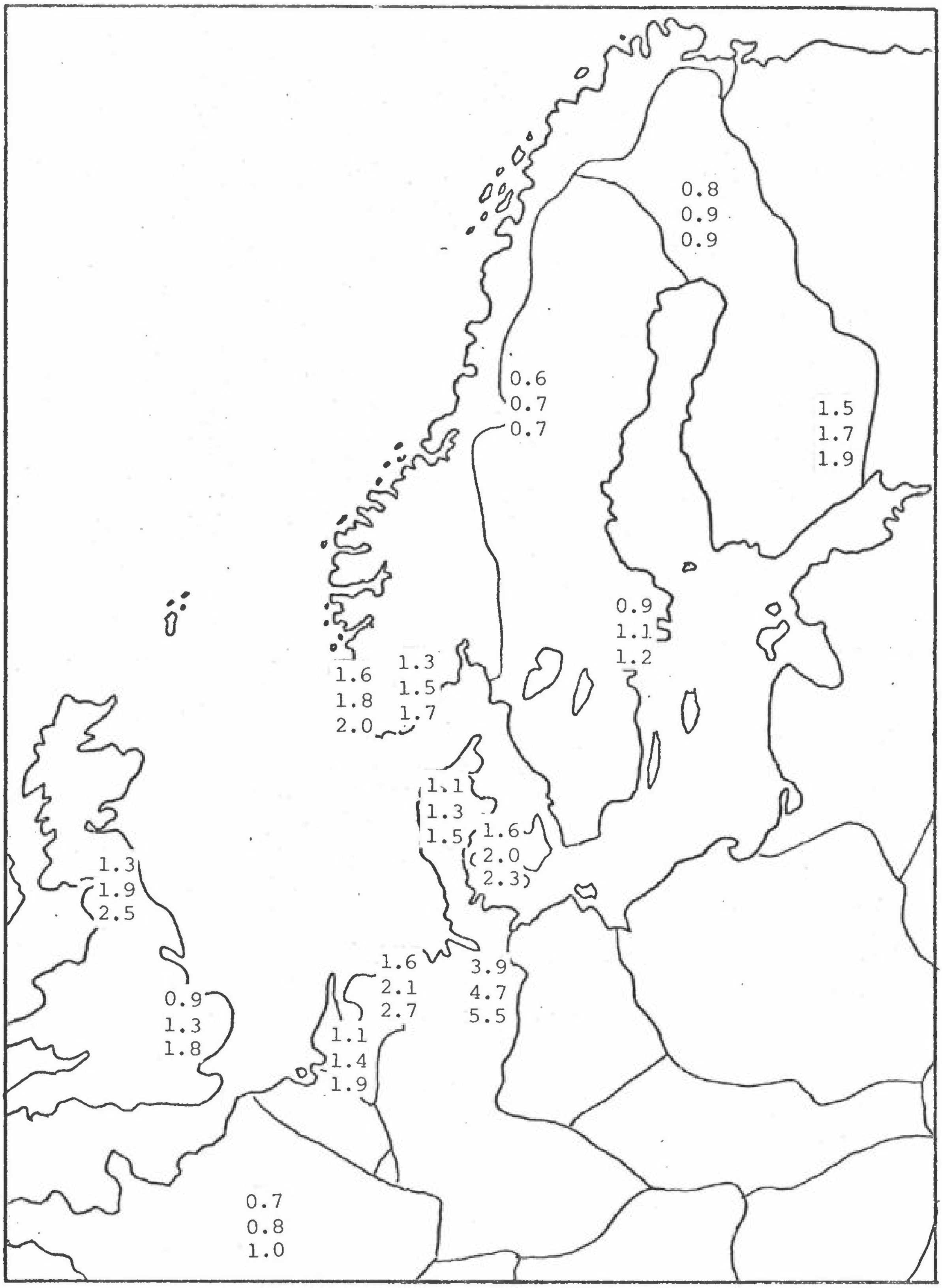

FIG. A33 DEC 73 - MARCH 74

96 HOURS SURFACE BACK TRAJECTORIES

RATIO OF $\overline{X4}$ / $\overline{X8}$ / $\overline{X12}$ TO SO_4 ON FILTER

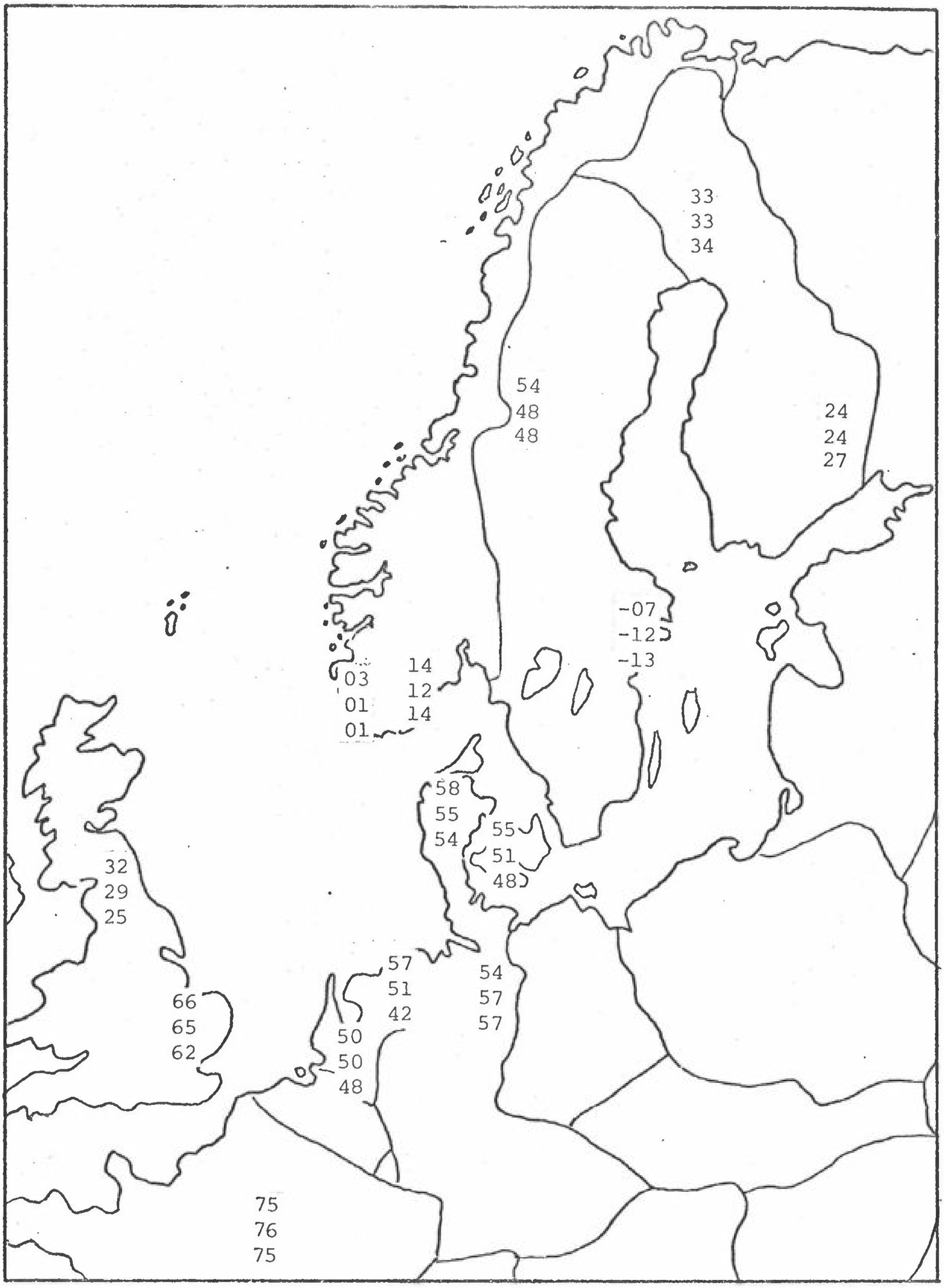

FIG. A34 DEC 73 - March 74

96 HOURS SURFACE BACK TRAJECTORIES

X4

CORRELATION OF X8 TO SO_4 ON FILTER

X12

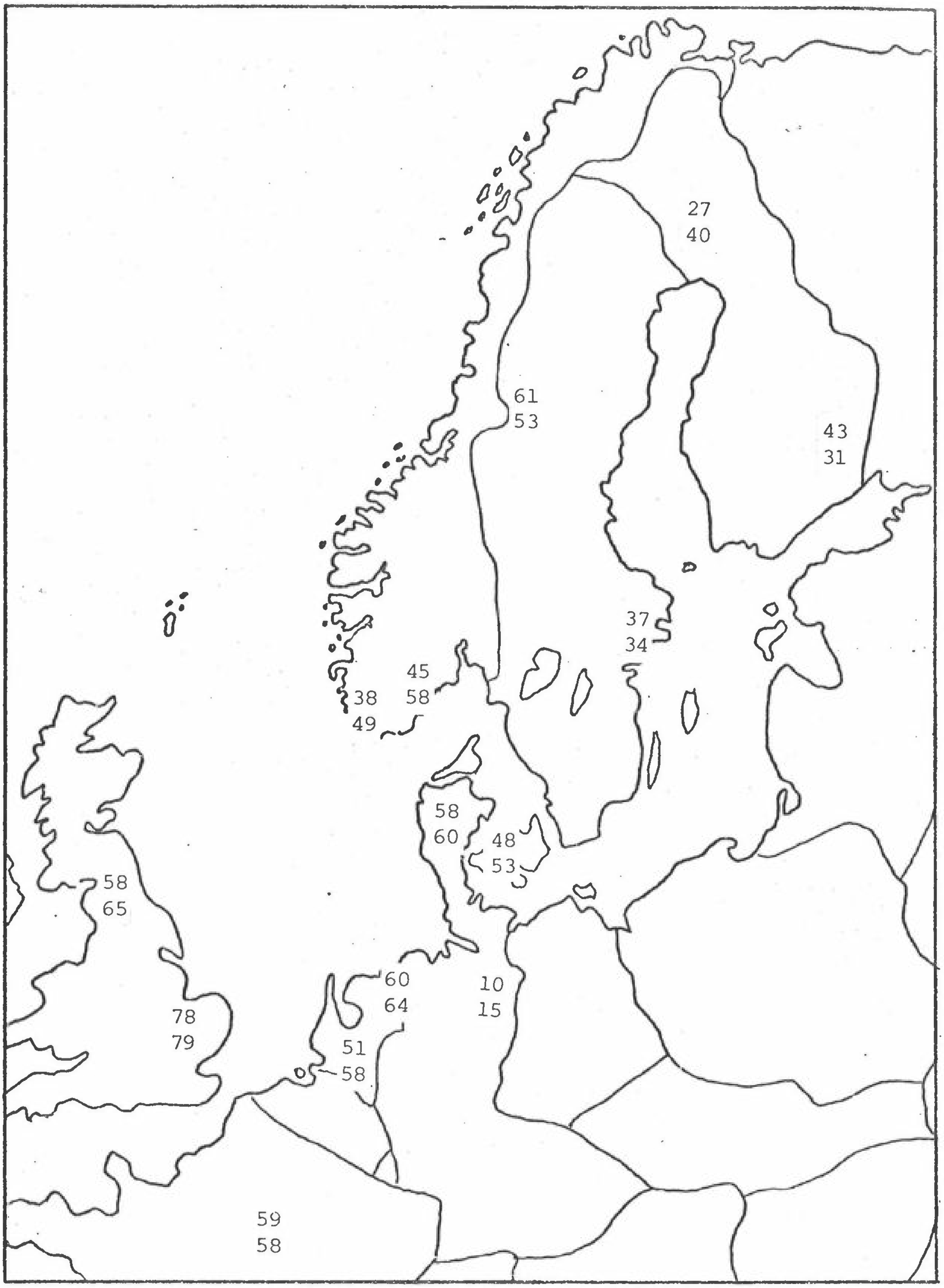

FIG. A35 DEC 73 - MARCH 74

48 HOURS 850 MB BACK TRAJECTORIES

CORRELATION OF X1 / X2 TO SO_4 ON FILTER

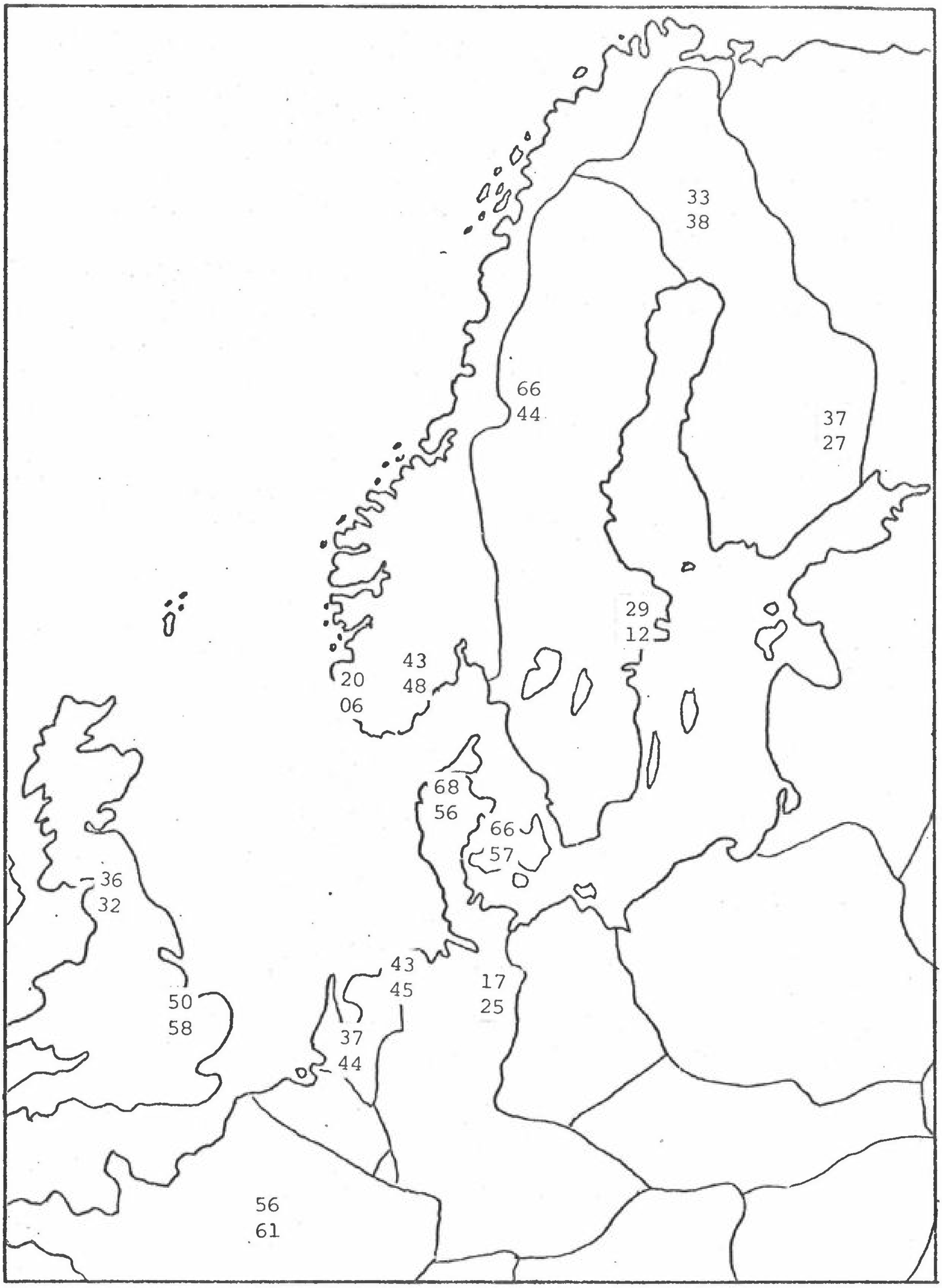

FIG. A 36 DEC 73 - MARCH 74
96 HOURS "CLARKE" BACK TRAJECTORIES

CORRELATION OF $\frac{X1}{X2}$ TO SO_4 ON FILTER

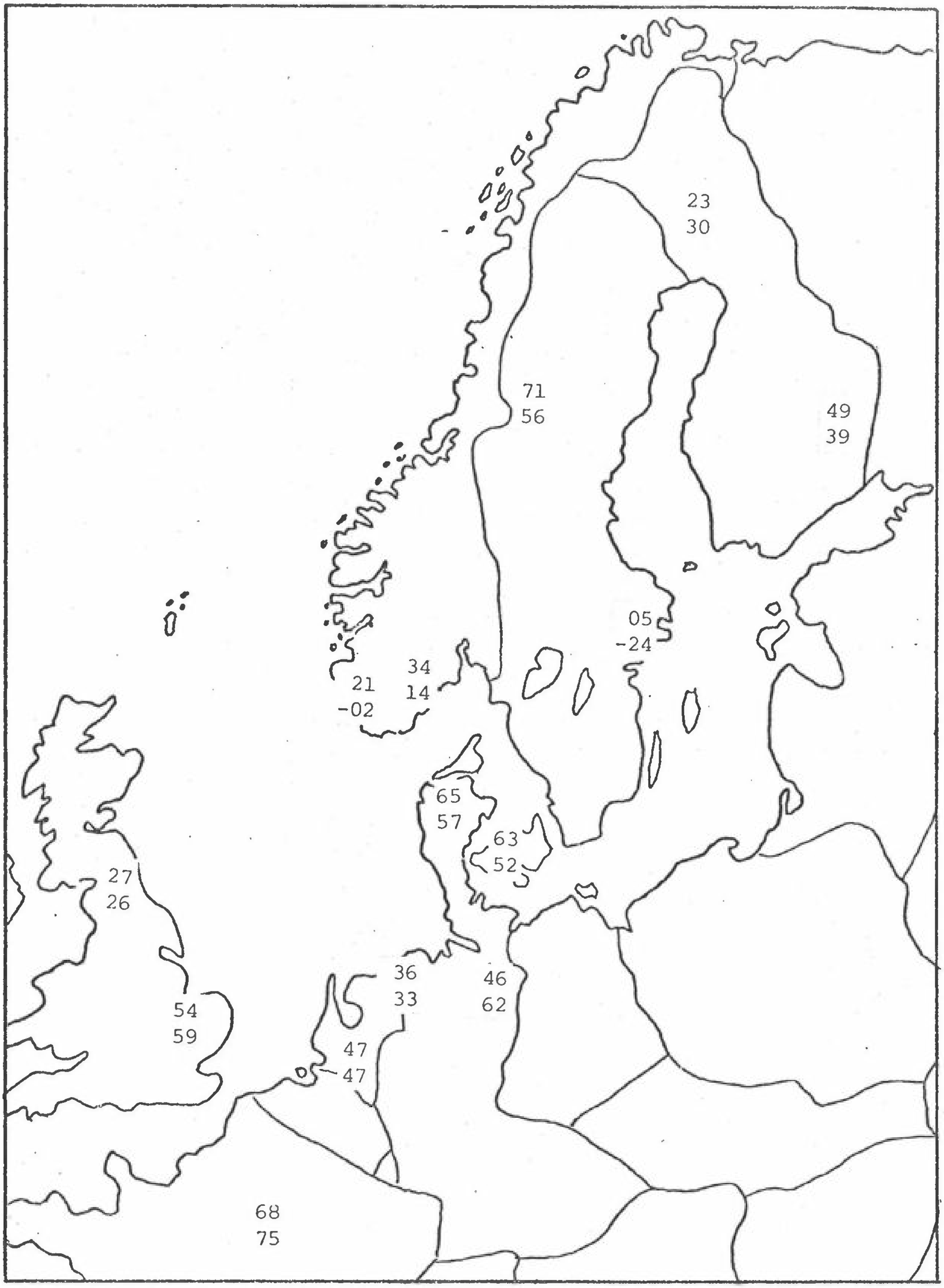

FIG. A37 DEC 73 - MARCH 74
96 HOURS SURFACE BACK TRAJECTORIES

CORRELATION OF $\frac{X1}{X2}$ TO SO_4 ON FILTER

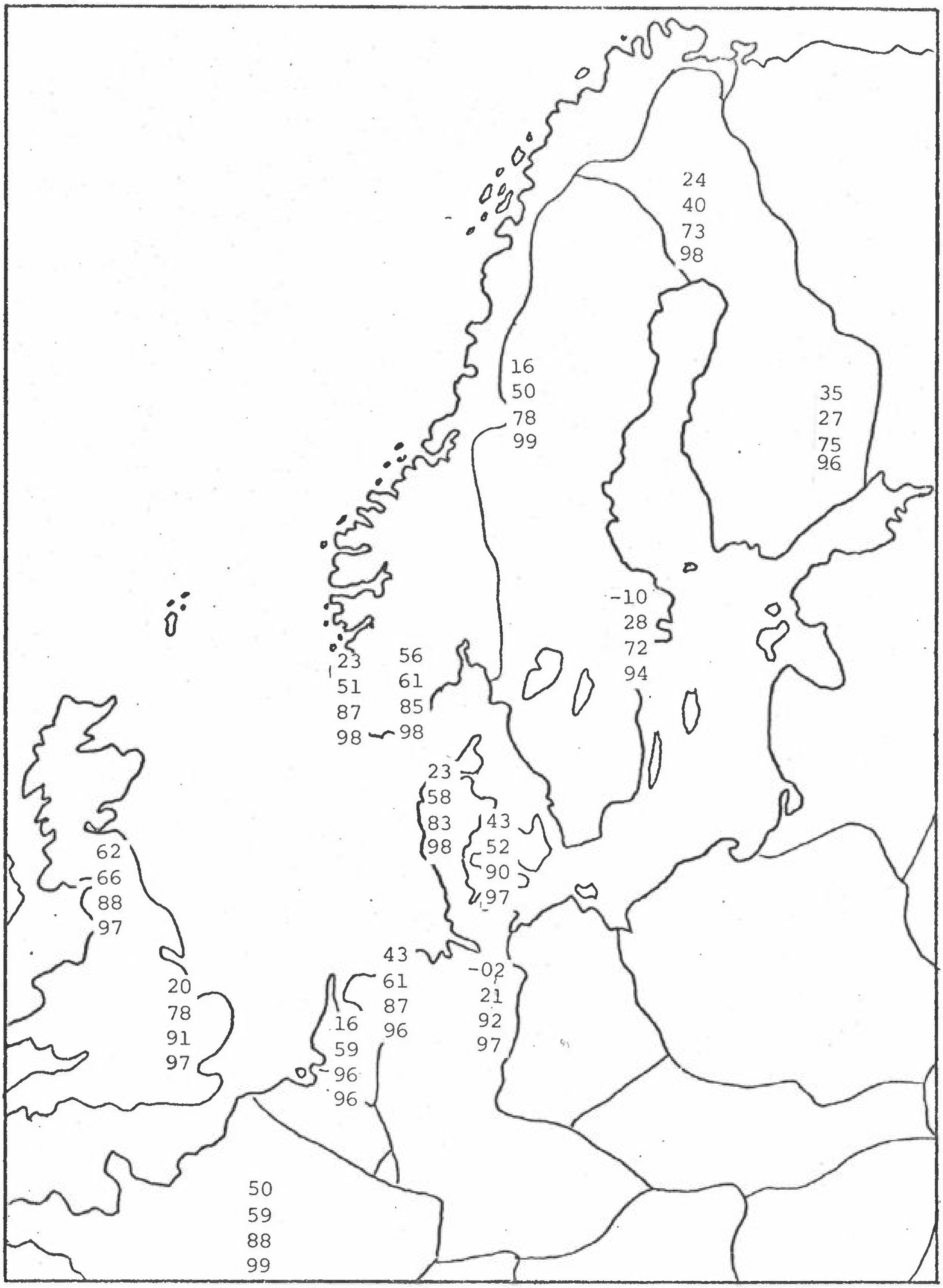

FIG A38 850 MB BACK TRAJECTORY ESTIMATES FOR DEC 73 - MARCH 74

CORRELATIONS BETWEEN TOTAL EMISSION ALONG TRAJECTORY AND

SO_2

SO_4 (on filter)

X1

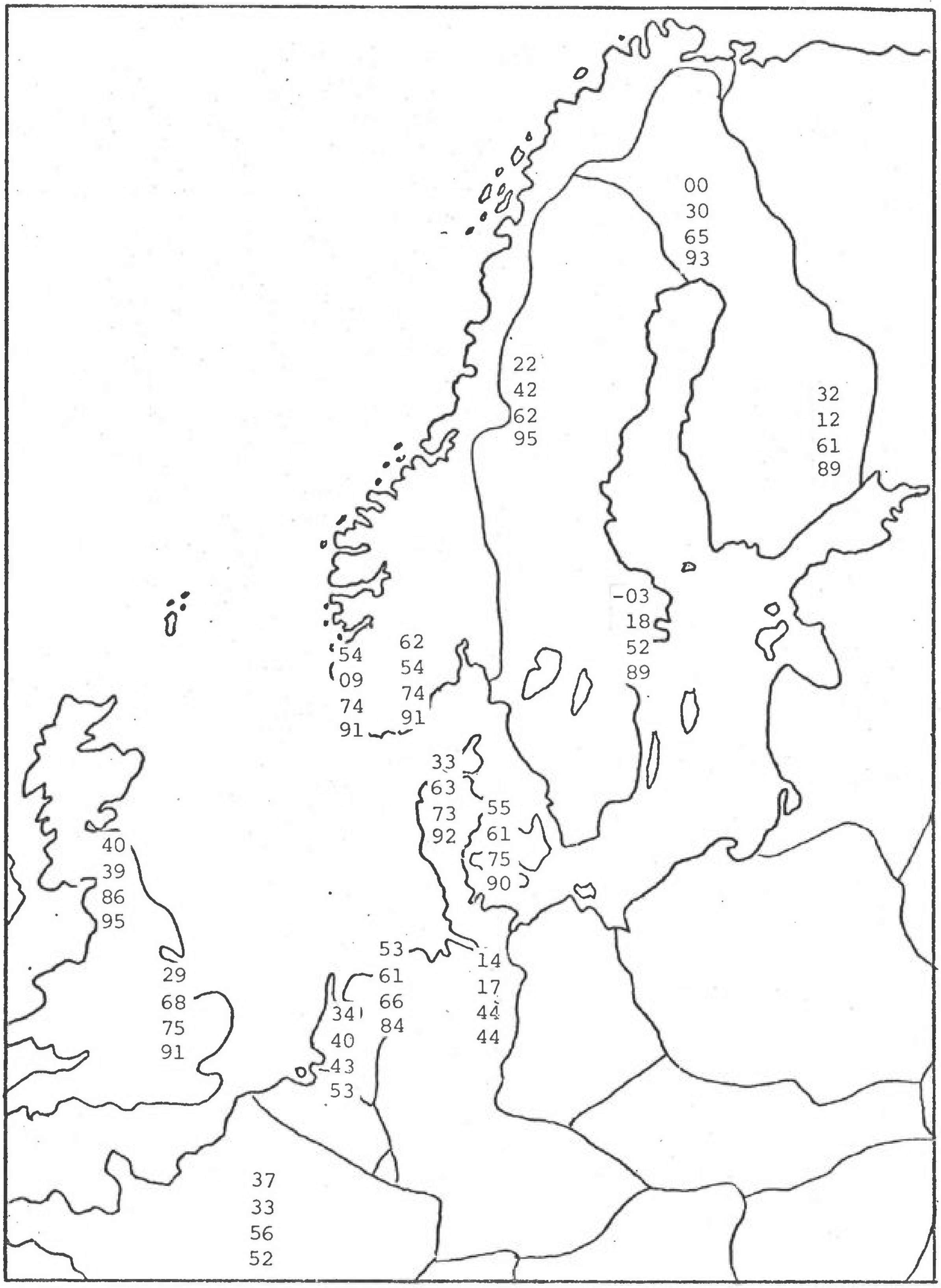

FIG. A39 "CLARKE" BACK TRAJECTORY ESTIMATES FOR DEC 73 - MARCH 74

CORRELATIONS BETWEEN TOTAL EMISSION ALONG TRAJECTORY AND

SO_2

SO_4 (on filter)

X1

X2

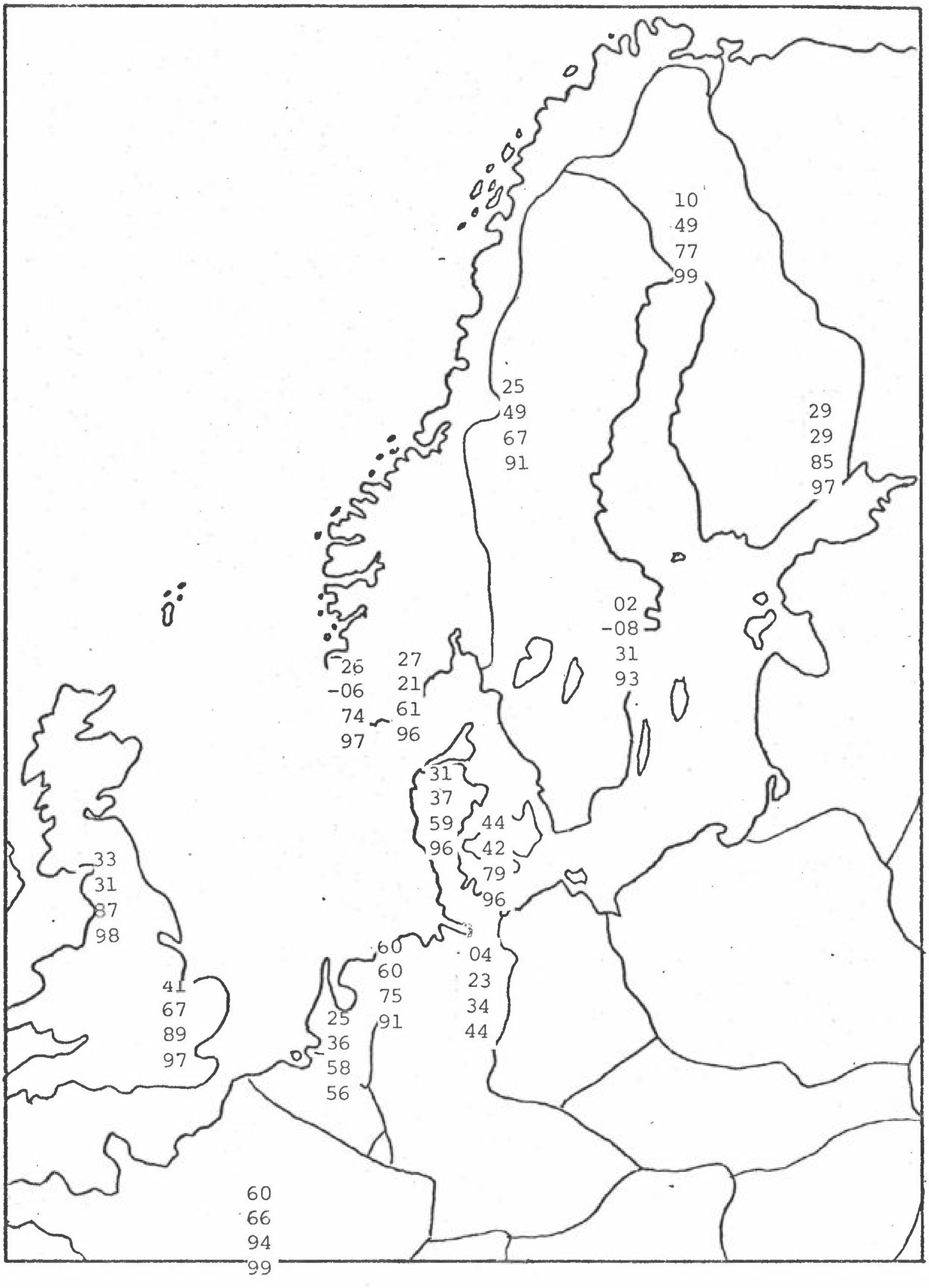

FIG. A40 "EKMAN" BACK TRAJECTORY ESTIMATES FOR DEC 73 - MARCH 74

CORRELATIONS BETWEEN TOTAL EMISSION ALONG TRAJECTORY AND

SO_2

SO_4 (on filter)

X1

X2

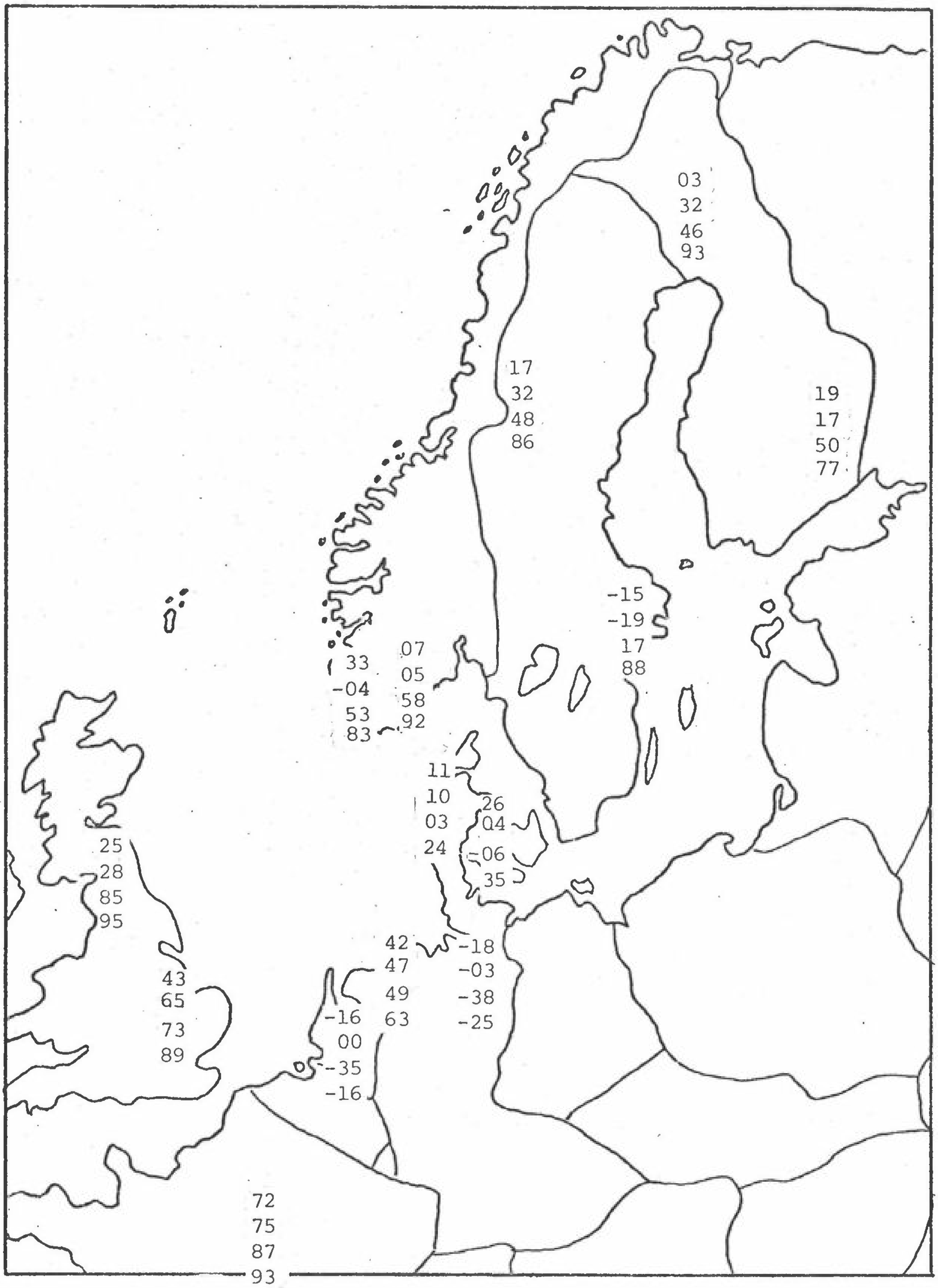

FIG. A41 SURFACE BACK TRAJECTORY ESTIMATES FOR DEC 73 - MARCH 74

CORRELATIONS BETWEEN TOTAL EMISSION ALONG TRAJECTORY AND

SO_2

SO_4 (on filter)

X1

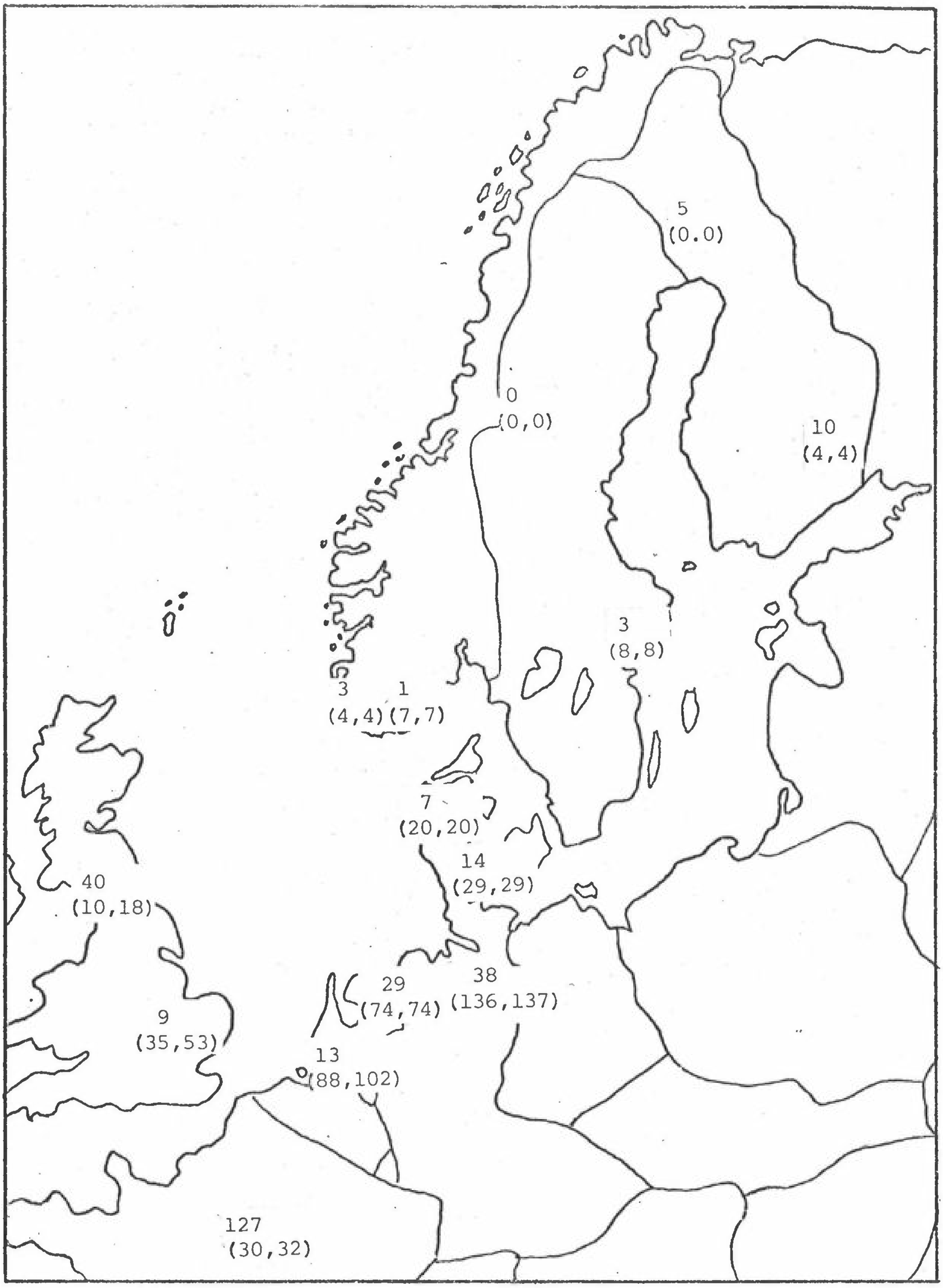

FIG. A42 EPISODE ON MARCH 27, 1974
OBSERVED DAILY MEANS OF SO_2
COMPARED TO 850 MB TRAJECTORY
ESTIMATES OF X1 AND X2
IN BRACKETS

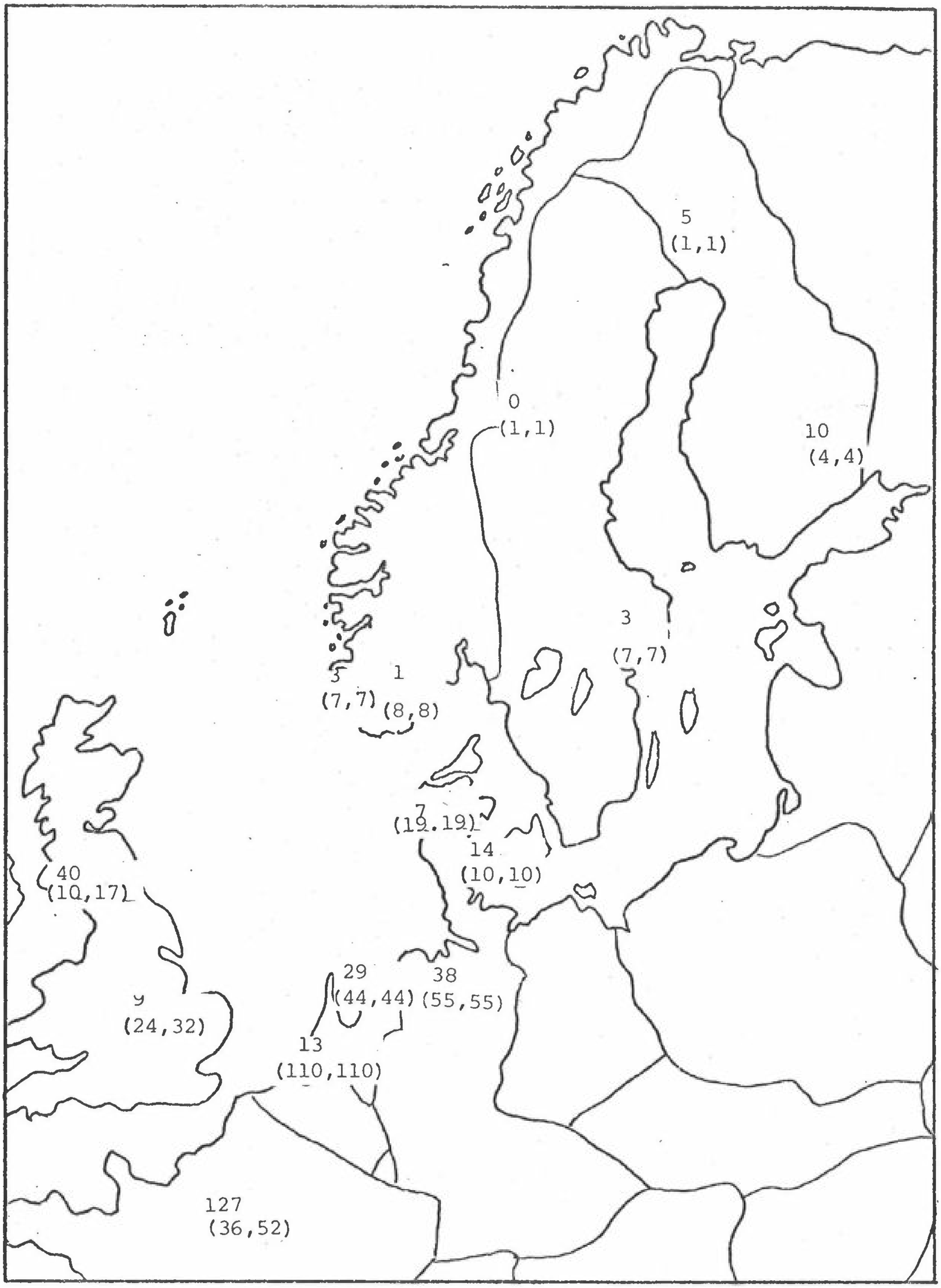

FIG. A43 EPISODE ON MARCH 27, 1974.

OBSERVED DAILY MEANS OF SO_2
COMPARED TO "CLARKE" TRAJECTORY
ESTIMATES OF X1 AND X2
IN BRACKETS

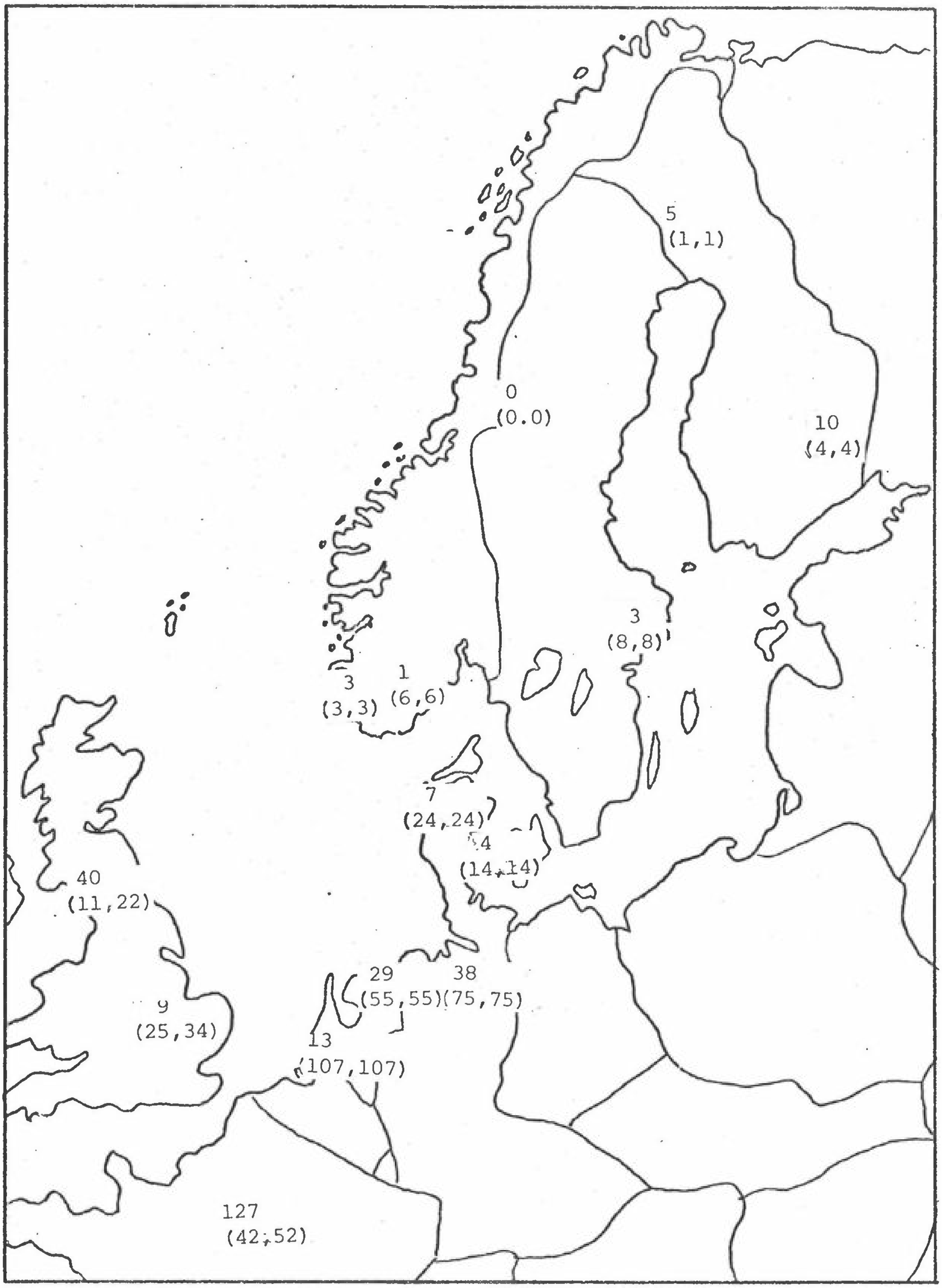

FIG. A44 EPISODE ON MARCH 27, 1974.

OBSERVED DAILY MEANS OF SO_2
COMPARED TO "EKMAN" TRAJECTORY
ESTIMATES OF X1 AND X2
IN BRACKETS

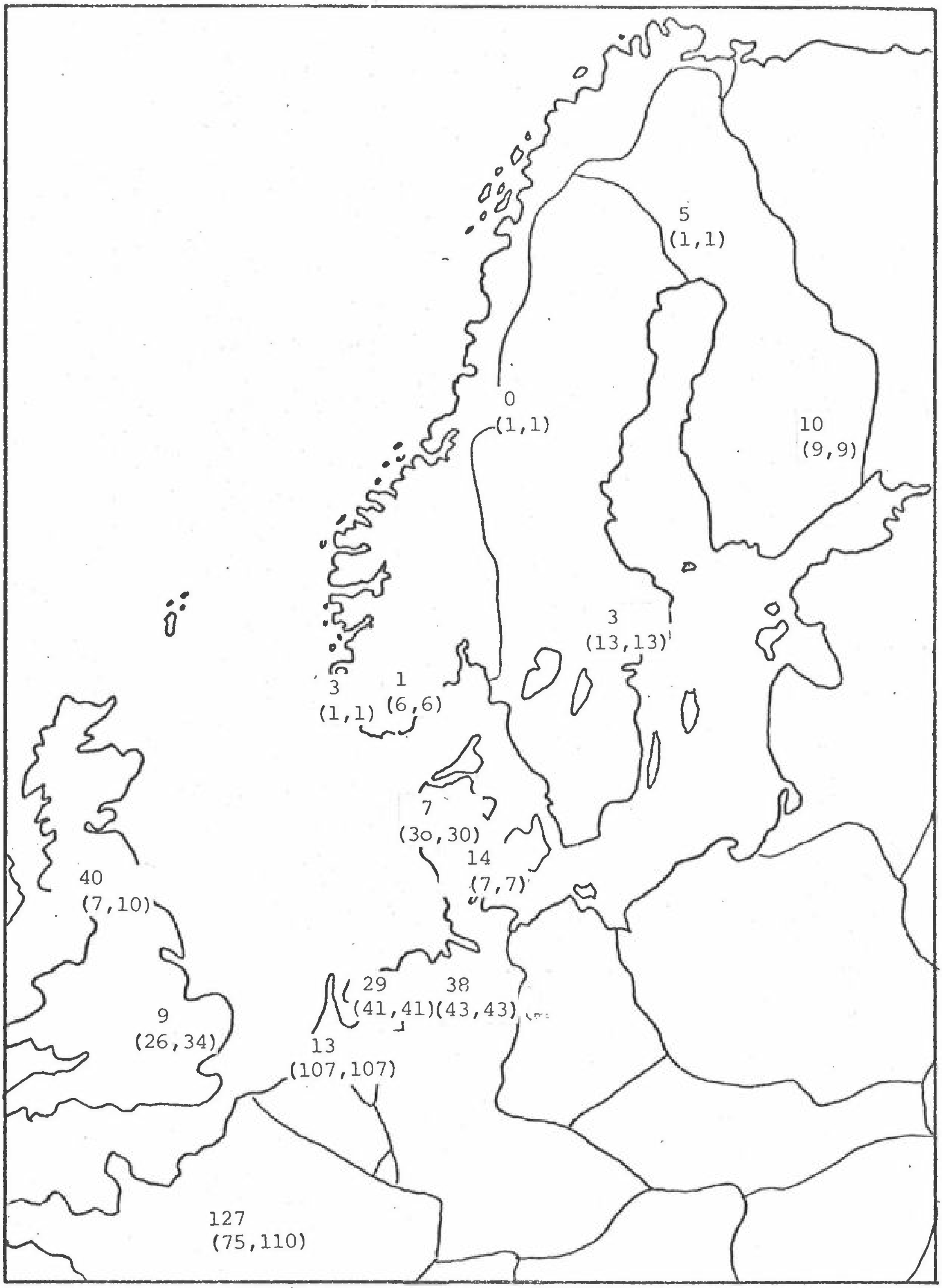

FIG. A45 EPISODE ON MARCH 27, 1974.

OBSERVED DAILY MEANS OF SO_2
COMPARED TO SURFACE TRAJECTORY
ESTIMATES OF SO_2

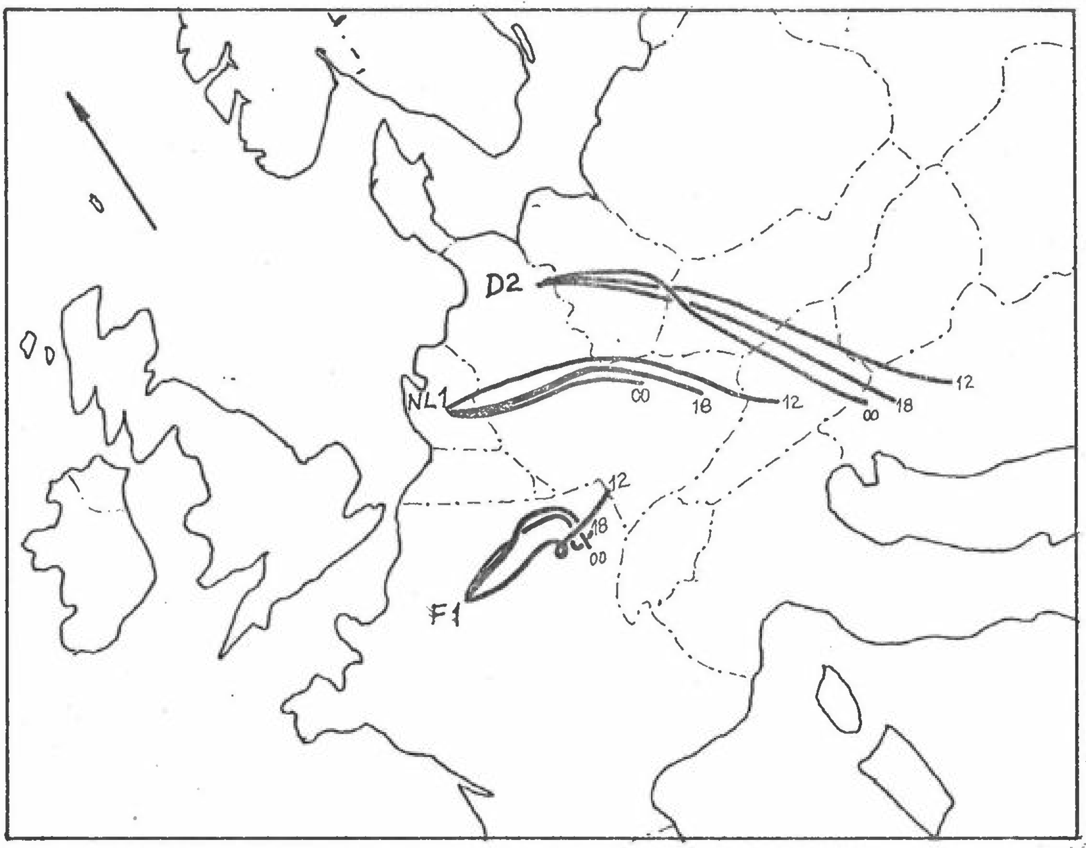

FIG. A46 48 HOURS BACK TRAJECTORIES WITH ARRIVALS BETWEEN 12 GMT MARCH 27 AND 00 GMT MARCH 28, 1974, 850 MB WINDS

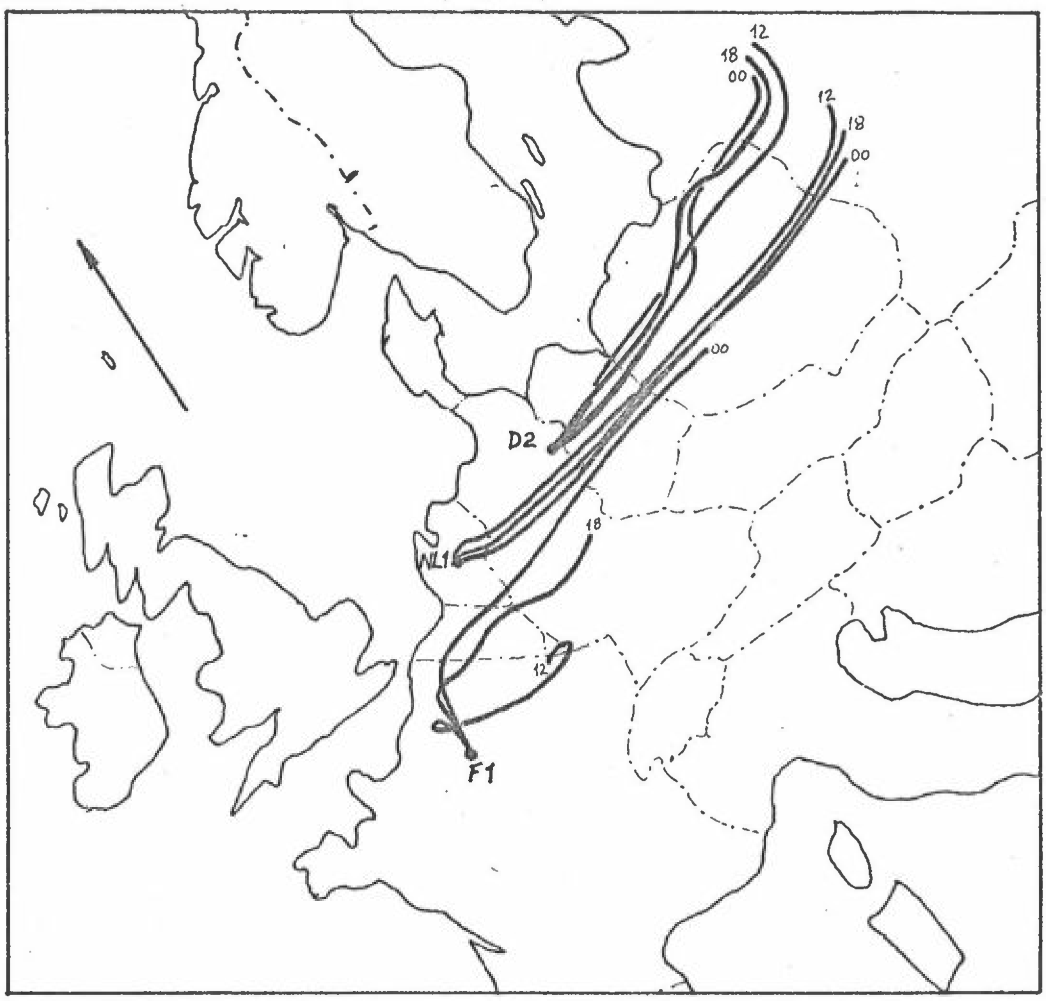

FIG. A47 96 HOURS BACK TRAJECTORIES WITH ARRIVALS BETWEEN 12 GMT MARCH 27 AND 00 GMT MARCH 28, 1974.
SURFACE WINDS.

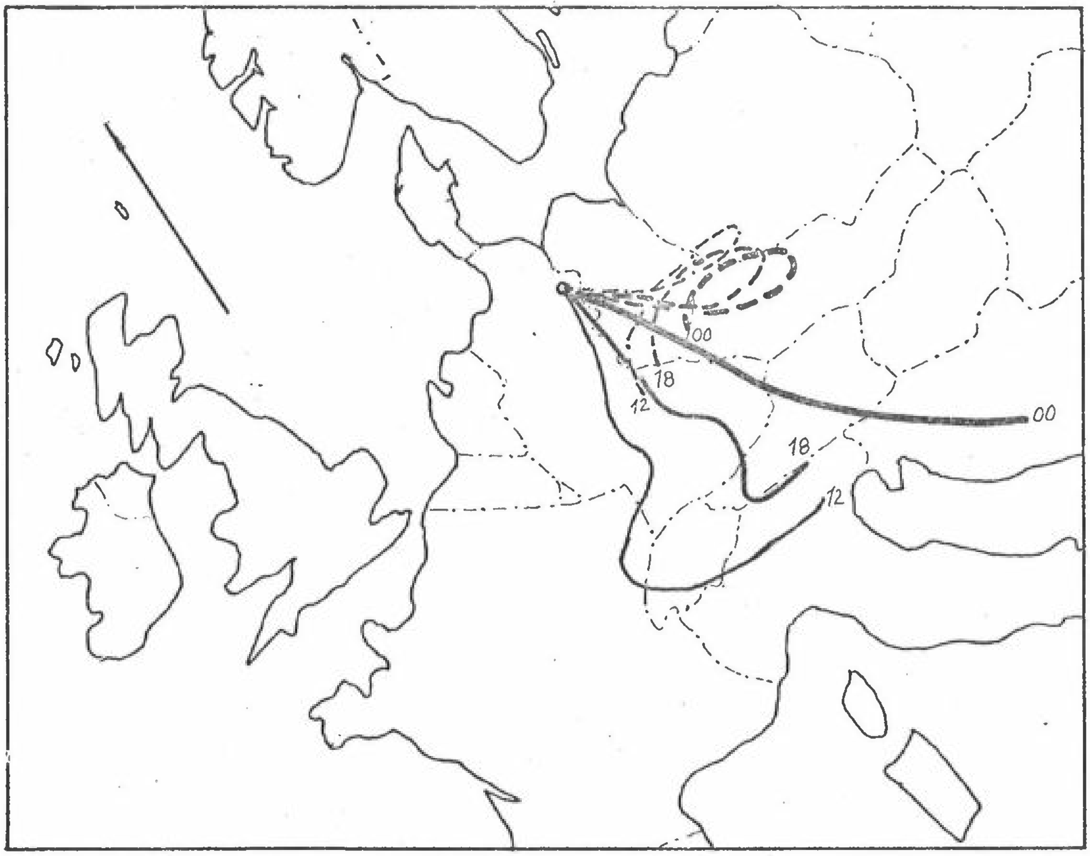

FIG. A48 48 HOURS 850 MB BACK TRAJECTORIES (FULL LINE)
96 " SURFACE " " (BROKEN LINE)
ARRIVAL AT D2 FROM 12 GMT JANUARY
3 TO 00 GMT JANUARY 4, 1974

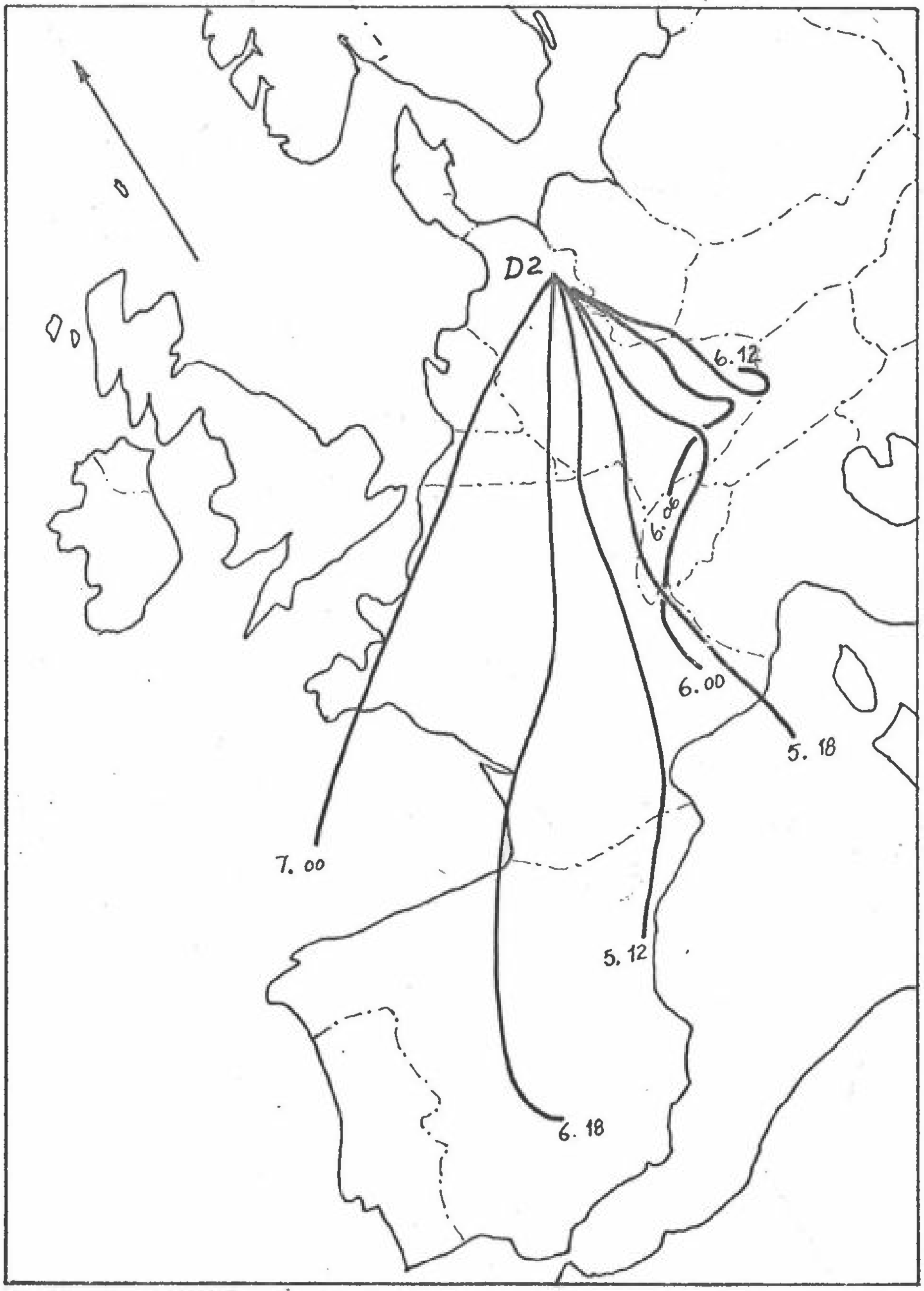

FIG. A49 48 HOURS 850 MB BACK TRAJECTORIES. ARRIVALS AT D2 FROM 12 GMT JANUARY 5 TO 00 GMT JANUARY 7, 1974

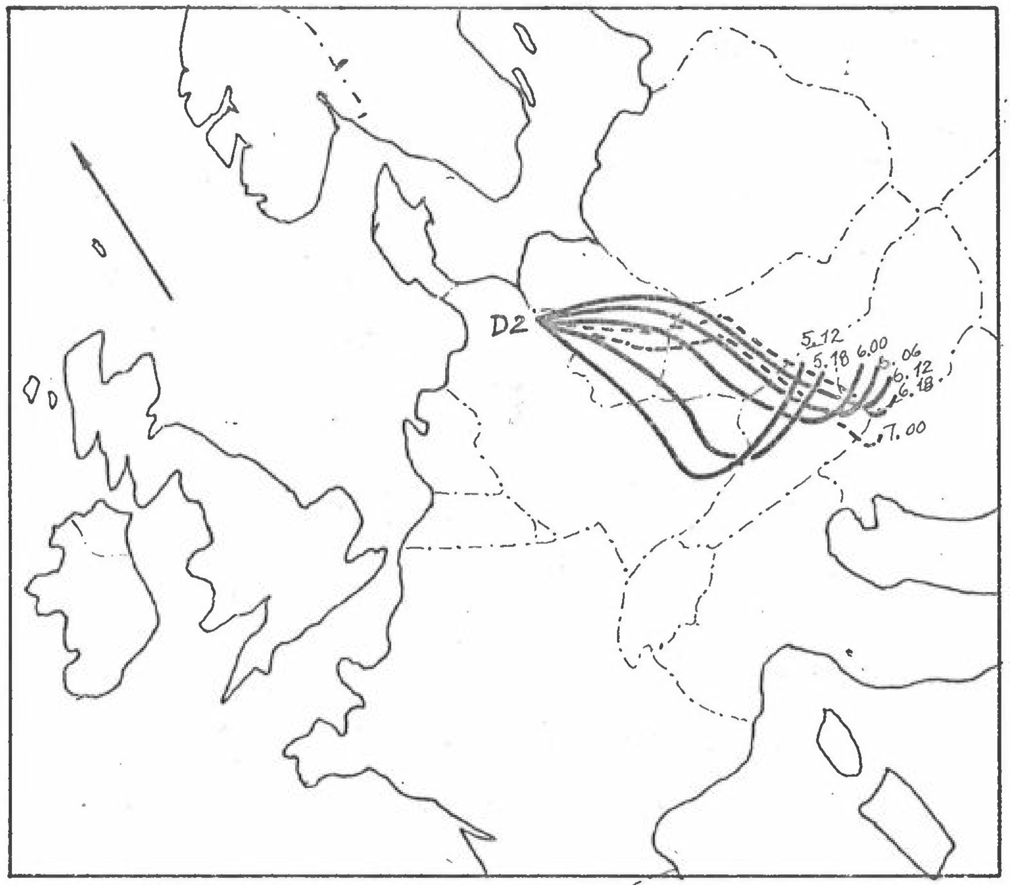

FIG. A50 96 HOURS SURFACE BACK TRAJECTORIES.
ARRIVALS AT D2 FROM 12 GMT JANUARY 5
TO 00 GMT JANUARY 7, 1974

SO_2 estimates	$\delta_N=1$	$\delta_N=0$ or $k_2 N < 0.6 s^{-1}$
X1	$k_0+k_1=3\times10^{-5}$, $k_1=2\times10^{-6}$, $k_2=0$	$k_0+k_1=0.8\times10^{-5}$, $k_1=2\times10^{-6}$, $k_2=0$
X2	$k_0=0$, $k_1=2\times10^{-6}$, 4×10^{-5}	" , " , "

SO_4 on filter estimate		$\delta_N = 1.$				$\delta_N = 0$ or $k_2 N < 0.6 s^{-1}$		
		k_0+k_1	k_1	k_2	K	k_0+k_1	k_1	K
(X1 as	X4	3×10^{-5}	2×10^{-6}	0	2×10^{-6}	0.8×10^{-5}	2×10^{-6}	2×10^{-6}
	X5	"	5×10^{-6}	0	"	"	"	"
	X6	"	10^{-5}	0	"	"	"	"
SO_2	X7	3×10^{-5}	2×10^{-6}	0	5×10^{-6}	"	"	"
	X8	"	5×10^{-6}	0	"	"	"	"
estimate)	X9	"	10^{-5}	0	"	"	"	"
	X10	3×10^{-5}	2×10^{-6}	0	10^{-5}	"	"	"
	X11	"	5×10^{-6}	0	"	"	"	"
	X12	"	10^{-5}	0	"	"	"	"
(X2 as	X13	2×10^{-6}	2×10^{-6}	4×10^{-5}	2×10^{-6}	0.8×10^{-5}	2×10^{-6}	2×10^{-6}
	X14	5×10^{-6}	5×10^{-6}	"	"	"	"	"
	X15	10^{-5}	10^{-5}	"	"	"	"	"
SO_2	X16	2×10^{-6}	2×10^{-6}	4×10^{-5}	5×10^{-6}	"	"	"
	X17	5×10^{-6}	5×10^{-6}	"	"	"	"	"
estimate)	X18	10^{-5}	10^{-5}	"	"	"	"	"
	X19	2×10^{-6}	2×10^{-6}	4×10^{-5}	10^{-5}	"	"	"
	X20	5×10^{-6}	5×10^{-6}	"	"	"	"	"
	X21	10^{-5}	10^{-5}	"	"	"	"	"

STATION	DATE D M J	OBSERVED AT SURFACE	COMPUTED VALUES OF X1 AND X2 USING			
			850 MB	"CLARKE"	"EKMAN"	SURFACE
D2	03 01 74	169	44-49	66-94	68-98	113-229
-	05 - -	153	23-26	68-74	56-59	128-133
-	06 - -	130	44-51	70-84	106-116	144-166
-	16 02 -	119	29-34	89-94	87-93	123-168
-	12 03 -	114	74-75	122-125	207-208	160-162
NLI	20 12 73	128	22-23	56-57	61-61	76-77
-	02 01 74	108	53-67	84-109	90-110	85-119
-	28 02 -	103	66-67	130-130	134-134	100-101
-	11 03 -	111	31-47	61-104	51-96	92-137
FI	27 03 74	127	30-32	36-52	42-52	75-110
-	28 - -	121	29-40	33-42	36-42	52-76

TABLE A2. DEC. 73 - MARCH 74. TRAJECTORY COMPUTATIONS FOR DAYS WHEN OBSERVED SO_2 CONSENTRATIONS WERW MORE THAN 100 MICROGRAMMES PER M^3. LEFT ESTIMATE IS X1, RIGHT ESTIMATE IS X2.